MARTIN MARIETTA ENERGY SYSTEMS LIBRARIES
3 4456 0361315 0

CENTRAL RESEARCH LIBRARY
DOCUMENT COLLECTION

SECRET

AEC RESEARCH AND DEVELOPMENT REPORT

ORNL-2703
C-83 – Reactors-Special
Features of Military Package
Power Reactors

79A

DECLASSIFIED
CLASSIFICATION CHANGED TO:
BY AUTHORITY OF: AEC - 3-30-62
BY: M. Bowman 9.10.62

ARMY PACKAGE POWER REACTOR PROJECT

PROGRESS REPORT

CENTRAL RESEARCH LIBRARY
DOCUMENT COLLECTION
LIBRARY LOAN COPY
DO NOT TRANSFER TO ANOTHER PERSON
If you wish someone else to see this document, send in name with document and the library will arrange a loan.

Inv. 60

OAK RIDGE NATIONAL LABORATORY
operated by
UNION CARBIDE CORPORATION
for the
U.S. ATOMIC ENERGY COMMISSION

SECRET

RESTRICTED DATA

This document contains Restricted Data as defined in the Atomic Energy Act of 1954. Its transmittal or the disclosure of its contents in any manner to an unauthorized person is prohibited.

[redacted]

ORNL-2703
C-83 - Reactors-Special
Features of Military Package
Power Reactors
M-3679 (22nd ed.)

This document consists of 100 pages.

Copy 79 of 200 copies. Series A.

Contract No. W-7405-eng-26

ARMY PACKAGE POWER REACTOR PROJECT

PROGRESS REPORT

A. L. Boch, Project Coordinator

Date Issued

MAR 24 1959

OAK RIDGE NATIONAL LABORATORY
Oak Ridge, Tennessee
operated by
UNION CARBIDE CORPORATION
for the
U.S. Atomic Energy Commission

[redacted]

MARTIN MARIETTA ENERGY SYSTEMS LIBRARIES

3 4456 0361315 0

[redacted]

[redacted]

[redacted]

[redacted]

SUMMARY

This report describes the Oak Ridge National Laboratory's participation in the Army nuclear power program. The information is presented in two parts based on two separate reactor types being studied by the Army Reactors Branch. Part I describes ORNL participation in the APPR-1 pressurized-water reactor program, and Part II deals with the gas-cooled reactor experiment.

PART I. PRESSURIZED-WATER REACTOR PROGRAM

Fabrication of the fuel and control elements for core I of the APPR-1 and the subsequent operating experience with core I suggested possible improvements in design and materials. Investigations were accordingly conducted in which it was found that type 347 stainless steel, which was thought to be desirable from the standpoint of mechanical properties as a substitute for type 304L as the fuel-plate cladding material and for type 304B as matrix material, would not be satisfactory because of the tantalum content of the alloy and because of the additional stainless steel that would be required in the matrix because of greater densification.

In order to reduce activity buildup in the primary system, a low-cobalt-content (0.005 wt % Co) type 304L stainless steel was procured by careful selection of inexpensive charge materials with cobalt concentrations of less than 0.006 wt %. The core II fuel elements and absorber sections will be constructed from this steel.

The Haynes-25 combs used as flux suppressors in the control rods of core I also contributed to the high cobalt activity of the system, and therefore dispersions of Eu_2O_3 in stainless steel were developed for use as the flux suppressor. A 28 wt % Eu_2O_3–stainless steel dispersion inserted into the billet frame in the gap between the fuel matrix and the frame was found to provide a satisfactory suppressor section.

In an effort to provide for operation of core II with a bank of five control rods rather than seven as in core I, means were studied for increasing the boron concentration in the fuel plates. It was found that higher concentrations of boron compounds resulted in considerably more diffusion into the cladding under the existing manufacturing procedures. Utilization of a master alloy of boron-stainless steel containing highly enriched boron appeared to be attractive until significant boron losses were observed when the material was sintered under hydrogen. Additional information indicated that this difficulty could be overcome by sintering in vacuum. Time limitations for procurement of the core II elements, however, dictated adherence to core I boron loadings until this problem could be completely solved.

Irradiation tests of fuel plates in the MTR failed to indicate any radiation damage to the specimens even for U^{235} burnup as high as 57%. Plates containing various quantities of UO_2 likewise showed no evidence of failure in postirradiation examinations. Similar results were obtained when the method of UO_2 preparation was varied and when various degrees of cold-rolling were used during fabrication.

Methods were developed for fabricating absorber sections for the control rods that consisted of a type 304 stainless steel-clad dispersion of 2.86 wt % B^{10} in electrolytic iron. Irradiation tests of miniature plates revealed that such plates could withstand 4 at. % B^{10} burnup without damage attributable to the helium generated by the boron (n,α) reaction. A test of a full-size APPR-1 absorber section which was substituted for an MTR control rod revealed no operational difficulty after five reactor cycles, and, after 11.5 megawatt-years of operation in core I of the APPR-1, the control rod containing the boron-iron absorber section is still functioning satisfactorily.

The known susceptibility of boron-containing materials to radiation damage suggested, however, that a more reliable absorber section be developed. Europium was selected for this service. The absorber section developed for core II consists of a roll-clad stainless steel composite plate containing a dispersion of 38 wt % Eu_2O_3 in stainless steel.

A study has been made of irradiation experiments conducted at other installations on fuel elements of the same general design as that of the APPR-1 fuel elements. A correlation of the irradiation damage results with burnup and temperature has provided information useful in design evaluations.

Experiments have been performed in which irradiated fuel plates were melted under controlled conditions simulating the loss-of-coolant accident. Tests with samples punched from a fuel plate have indicated dependence of the quantity of fission products released on the preheating time. Further melting experiments with clad, miniature coupons are planned in order to evaluate the effect of the exposed fuel edge of the punched sample.

A review has been made of the critical experiments performed in connection with the APPR-1. The discrepancy between the results obtained with matrix fuel plates and with foil fuel plates has been tentatively explained as being due to a heterogeneous effect in the foil-type plates.

PART II. GAS-COOLED REACTOR PROGRAM

A gas-cooled loop was designed for in-pile testing of advanced fuel specimens in two adjacent lattice positions in the ORR. The design provided for operation with various coolant gases, including N_2, He, CO_2, and air at temperatures up to 815°C and 300 psia. In order to remove up to 60 kw of fission and gamma-ray heat, the maximum gas velocity over the specimens was to be 350 fps. Most of the components, materials, and facility alterations had been specified by the time the project was terminated in April 1958. Some of the materials and components had been received.

A general review of the Army gas-cooled reactor design culminated in an outline of critical problem areas in the GCRE design and suggestions for their resolution. The problems specified were (1) the "hot" spot temperature on the fuel element, (2) corrosion, (3) the gas ducting system design, and (4) the control rod design.

CONTENTS

SUMMARY iii

INTRODUCTION viii

PART I. PRESSURIZED-WATER REACTOR PROGRAM

1. METALLURGICAL DEVELOPMENTS 3

APPR-1 Fuel Elements 3
Fabrication Process 8
Evaluation of Type 347 Stainless Steel as a Replacement for Type 304 Stainless Steel 11
Reduction of Cobalt Content of Type 304 Stainless Steel 14
Replacement of Haynes-25 Combs 17
Modified Control Rod Bank 18

Irradiation Testing of APPR Fuel Material 25

Control Rod Development for the APPR-1 33
Fabrication Procedures 33
Irradiation Tests of Boron-Iron Compacts 34
Core II Absorber Section 42

2. CORRELATION OF FUEL ELEMENT IRRADIATION EXPERIENCE AT VARIOUS AEC INSTALLATIONS 50

3. EXPERIMENTAL DETERMINATION OF FISSION-PRODUCT RELEASE AS A RESULT OF MELTDOWN OF AN APPR-1 FUEL ELEMENT 52

4. CALCULATION OF TANTALUM AND COBALT ACTIVATION IN TYPE 347 STAINLESS STEEL 54

5. CORRELATION OF APPR CRITICAL EXPERIMENTS 56

PART II. GAS-COOLED REACTOR PROGRAM

6. GAS-COOLED IN-PILE TEST LOOP 63

Design Criteria 63

Major Components and Features 65
Compressors 65
Economizer 67
Preheater 67
Cooler 67
Filters 67
Instrumentation and Controls 68
Retraction and Withdrawal Devices 69
Other Features 70

Analog Computer Study 70

Gas Velocity Measurements 72

Determination of Coefficient of Heat Transfer in Loop Insulation 76

Reactivity and Flux Measurements Pertinent to Loop Operation 81

7. GAS-COOLED REACTOR EXPERIMENT SUPPORT 84

Review of GCRE Design 84

Simulator Analysis 85

ARMY PACKAGE POWER REACTOR PROJECT PROGRESS REPORT

INTRODUCTION

The Oak Ridge National Laboratory has been associated with the Army nuclear power program continuously throughout the history of the program. Shortly after the Army Reactors Branch (ARB) was organized in the Division of Reactor Development of the Atomic Energy Commission in December 1952, the package power reactor project was formed at ORNL for the purpose of providing technical support to the new branch.

In the periods before, during, and immediately after the construction of the APPR-1 pressurized-water reactor at Fort Belvoir, Virginia, the ORNL Package Reactor Group served essentially as an extension of the ARB technical staff. The Laboratory's contributions to the APPR-1 project included: (1) conceptual design of the reactor and power plant, (2) assistance in technical aspects of bid preparation and evaluation, (3) design and performance of critical experiments, (4) development and fabrication of the reactor core, which was the first of its kind, (5) irradiation testing of fuel and control materials, and (6) technical review during design and construction phases.

Following completion of the APPR-1 construction and test operation, metallurgical development at ORNL continued on core materials. Also, specifications were prepared to permit the fabrication of core II stationary fuel elements by a private contractor.

The remainder of the Laboratory's effort was directed largely toward support of Army Reactors Branch activities in developments other than the pressurized-water reactor. Specifically, the design and construction of a gas-cooled in-pile test loop was undertaken in 1956. This loop was to be installed in the Oak Ridge Research Reactor (ORR) for use in support of the Army gas-cooled reactor program. A limited amount of technical review assistance was also provided on design aspects of the gas-cooled reactor experiment (GCRE), and a technical evaluation was made of proposals for the Army compact reactor experiment.

Several ORSORT design studies were sponsored which provided the initial design concepts for reactor development programs, including the GCRE.

In the spring of 1958 a decision was made to remove ORNL from the direct support role which they had occupied on the APPR-1 project. Work on the gas-cooled loop and design review on the GCRE was terminated. A reduced level of effort was established in order to retain the Laboratory in a role of continued general support of the Army nuclear power program. This effort has been mainly devoted to research and development work on metallurgical aspects of pressurized-water systems, with occasional consultation in other areas.

This report, which summarizes the activities of the ORNL Package Reactor Project during calendar year 1958, reflects the changing role of the Laboratory in the Army nuclear power program.

PART I. PRESSURIZED-WATER REACTOR PROGRAM

1. METALLURGICAL DEVELOPMENTS

APPR-1 FUEL ELEMENTS

The APPR-1 fuel elements utilize enriched fuel in order to provide for operation at a high specific power density and to minimize the core volume. A burnable poison is included to extend the reactivity lifetime of the element, and the fuel and poison are dispersed in stainless steel to maximize heat transfer. The fuel-bearing portions of the elements are clad in stainless steel for corrosion protection and retention of fission products. The use of stainless steel in the fuel-bearing core matrix and as the cladding assures the metal-to-metal bond of the core and cladding and the thin-plate type of construction necessary for efficient heat removal.

The fuel and burnable poison are incorporated into the fuel plates as a dispersion of uranium dioxide and boron carbide powder in austenitic stainless steel powder. The powder dispersion containing these active ingredients is hermetically sealed in a jacket of wrought stainless steel, which is then rolled to obtain the required metal-to-metal bond between cladding and matrix steel. A representative cross section of a fuel plate with 0.005-in. cladding is shown in Fig. 1.1.

The active core of the APPR is composed of 38 stationary fuel elements and seven movable control rod assemblies immersed in water. The water serves as moderator, reflector, and heat transfer medium. The system operates at an outlet temperature of 230°C and is pressurized to 1200 psia; water flows through the channels between adjacent fuel plates at an average velocity of 4.3 fps.

A stationary fuel element, as illustrated in Fig. 1.2, consists of 18 flat composite plates joined to a pair of spacer plates by brazing to form an integral assembly with a nominal water-gap spacing of 0.133 in. between plates. An element with attached end adapters is shown in Fig. 1.3 ready for insertion in the reactor grid. The control rod assembly for core I, shown in Fig. 1.4, differs from the stationary

UNCLASSIFIED
Y-25961

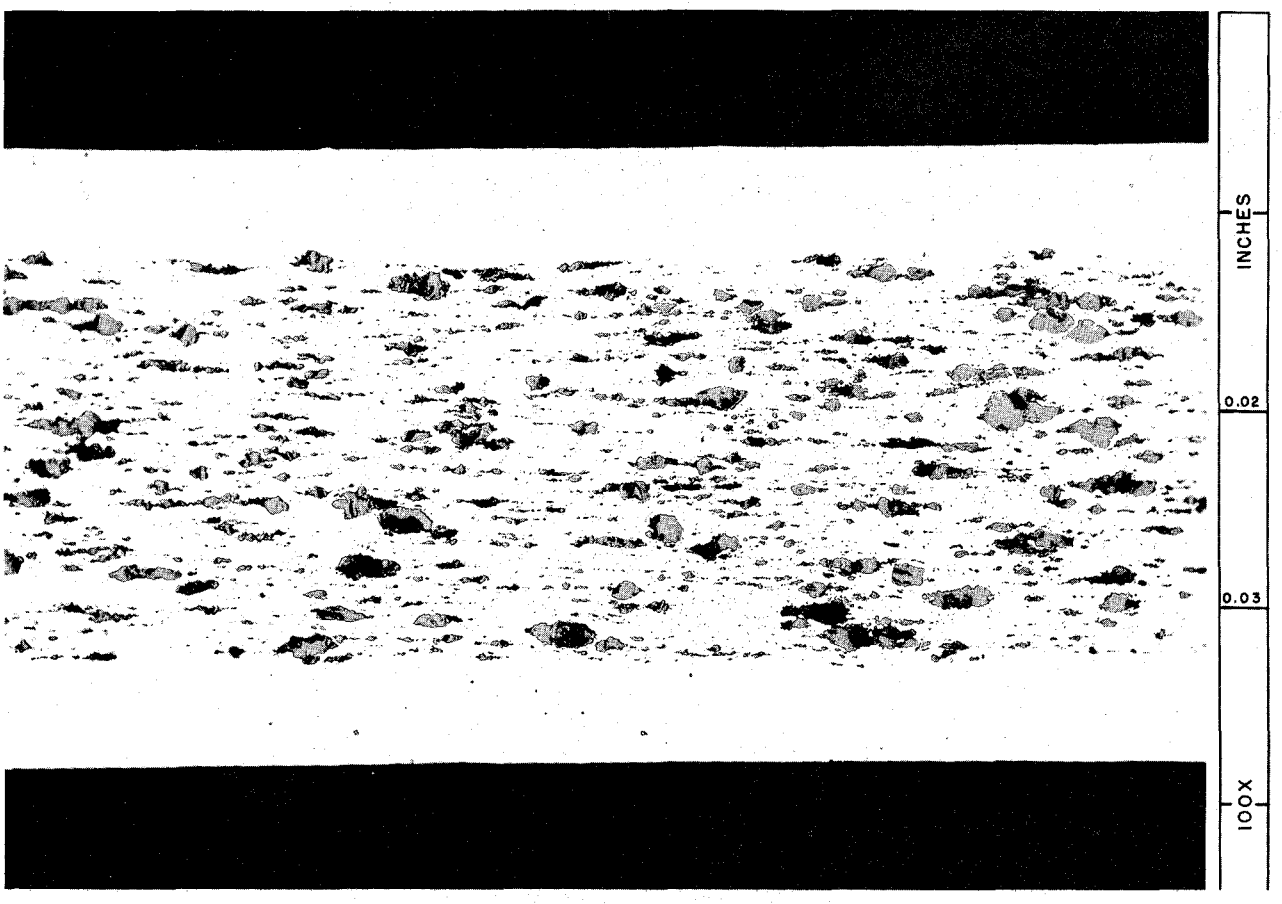

Fig. 1.1. Cross Section of an APPR-1 Composite Fuel Plate. As polished.

UNCLASSIFIED
Y-24067

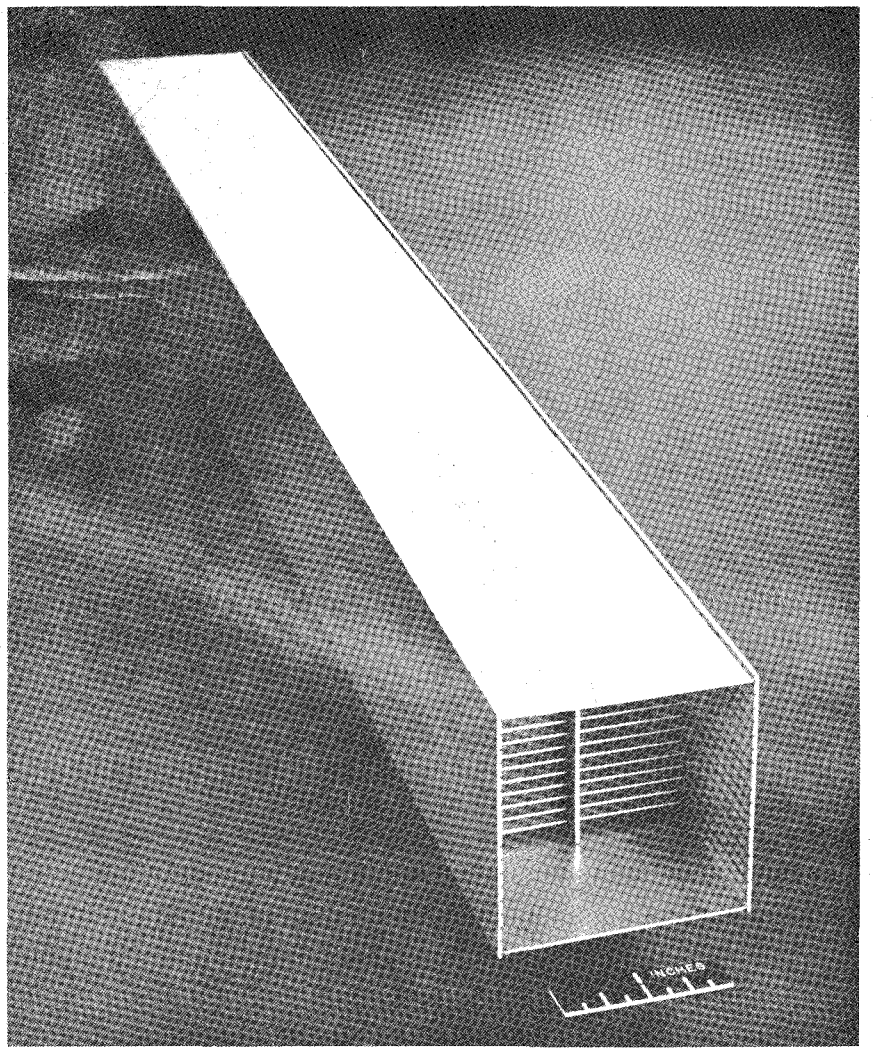

Fig. 1.2. APPR-1 Stationary Fuel Element Without End Adapters.

UNCLASSIFIED
Y-19729

Fig. 1.3. APPR-1 Stationary Fuel Element with End Adapters Attached.

UNCLASSIFIED
Y-22201

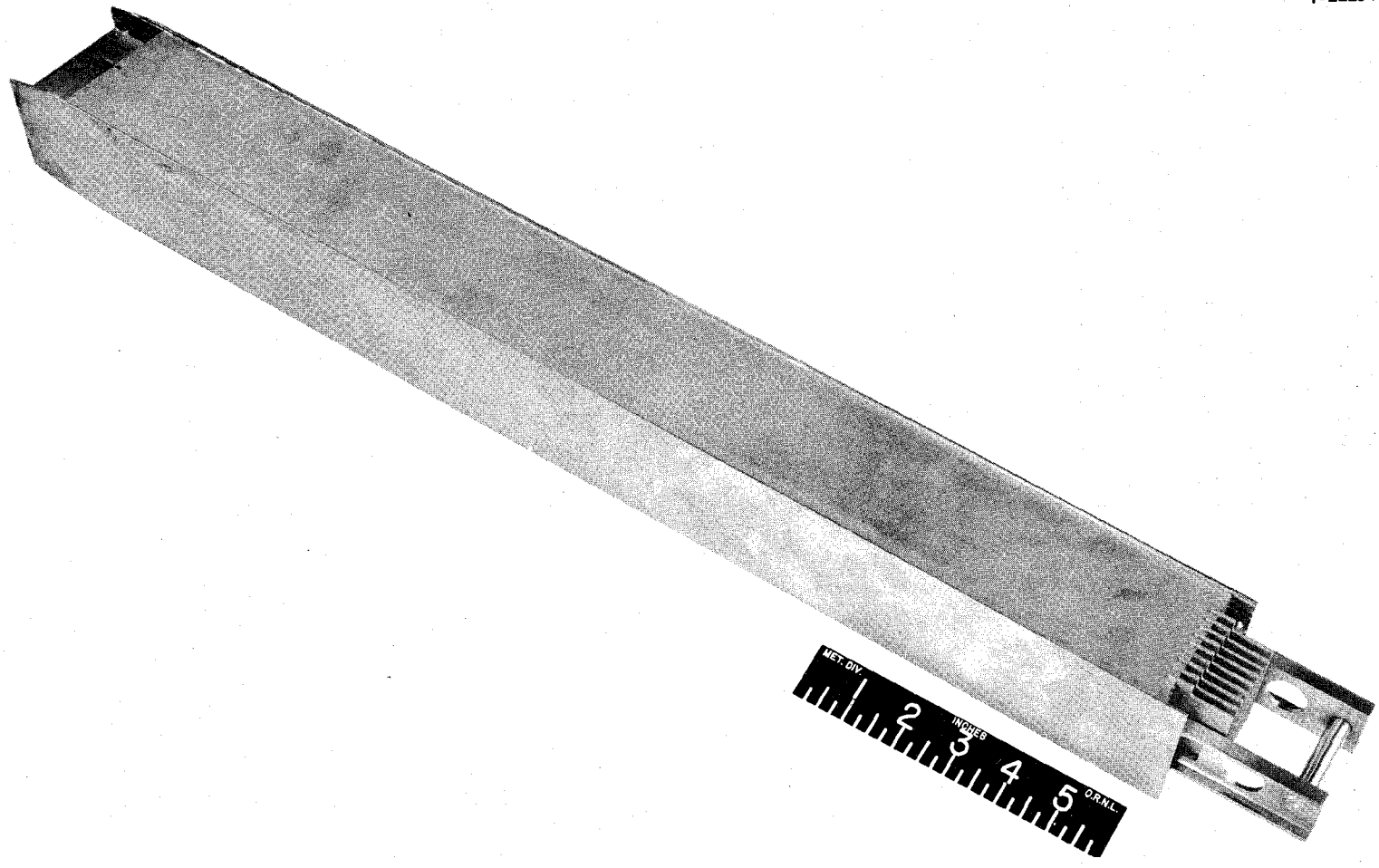

Fig. 1.4. Control Rod Assembly for Core I of APPR-1.

fuel element in that it consists of 16 fuel plates; and, instead of end adapters, it has a series of Haynes-25 combs at the end adjacent to the adsorber section, and a handle at the opposite end to permit insertion and removal. The Haynes-25 combs used in the core I rods contained 51 wt % Co for controlling the flux peaking in the region between the fuel plates and the absorber section. Pertinent data on the core I fuel and control elements are listed in Tables 1.1 and 1.2.

Table 1.1. Design Data on APPR-1 Core I Fuel and Control Elements

	Stationary Fuel Element	Control Rod Assembly
Number of fuel-bearing plates per assembly	18	16
Number of Haynes-25 combs per assembly		9
Fuel plate cladding thickness, in.	0.005	0.005
Core thickness, in.	0.020	0.020
Water-gap spacing, in.	0.133	0.133
B^{10} content per assembly, g	0.464	0.363
U^{235} content per assembly, g	515.16	417.76
Fuel density per plate, g/cm^2	0.079 (min) 0.085 (max)	0.078 (min) 0.082 (max)

Fabrication Process. The methods which were developed and adopted for manufacturing the fuel elements for core I of APPR-1 are illustrated in Fig. 1.5. The exact quantities of material for each fuel core are separately weighed, blended, and pressed at room temperature under a load of 33 tsi to form the fuel compact. After sintering for 1 1/4 hr at 1175°C, the core is coined to a density of approximately 87% of theoretical. The core is enclosed in a stainless steel frame, cover plates are attached to the frame, and the stainless steel cladding is bonded to the fuel core by rolling at 1150°C to a

Table 1.2. Materials Data on APPR Fuel and Control Elements

Composition of Fuel Matrix	Particle Size (μ)	Stationary Fuel Element			Control Rod Assembly		
		Grams	Wt %	Vol %	Grams	Wt %	Vol %
UO_2	44-88	35.09	25.98	19.04	32.01	25.87	16.90
B_4C	< 44	0.188	0.14	0.50	0.172	0.14	0.42
Type 304B stainless steel	< 149	99.80	73.88	82.46	91.56	73.99	82.68

UNCLASSIFIED
Y-25687

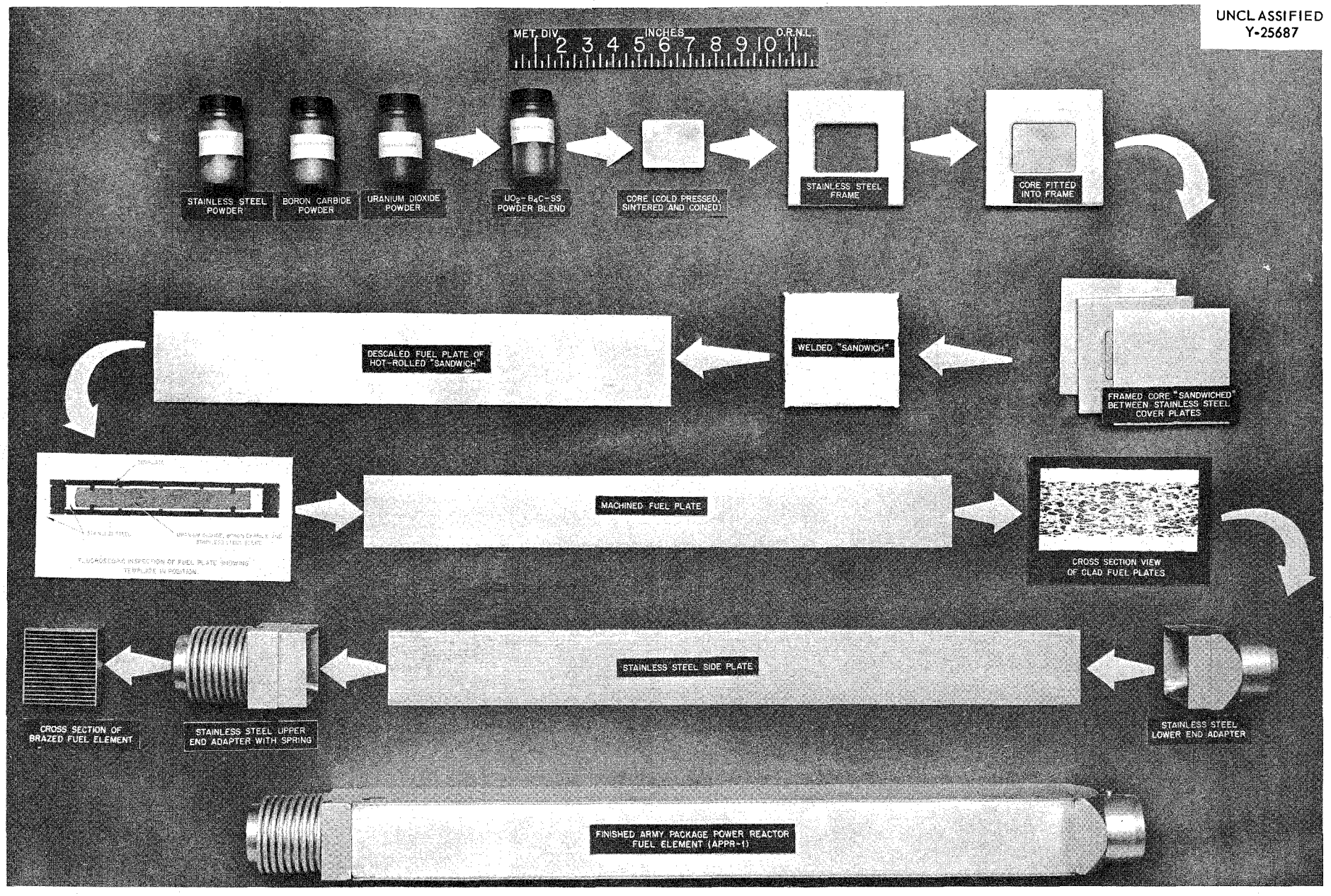

Fig. 1.5. Procedure for Manufacturing APPR-1 Fuel Element Components.

reduction in thickness of 90.5%. The hot-rolled mill scale is removed by pickling in 15% HNO_3–5% HF aqueous solution, and the plates are cold-rolled, with a reduction of approximately 25% in thickness, to the specified core dimensions. After fluoroscopic examination and shearing and machining to the specified over-all plate dimensions, the composites are flattened by annealing between steel platens for 3 hr at 1130°C. The fuel element is assembled by sliding the plates into the grooved side plates; Coast Metals NP alloy powder is preplaced at the joints; and the fuel element is brazed by slowly heating it to 1130°C and furnace cooling it. The stationary fuel elements are completed by welding adapters to each end and machining them to the specified size. Since the gusset plates of the control rod assembly are welded to the side plates prior to brazing, the only work required after brazing is welding the handle to the gusset plates.

After completion of the fuel and control elements for core I and the subsequent reactor experience, several changes appeared to be desirable. These included the following:

1. replacement of the low-carbon stainless steel plate (type 304L) and the boron-containing stainless steel powder (type 304B) in the fuel elements with a stabilized stainless steel,
2. utilization of a stainless steel with appreciably less cobalt than that present in the steel used in core I fuel elements,
3. replacement of the high-cobalt-content Haynes-25 combs at the end of the control rod assembly with a more suitable flux suppressor,
4. operation of the reactor with a bank of five control rod assemblies, rather than seven, by increasing the boron content of the control rod fuel plates.

Evaluation of Type 347 Stainless Steel as a Replacement for Type 304 Stainless Steel. The incentive to use a stabilized stainless steel was the knowledge that the carbon in the type 304B stainless steel matrix of the fuel-plate core diffused into the cladding and the heat treatments specified in the manufacture of the fuel elements caused chromium carbide precipitation at the grain boundaries of the type 304L stainless steel cladding. If material sensitized in this manner were

then cleaned in a reducing acid it would be susceptible to intergranular attack such as that shown in Fig. 1.6. Although such treatment is not specified for plates which have been heat treated, the possibility that they might be cleaned with a reducing acid exists. There is no economical nondestructive inspection procedure available with which to detect such attack. In addition, the grain size of the type 304L stainless steel cladding of the finished fuel plate was larger than desired.

Since the use of a stablized steel, such as type 347, would avoid the sensitization difficulty, and since such steel is not as susceptible as type 304L stainless steel to exaggerated grain growth, an investigation was conducted to determine whether type 347 stainless steel sheet and powder containing 2.3% silicon could be substituted for the originally specified types 304L and 304B stainless steel sheet and powder, respectively, without modification of the established specifications for the manufacture of APPR-1 fuel elements. After fabrication of 23 plates containing depleted UO_2, it was concluded that the substitution had no effect on the densification of the cold-pressed, sintered, and coined compact. Based on picnometer density values of 10.33 and 7.45 g/cm^3 for UO_2 and type 347 stainless steel, respectively, the green-pressed densification was 78.5%. After sintering at 1175°C for 75 min and coining under a pressure of 33 tsi, the densification increased to approximately 87%, which is the same as the density obtained previously with compacts containing type 304B stainless steel.

Billets containing the compacts, framed, and clad with wrought type 347 stainless steel exhibited fabrication characteristics quite similar to those of the plates fabricated with type 304L stainless steel. It was observed, however, that the length of the fuel core in the completely fabricated plate was approximately 3% shorter than the nominal length; it thus appeared that the substitution of the type 347 stainless steel resulted in greater final densification, which slightly modified the weight-percentage values for the element.[1]

---

[1] R. J. Beaver and C. F. Leitten, Talks Presented Before APB, Washington, D. C., September 1957, ORNL CF 58-2-128 (Feb. 11, 1958).

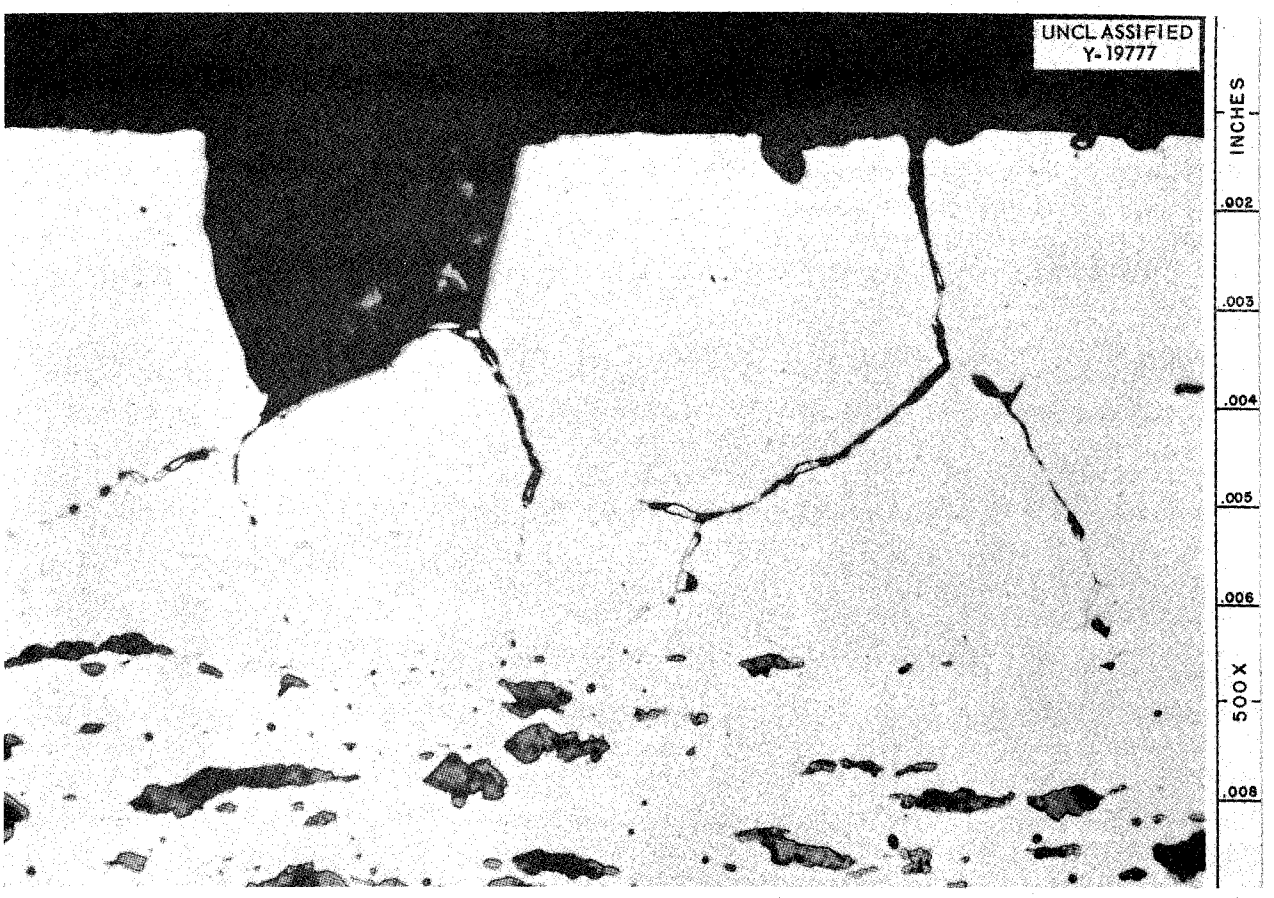

Fig. 1.6. Microstructure of a Type 304L Stainless-Steel-Clad Fuel Plate After Exposure to an Aqueous Solution Containing 15% HNO_3 and 5% HF.

The first type 347 stainless steel element containing depleted UO_2 was brazed successfully. There was no indication that the use of the different steel had any effect on the brazing process. The microstructures of the UO_2 dispersion in type 347 stainless steel are shown after hot-working in Fig. 1.7 and after hot-working, 25% cold-reduction, and annealing in Fig. 1.8. The grain size of the cladding on the cold-rolled and annealed plates, as shown in Fig. 1.7, is significantly finer than the grain size of type 304 stainless steel cladding on similar plates. The finer grain structure combined with stabilization of the stainless steel inhibits intergranular attack of the type[2] shown in Fig. 1.6. It is to be emphasized, however, that intergranular corrosion is not likely to occur during operation of the APPR-1 pressurized-water system.

The greater densification of the type 347 stainless steel powder required that the amount of stainless steel added to the fuel compact be increased in order to meet the dimensional specifications. Since the time schedule for production of the core II elements would not permit the extensive investigation that would have been required to determine the effect of the added steel on reactivity and the effect of the tantalum content of commercial type 347 stainless steel on the activity of the system, it was decided to fabricate the core II fuel elements with type 304 stainless steel. As stated above, and as borne out by operation with core I, intergranular corrosion is not likely to occur in the pressurized-water system, and steps were taken to ensure that heat-treated plates would not be cleaned with a reducing acid during fabrication.

Reduction of Cobalt Content of Type 304 Stainless Steel. Experience during reactor operation with core I indicated potential maintenance difficulties because of high activity buildup in the primary-loop system.[3]

---

[2] R. J. Beaver et al., Investigation of the Factors Affecting Sensitization of APPR-1 Fuel Elements, ORNL-2312 (Oct. 8, 1957).

[3] W. J. Small, J. L. Zegger, and A. L. Medin, Long-Lived Circulating Activity in the APPR, APAE-20 (Aug. 28, 1957).

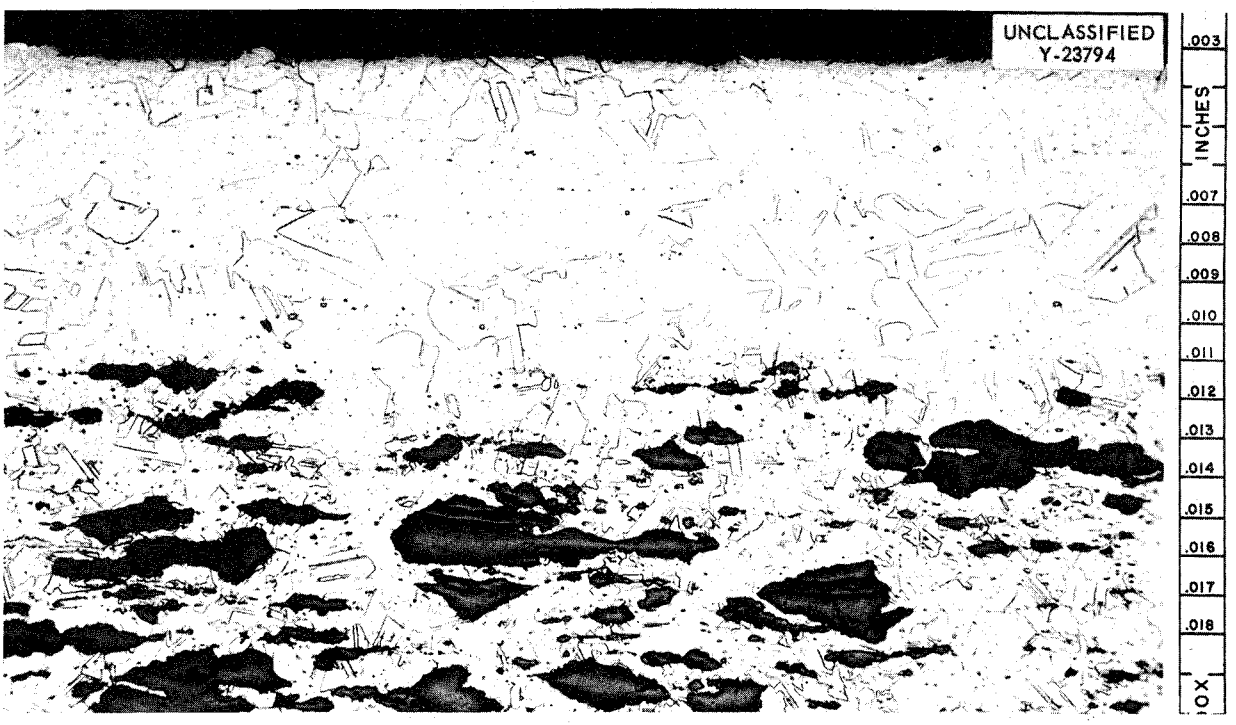

Fig. 1.7. Microstructure of a Type 347 Stainless Steel Fuel Plate in the As-Hot-Rolled Condition.

Fig. 1.8. Microstructure of a Type 347 Stainless Steel Fuel Plate in the Hot-Rolled, 25% Cold-Reduced, and Annealed Condition.

One of the major causes of the activity was Co^{60}, an irradiation-transformation product of Co^{59}, which is a tramp element in stainless steel. The concentration of cobalt in stainless steels normally ranges from 0.03 to 0.3 wt %, with the cobalt content in type 304L stainless steel being approximately 0.07 wt %. It was felt that to minimize this source of activity, the stainless steel in fuel elements for core II would have to be limited to a cobalt content of less than 0.006 wt %. The price of stainless steel with a guarantee of such a specification would, of course, be exorbitant. However, by careful selection of charge materials with extremely low-cobalt content, and close cooperation of the vendor, in this case, Allegheny Ludlum Steel Corp., Pittsburgh, Pennsylvania, it was possible to produce a type 304L stainless steel containing 0.005 wt % Co. The steel heat consisted of 18,000 lb of the charged material. From this material, a 57% yield of plates and sheets was realized at a cost of approximately $2.60/lb for the finished product.

The cobalt content of the materials selected for this heat of steel are itemized below:

Charge Materials	Cobalt Content (wt %)
Armoc iron	0.005
Mond nickel	0.0005
Electrolytic chromium	< 0.001
High-purity ferro-silicon	0.002
Electrolytic manganese	< 0.001
Iron ore	< 0.001
Aluminum	< 0.001
Fluorspar	< 0.001
Limestone	< 0.001
Periclase furnace lining	< 0.001
Magdolite	< 0.001

An analysis of the finished product showed the following:

Components of Finished Product	Analysis (wt %)
Cobalt	0.005
Carbon	0.018
Iron	68.2
Nickel	9.57
Chromium	18.70
Manganese	1.72
Silicon	0.82
Phosphorus	0.010
Sulphur	0.020
Copper	0.100
Tantalum	<0.001

Measurements of the mechanical properties of the 1-in.-thick plate stock revealed yield and tensile strengths of 34,000 and 83,000 psi, respectively, with a reduction in area of 80%. These values compare favorably with those for commercially available type 304L stainless steel. It was thus demonstrated that by careful monitoring of the inexpensive materials required in the makeup of this stainless steel, the desired maximum cobalt content of 0.006 wt % could be obtained at a cost which was not unreasonable.

Replacement of Haynes-25 Combs. Another factor that obviously contributed to the high cobalt activity of the reactor was the corrosion products of the Haynes-25 combs which were attached to the control rods to serve as flux suppressors. An alternate technique for suppressing the flux is to enclose a volume of material containing the required quantity of a neutron absorbing element within the composite fuel plate at the end of the fuel-bearing section. Boron could not be used for this service because it is subject to irradiation damage by the (n,α) reaction and because there would be appreciable burnup of the large quantity required. A dispersion of Eu_2O_3 in stainless steel was selected as the neutron-absorbing material, since it undergoes an (n,γ)

reaction and should not be susceptible to serious irradiation damage. Calculations based on a flux-suppressor length of 0.875 in. in the completely fabricated plate revealed that a 28 wt % Eu_2O_3-stainless steel dispersion would be required.

The method selected for incorporating the required quantity of Eu_2O_3 in the desired volume was to prepare a 0.065-in.-thick sheet of the 28 wt % dispersion, precision shear the desired volume of material from the sheet, and snugly fit the material into the billet frame in the gap between the fuel matrix and the frame.[4]

The Eu_2O_3-stainless steel dispersion was easily and simply prepared by dry-blending for 3 hr in an oblique blender. After blending, the dispersion was cold-pressed at a pressure of 33 tsi. The compact was sintered at 1230°C for 1 1/4 hr, and finally coined at a pressure of 33 tsi to a densification of 87%. Procedures already established for rolling APPR-1 fuel plates were utilized in the fabrication of the plate, except that the plate was rolled in only one direction. No difficulties were encountered during processing.

A radiograph of a finished control rod fuel plate is shown in Fig. 1.9. The length of the Eu_2O_3-bearing section is approximately 7/8 in. As may be seen in Fig. 1.9, there was a slight tendency for the suppressor material to tail. The uniformity of the rare-earth dispersion in the finished plate is illustrated in Fig. 1.10. Measurements of this type of plate revealed that the cladding thickness above the rare-earth section was approximately 0.5 mil less than the cladding thickness above the fuel-bearing section of a fuel plate for a fuel element. More than 100 of these plates were produced for the core II control rods.

Modified Control Rod Bank. The desire to operate core II with a bank of five control rods instead of seven suggested increasing the boron concentration in the fuel plates from 0.11 wt % B to a nominal

[4] J. E. Cunningham et al., Specifications and Fabrication Procedures for APPR-1 Core II Stationary Fuel Elements, ORNL-2649 (Jan. 29, 1959).

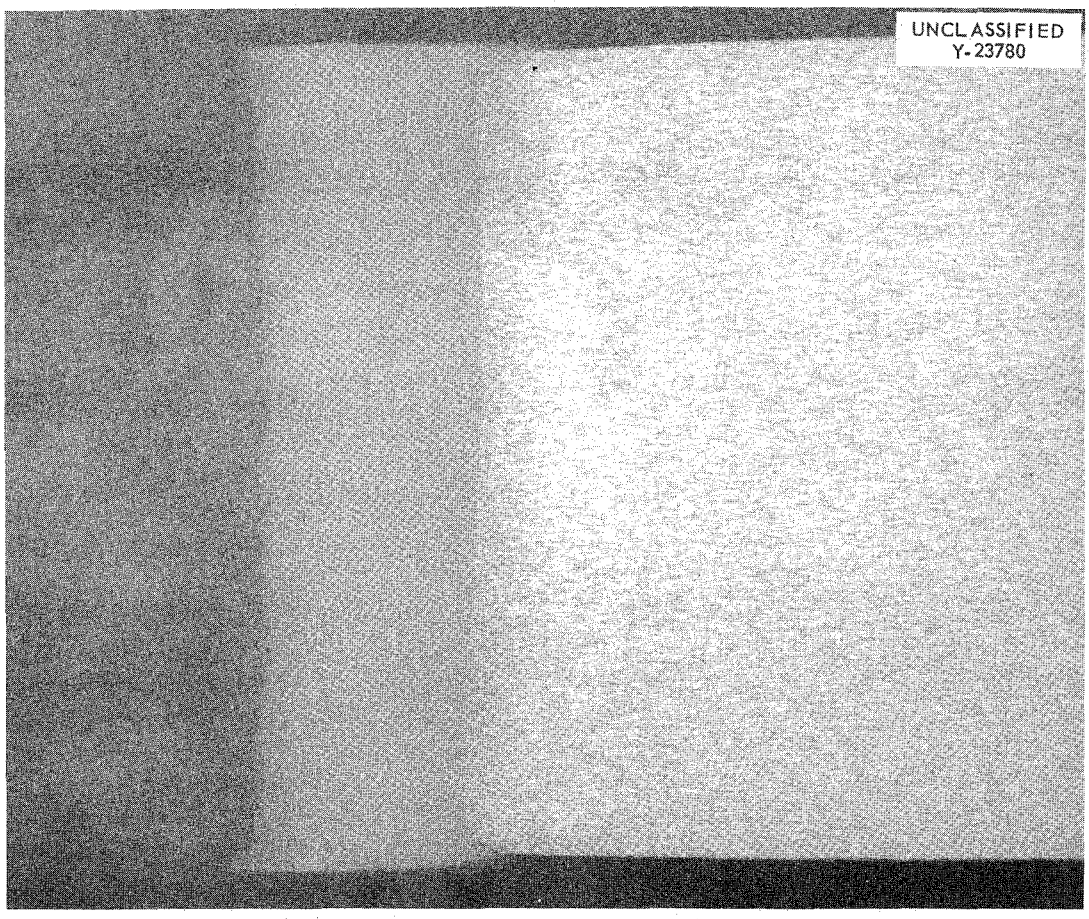

Fig. 1.9. Radiograph Showing Fuel and Eu_2O_3 Flux Suppressor Sections of a Completed Core II Control Rod Fuel Plate.

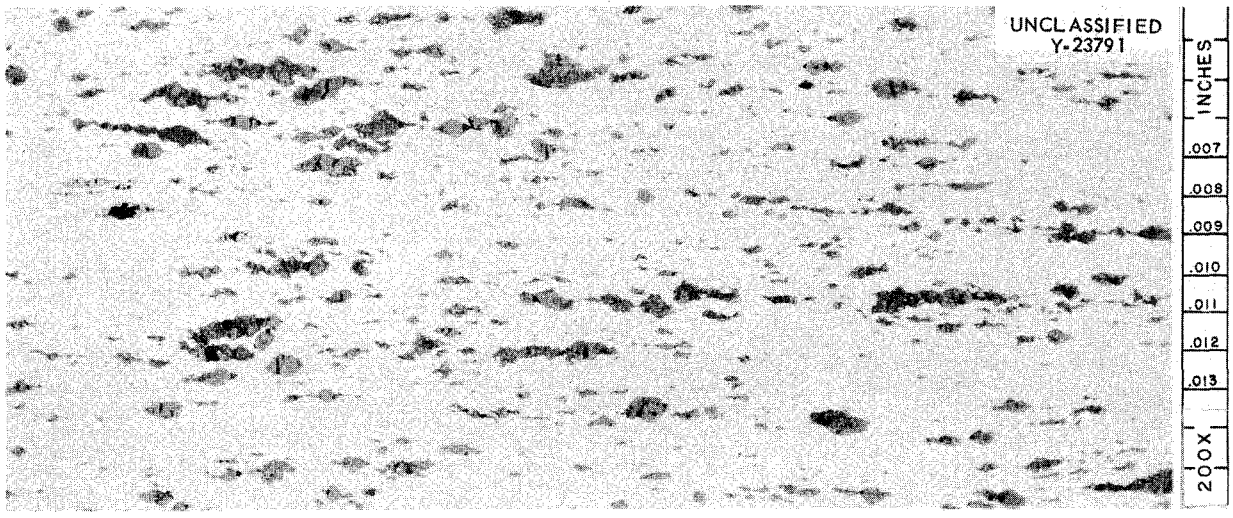

Fig. 1.10. Flux Suppressor Section of a Fabricated Control Rod Fuel Plate Showing Eu_2O_3 in Stainless Steel Matrix.

0.25 wt % B.[5] Potential reactions between stainless steel and boron of this concentration at established manufacturing temperatures stimulated investigations with the reference material, B_4C, as well as with ZrB_2 and BN. The objectives of the investigation were to determine the presence of reactions and to evaluate the extent of boron diffusion into the cladding. A master boron-stainless steel alloy containing 0.25 wt % boron, highly enriched in the B^{10} isotope, was also studied. The materials combinations and loadings used in the study are listed in Table 1.3. In all cases, the boron-containing addition was blended with the appropriate core matrix material, and the mixture was compacted, sintered, and coined. These cores were then clad with type 304L stainless steel and rolled according to standard APPR procedures. In some cases type 304B stainless steel was used in the cores rather than type 304LB, since type 304LB stainless steel was not available at the initiation of this program. Calculations were made to determine the amount of each compound required for core II boron loadings, and plates were fabricated containing the required amount of boron, a 25% excess, and a 25% deficiency. Originally, evaluation tests at 1100, 1150, and 1200°C were planned for each combination of materials in order to determine the effect of temperature on compatibility, but insufficient time prevented completion of tests at each temperature.

Plates of each combination were initially fabricated and tested at 1150°C, the temperature of primary interest. Metallographic samples were taken after rolling and after each of three thermal cycles. Each thermal cycle consisted of slowly heating the sample to the reference temperature, holding at that temperature for 1 hr, and furnace-cooling. In the plates to which boron was added as a compound, a globular, colorless, precipitated phase was found in the core after rolling and after thermal-cycling. The formation of the precipitated phase, which was thought to be a complex metallic boride, suggested that the boron-containing compounds were unstable.

---

[5] D. T. Bourgette, Minutes of Meeting Held at ORNL on May 1, 1958 Concerning Core II Loading for APPR-1, ORNL CF 58-9-65 (Sept. 9, 1958).

Table 1.3 Materials and Loadings Used in Investigation of Compatibility of Boron Compounds with Stainless Steel

Plate cladding: Type 304L stainless steel

Boron-Containing Material	Type of Stainless Steel Powder Used in Matrix	Quantity of Boron-Containing Material in Core (wt %)
ZrB_2	304B	1.128
	304B	1.499
	304B	1.867
BN	304B	0.498
	304B	0.655
	304B	0.805
	304LB	0.655
Master alloy (0.25 wt % B)	304LB	14.3
	304LB	19
	304LB	23.8
B_4C	304LB	0.288
	304LB	0.384
	304LB	0.481

The progress of a definite reaction in the ZrB_2 particles could be observed as the fabrication temperature was increased from 1100 to 1200°C. On the other hand, particles of B_4C could not be found in the stainless steel matrix after two cycles at 1150°C. Boron nitride was the most stable of the three compounds investigated, inasmuch as stringers, as well as the new phase, were present in the BN-containing cores even after three cycles at 1200°C. No positive signs of melting were observed in

any of the cores. In every case chromium carbide precipitates were found at the grain boundaries of the cladding after thermal cycling. An additional unidentified precipitate was present in the cladding adjacent to the core. The depth of penetration of the precipitated material, measured from the interface of core and cladding, increased with increases in the maximum temperature of the thermal cycle, and, in extreme cases, random particles reached the outer surface of the cladding. Preliminary attempts to identify this precipitate were unsuccessful. It is suspected that it is a boride similar to the compound precipitated within the core matrix. A sample of plate with cladding that was fairly rich in the precipitate was heated to 1150°C, held for 1 hr, and quenched in ice water. Metallographic examination showed that most of the precipitated material had dissolved. The significant effects observed in these experiments are illustrated in Figs. 1.11 through 1.14.

The boron-containing master alloy that was used in this investigation contained 0.25 wt % B in type 304LB stainless steel. In the preparation of the material, elemental boron powder 90% enriched in the B^{10} isotope was blended with carbonyl nickel powder, compacted, and sintered. The sintered compacts were then arc-melted under argon, crushed, sampled, and analyzed. The resulting nickel-boron powder then served as the additive to type 304LB stainless steel to produce the 0.25 wt % B^{10} alloy. The alloy was atomized to -100-mesh powder. This master alloy was then diluted with type 304LB powder to obtain the aforementioned experimental boron concentration; UO_2 was added; and the mixture was blended, compacted, and sintered. This method of adding boron to the control rod was found to be advantageous in that (1) the boron-stainless steel master alloy and type 304LB powders could be blended homogeneously, since their densities and particle sizes were nearly equal; (2) the amount of boron added to the core could be closely controlled because the quantity of master alloy required (~20 g) could be accurately weighed; and (3), since the master alloy is low in residuals, there was no contamination from impurities. In comparison, the reaction between stainless steel and the compounds B_4C, ZrB_2, and BN led to undesirable

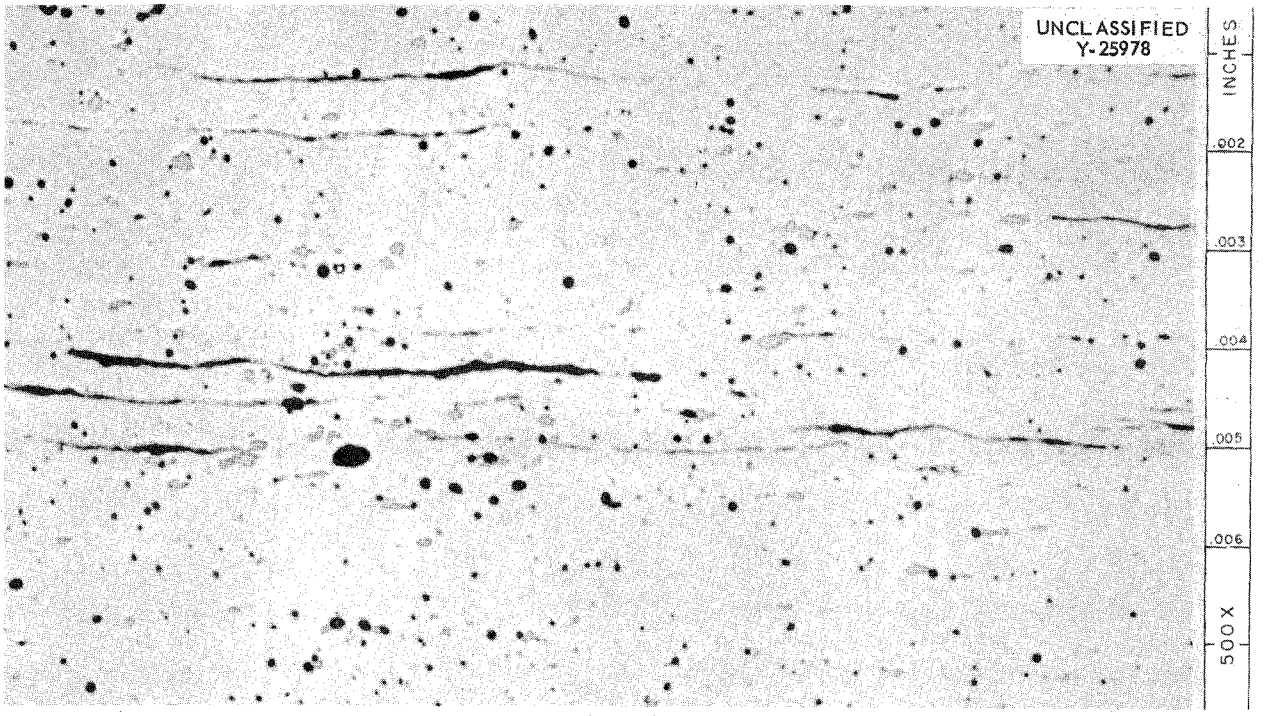

Fig. 1.11. Section of Experimental Plate Containing 0.65 wt % BN in Type 304LB Stainless Steel That Was Fabricated and Heat Treated for 1 hr at 1150°C. The stringering of the boron nitride that occurred during fabrication and the globular precipitate caused by the heat treatment may be seen.

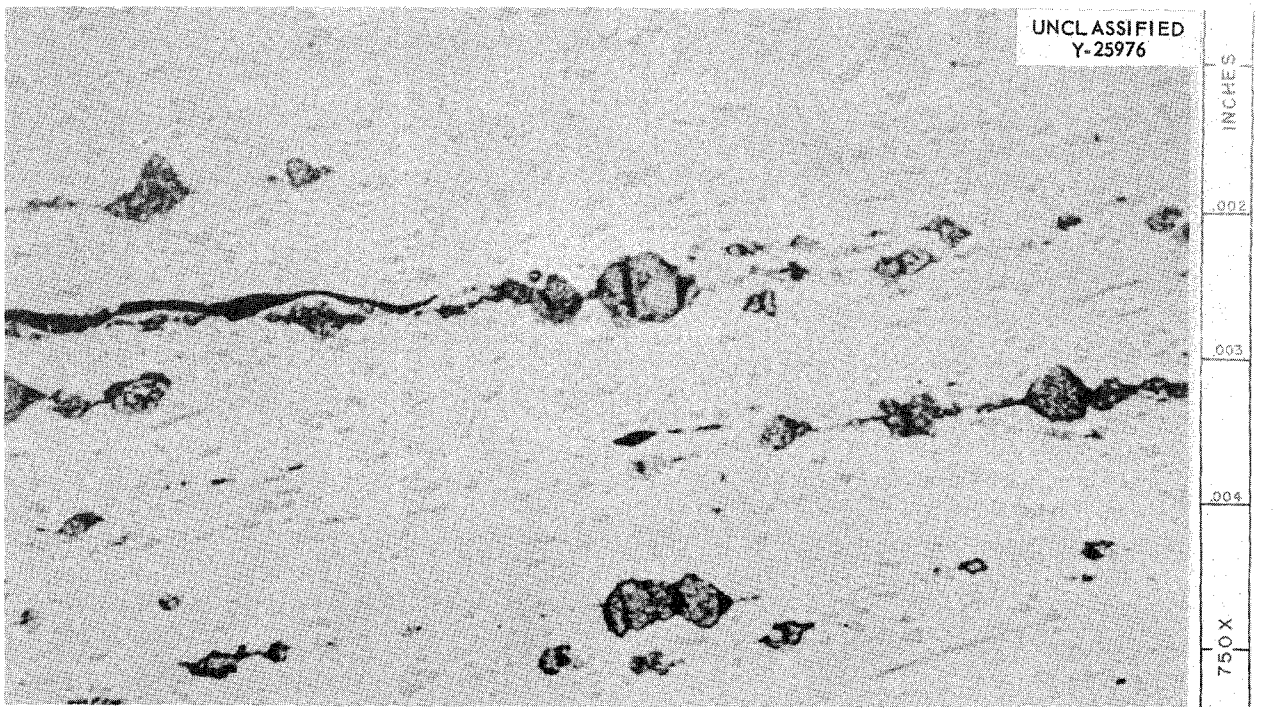

Fig. 1.12. Section of Experimental Plate Containing 1.5 wt % ZrB_2 in Type 304B Stainless Steel That Was Fabricated and Heat Treated at 1150°C. The effect of the reaction of the ZrB_2 with the stainless steel may be seen, as well as the globular precipitates caused by the heat treatment.

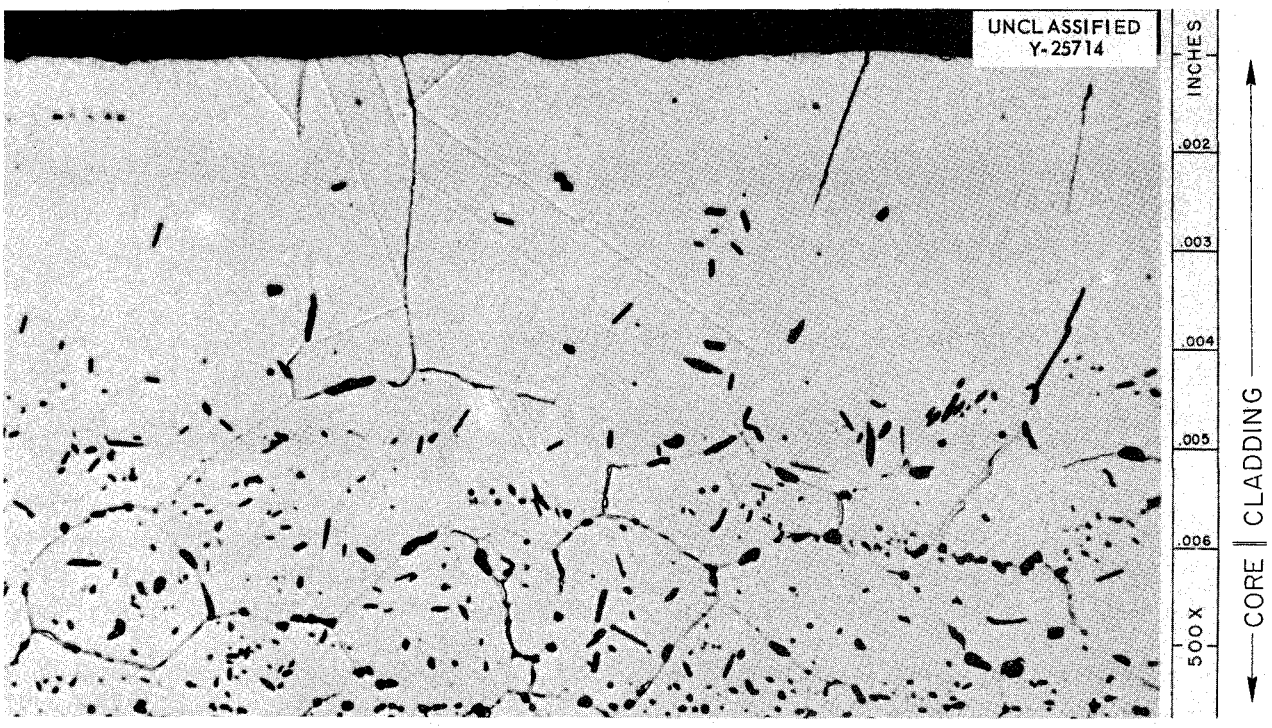

Fig. 1.13. Section of Experimental Plate Containing 0.5 wt % B_4C in Type 304LB Stainless Steel That Was Fabricated and Heat Treated 3 hr at 1150°C. The boride particles that diffused into the cladding during the heat treatment may be seen.

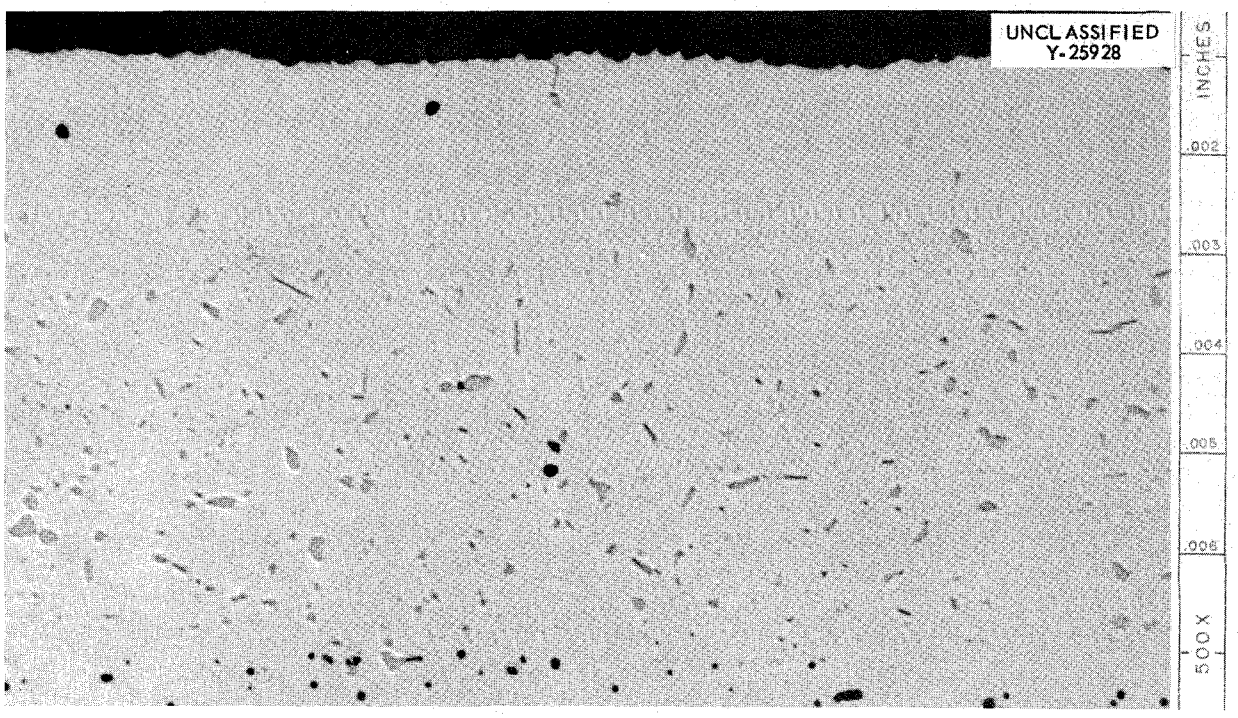

Fig. 1.14. Section of Experimental Plate Containing 0.65 wt % BN in Type 304B Stainless Steel That Was Fabricated and Heat Treated 3 hr at 1150°C. The boride particles that diffused into the cladding during the heat treatment may be seen.

contaminants in the core matrix and the cladding. Metallographic examination after fabrication and heat-treatment of plates containing the master alloy indicated carbide precipitates at grain boundaries of the cladding, but there were no boride particles at the interface of the core and cladding or in the cladding. Additional experiments revealed, however, that a significant loss of boron had occurred in these cores while sintering under hydrogen at 1150°C. Further work indicated that cores sintered in vacuum lost little, if any, boron. Data on the amount of boron lost during sintering in various atmospheres are presented in Table 1.4.

IRRADIATION TESTING OF APPR FUEL MATERIAL

The short time schedule for obtaining information on irradiation damage effects in the UO_2-stainless steel dispersion of the APPR fuel plates necessitated testing in the MTR at the prevailing temperature. The surface temperature of the plates during irradiation was estimated to be 200°F. No failures were observed in any of the irradiated specimens, even though the burnup of U^{235} atoms in some instances was as high as 57%.

The primary purpose of the phase I of the irradiation program was to determine the effects of irradiation upon the structural integrity and hardness of the fuel elements as a function of UO_2 particle size and burnup.[6] The data obtained (Table 1.5) confirmed, in general, the theory that damage to elements of this type during irradiation at relatively low temperatures can be reduced by increasing the particle size of the fissile material.

Phase II of the irradiation program consisted of the irradiation of a full-sized APPR type fuel element in the MTR.[7] The assembly

---

[6] F. H. Neill, Irradiation of Stainless Steel Fuel Element Samples in MTR - Irradiation Request ORNL-21, ORNL CF 55-4-153 (April 26, 1955).

[7] R. J. Beaver, Specifications for Stainless Steel MTR Irradiation Test Element, Irradiation Request ORNL-17, ORNL CF-55-6-31 (June 2, 1955).

Table 1.4. Boron Losses During Sintering of Stainless Steel Compacts Containing 0.04 wt % Boron That Were Prepared With the 0.26 wt % Boron Master Alloy

Sintering time: 75 min
Sintering temperature: 1150°C

Experiment No.	Matrix Material	Sintering Atmosphere	Boron Lost* (%)
1	Type 304LB stainless steel	H_2	40
2	Type 304LB stainless steel	H_2	24
3	Type 304LB stainless steel	H_2	57
4	Type 304LB stainless steel	H_2	39
5	Type 304LB stainless steel with low silicon content	H_2	50
6	Type 304LB stainless steel with low silicon content	H_2	25
7	Type 304LB stainless steel with low silicon content	Vacuum	4
8	Type 304LB stainless steel with low silicon content	He	8
9	Type 304LB stainless steel with low silicon content	Vacuum	5

*Value is average for three samples.

Table 1.5. Effect of UO_2 Particle Size on Irradiation-Induced Hardening of UO_2-Stainless Steel Fuel Elements

Core composition: 25.81 wt % UO_2 (5.84 at. % U)
0.35 wt % B_4C
73.84 wt % stainless steel

UO_2 Particle Size (μ)	Burnup (%)		Core Hardness (DPH)	
	U^{235}	Total Core Atoms*	Prior to Irradiation	After Irradiation
7-11	21.1	1.23	204	486
16-22	17.1	1	198	483
22-31	22	1.28	189	475
31-44	21.4	1.25	184	459
53-62	20.1	1.17	179	423
74-88	16.9	0.99	184	412
88-105	21.4	1.25	178	394

*Burnup of B^{10} from B_4C burnable poison neglected.

consisted of three types of fuel plates with core loadings of 18.75, 22.18, and 26.89 wt % UO_2, respectively. Postirradiation examination of the test element revealed no evidence of dimensional growth beyond fabricational tolerances or evidence of structural failure of core, cladding, or brazed joints. Hardness and burnup values for the three types of plates are shown in Table 1.6.

Further fuel element irradiations (phase III) were undertaken to determine the effect of the method of preparation of the uranium dioxide and the various degrees of cold-rolling during fabrication upon the resultant radiation damage of the fuel plate.[8] Unfortunately, wide

[8] R. C. Waugh, Preliminary Specifications for APPR Phase III MTR Irradiation Experiment, ORNL CF 55-10-111 (Oct. 21, 1955).

Table 1.6. Effect of UO_2 Quantity on Irradiation-Induced Hardening of UO_2-Stainless Steel Fuel Elements

Core composition of 15-Mwy plate: 18.75 wt % UO_2, 0.21 wt % B_4C, 81.04 wt % type 304B stainless steel

Core composition of 22.5-Mwy plate: 22.18 wt % UO_2, 0.27 wt % B_4C, 77.55 wt % type 304B stainless steel

Core composition of 30-Mwy plate: 26.89 wt % UO_2, 0.39 wt % B_4C, 72.72 wt % type 304B stainless steel

Core Lifetime (Mwy)[a]	Irradiation Position of Specimen[b]	Burnup (%)		Cladding Hardness (DPH)		Core Hardness (DPH)	
		U^{235}	Total Core Atoms[c]	Prior to Irradiation	After Irradiation	Prior to Irradiation	After Irradiation
15	High-flux region	15.6	0.65	119	195	172	369
	Low-flux region	5.4	0.22	119	166	172	307
22.5	High-flux region	18.2	0.89	138	197	168	398
	Low-flux region	6.5	0.32	138	178	168	340
30	High-flux region	12.4	0.76	137	184	169	370
	Low-flux region	5.9	0.36	137	190	169	313

[a]The abbreviation Mwy refers to megawatt-years.

[b]Specimens were taken from both the high-flux and the low-flux regions of each plate.

[c]Burnup of B^{10} from B_4C burnable poison neglected.

variations in burnup during irradiation prevented close comparison between the different types of specimen. Post-irradiation hardness values indicated that dispersions fabricated with UO_2 prepared by steam oxidation of metal chips or by reduction of uranium trioxide were superior to those fabricated with UO_2 prepared from the reduction of burned chips or precipitated by hydrogen peroxide. The latter two oxide types were more susceptible, however, to fragmentation during fabrication, as shown in Fig. 1.15, and the irradiation results were probably an effect of the as-fabricated UO_2 particle size. No evidences of structural failure or dimensional growth were noted in the specimens, even after burnup of more than 50% of the U^{235} atoms (2% of total core atoms). Slight changes in the structure of the UO_2 particles that were fragmented during fabrication indicated that the fragments sintered early in the irradiation period. At a burnup of approximately 10% of the U^{235} atoms, the UO_2 particles were fully sintered and relatively dense, as shown in Fig. 1.16. At higher burnups, small pores appeared in the UO_2, as shown in Figs. 1.17 and 1.18, with the degree to which they occurred apparently being proportional to the amount of burnup.

Sections of specimens from phase I and phase III irradiations were subjected to postirradiation annealing. The specimens from phase I irradiations showed additional increases in core hardness upon annealing at temperatures up to 400°C, with the amount of the hardness increase being a function of the UO_2 particle size. Specimens from phase I irradiations to burnups of approximately 20% of the U^{235} atoms also showed evidence of structural failure of the core and blistering when annealed for 24 hr at 600°C under a pressure of 1 atm. Structural failure of the core and blistering were also noted, as shown in Fig. 1.19, in specimens from phase III irradiations to burnups of over 40% of the U^{235} atoms when annealed for 24 hr at 315°C under a pressure of 1 atm. Since previous work with fuel elements of a similar type failed to reveal evidences of structural failure even though the specimens were irradiated at estimated surface temperatures up to 600°C and to burnups of 30% of the U^{235} atoms, the validity of attempting to extrapolate failure produced by postirradiation annealing to failures occuring during irradiations at temperature is doubtful.

Fig. 1.15. As-Fabricated UO_2–Stainless Steel Fuel Element. 250X.

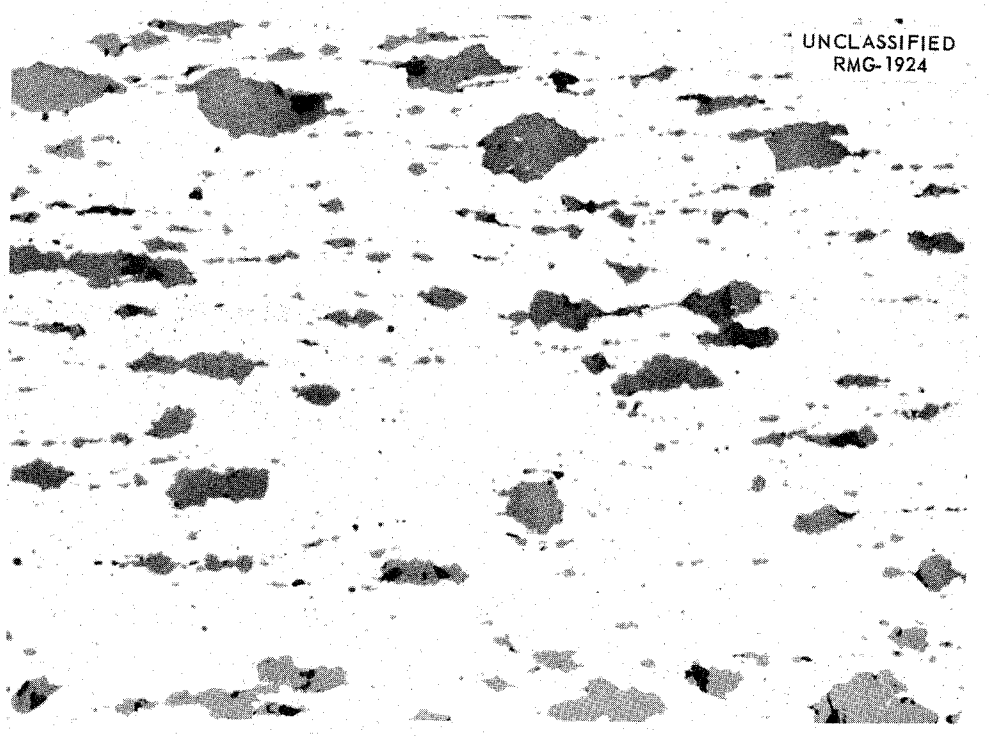

Fig. 1.16. A UO_2–Stainless Steel Fuel Element After 10% Burnup of the U^{235} Atoms. 250X.

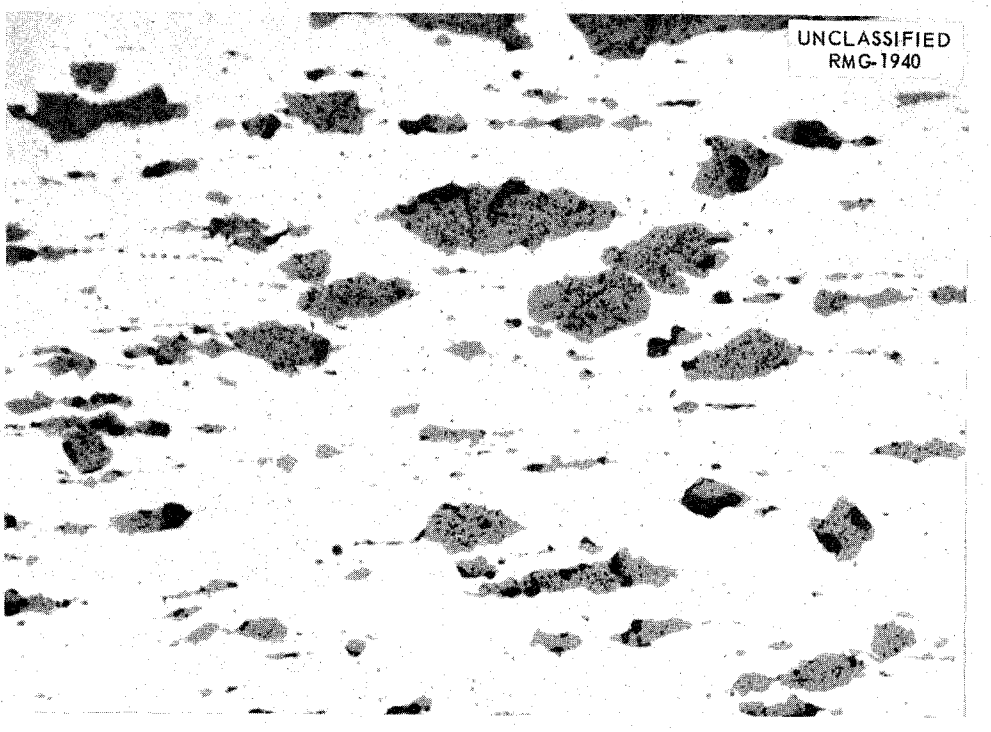

Fig. 1.17. A UO_2–Stainless Steel Fuel Element After 30% Burnup of the U^{235} Atoms. 250X.

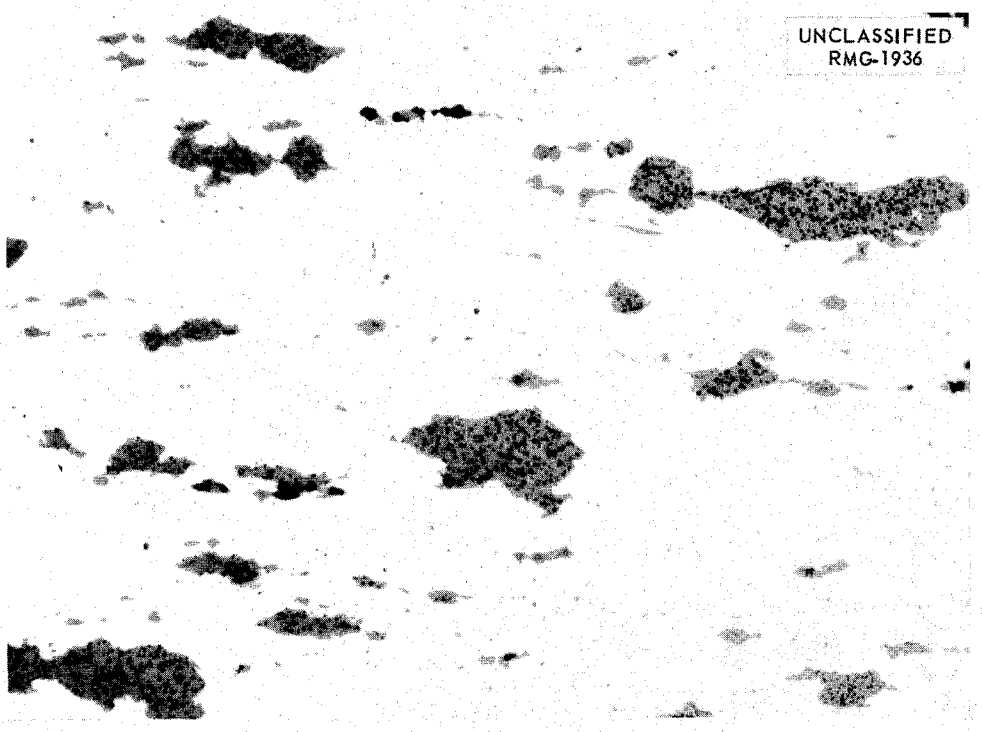

Fig. 1.18. A UO_2–Stainless Steel Fuel Element After 50% Burnup of the U^{235} Atoms. 250X.

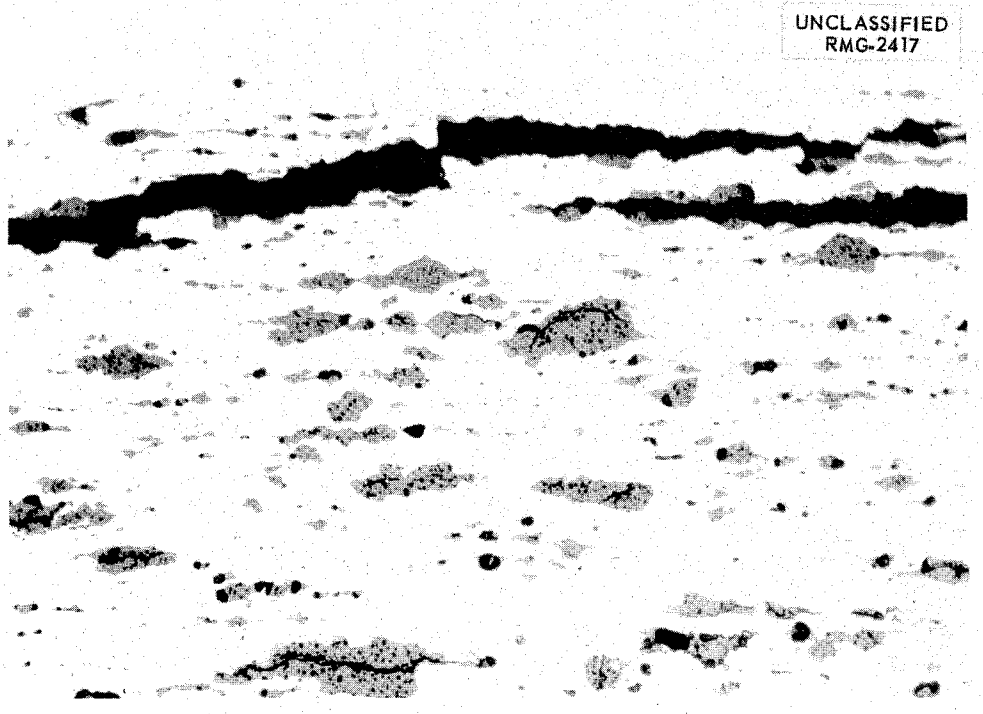

Fig. 1.19. A UO_2–Stainless Steel Fuel Element After 50% Burnup of the U^{235} Atoms and Postirradiation Annealing for 24 hr at 315°C. 250X.

CONTROL ROD DEVELOPMENT FOR THE APPR-1

Fabrication Procedures. The absorber section of the control rod assembly presently being used in the APPR-1 consists of a type 304 stainless steel-clad dispersion of 2.86 wt % B^{10} in electrolytic iron. At the time this material combination was selected, it appeared to be an expedient alternative for hafnium, which was not readily available, and for high-boron-content stainless steels, which are difficult to fabricate, are prone to serious irradiation damage, and, at that time, had questionable corrosion resistance in pressurized water at 500°F.

Procedures were developed which led to consistent and reliable methods for powder-metallurgical processing of the boron-iron dispersion and fabrication of roll-bonded composite plates.[9] The elemental powder material (electrolytic iron) and enriched crystalline boron, both of -100 mesh particle size, were individually weighed for each compact to assure accurate accounting for the boron. The weighed powders were blended in an oblique blender for 2 hr to provide uniform mixing prior to being cold-pressed in a double action powder-metallurgy die at a pressure of 31 tsi. To improve the density of the compact, the pressed cores were sintered in dry hydrogen at 1120°C and coined to final size at a pressure of 31 tsi. The density of the sintered and coined compact was 88% of theoretical. Data obtained by x-ray diffraction of the sintered material revealed that the elemental boron had combined with the iron in a solid-state reaction to yield the iron borides Fe_2B and FeB. Thus, the final product was actually a dispersion of iron borides in α-iron.

The core compacts were clad with wrought stainless steel and roll-bonded into plate. Standard "picture-frame" procedures were utilized in which three of the boron-iron compacts were stacked on each other

---

[9] C. F. Leitten, R. J. Beaver, and A. E. Richt, Stainless Steel-Clad Dispersion of Boron in Iron for Pressurized-Water Reactors, American Nuclear Society Programs, p 74 (June 2, 1958).

in a machined stainless steel frame that was previously provided with an evacuation tube. Cover plates were welded to each side of the frame. The billets were then inspected for leaks, evacuated, and sealed. The billet was heated before rolling in a semiprotective hydrogen atmosphere at a temperature of 1100°C for 90 min, and sound metallurgical bonding was achieved with a reduction per pass of 10% and a total reduction in thickness of 90%. In order to eliminate adverse core end effects, it was necessary to employ a single rolling direction.

A transverse section of the fabricated composite is shown in Fig. 1.20. As may be seen, there is some porosity in the iron-base dispersion. A transverse section near the edge of the core is shown at a higher magnification in Fig. 1.21. The boron diffusion which occurred during rolling is apparent. The easily observable grain growth across the interface between the cladding and the frame demonstrates the sound metallurgical bonding of the stainless steel cladding to the frame. Plates with these characteristics were perfectly sound after thermally cycling 50 times between 540°C and an ice-water quench.

The absorber section was assembled by edge-welding together four uniformly dimensional boron-bearing plates to form a rectangular parallelpiped 26 in. in length and 2.6 in.^{2} in cross section, as shown in Fig. 1.22. The individual absorber plates were clad with 0.033-in.-thick stainless steel and contained a core which was 20 3/4 in. long, 2.4 in. wide, and 0.90 in. thick.

The mechanical properties of the fabricated boron-iron dispersion are listed in Table 1.7. Between room temperature and 540°C the material has high strength but low ductility.

Irradiation Tests of Boron-Iron Compacts. The chief concern in the use of the boron-iron material is its potential susceptibility to irradiation damage because of the boron (n,α) reaction which yields lithium and helium gas. For irradiation testing, miniature absorber-section plates containing 1.7, 2.8, and 3.5 wt % B^{10} in iron were assembled in aluminum jackets. The specimens were irradiated in the

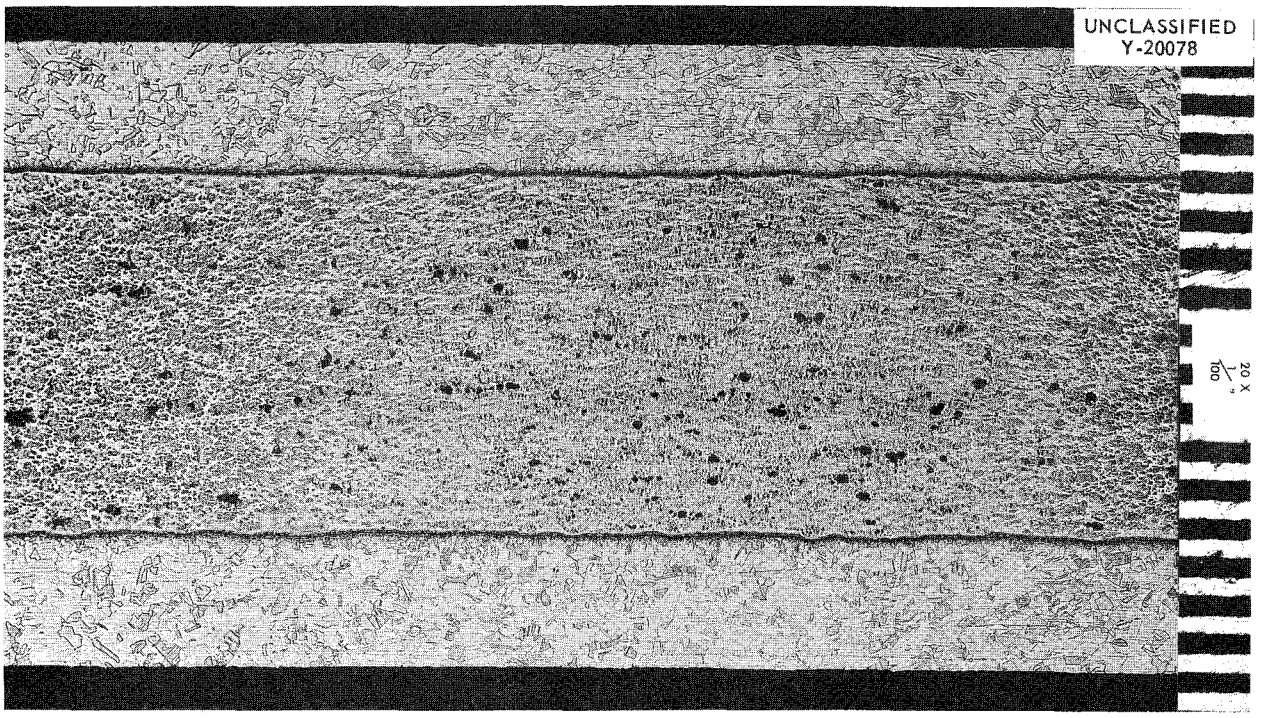

Fig. 1.20. Cross Section of a 3 wt % Boron Dispersion in Iron with a Cladding of Type 304L Stainless Steel After Rolling at 1100°C to a Total Reduction in Thickness of 90%.

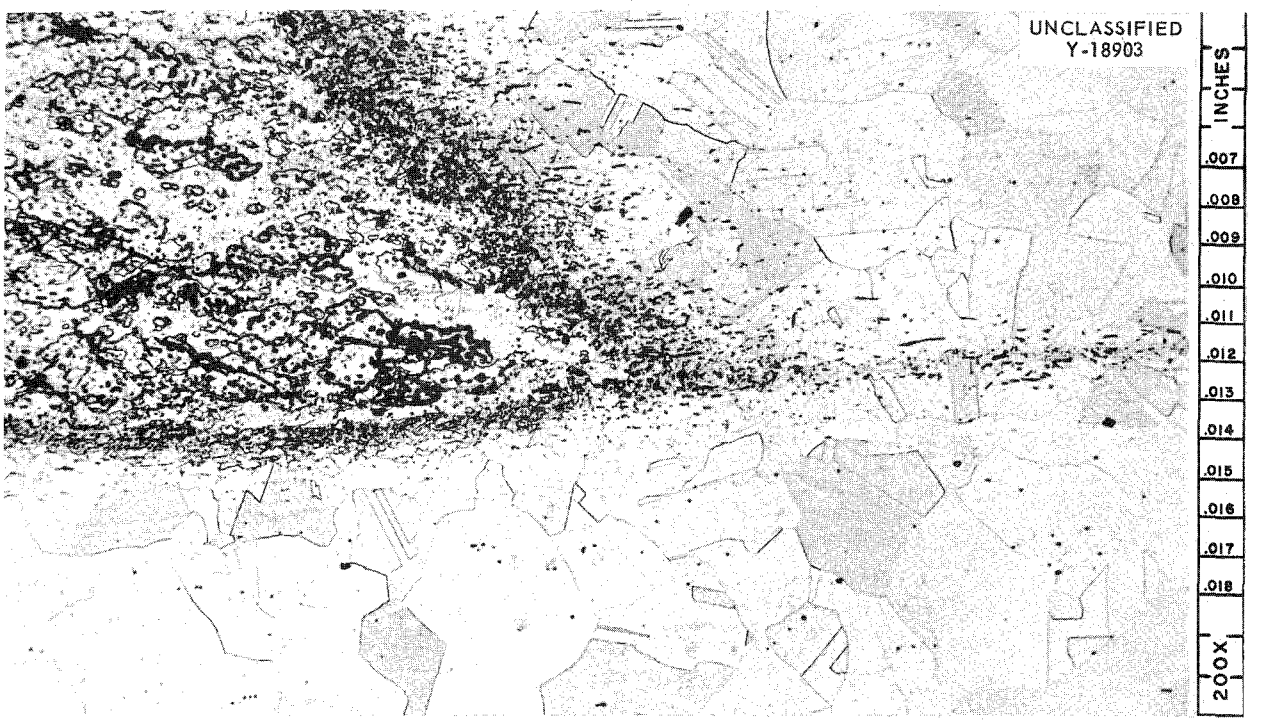

Fig. 1.21. Core-Frame-Cladding Interface of a 3 wt % Boron-Iron Dispersion Roll Clad with Stainless Steel at 1100°C. Cathodic etch.

Table 1.7. Mechanical Properties of Fabricated Boron-Iron Dispersion Compacts Containing 3 wt % Boron

Temperature (°C)	Yield Strength, 0.2% Offset (psi)	Tensile Strength (psi)	Elongation (%)
Room	40,500	42,600	0.5
150	40,000	41,100	0.5
260	39,700	40,000	0.5
400	34,500	39,300	3
540	21,500	28,200	5
980	3,850	5,050	16

beryllium reflector of the MTR to varying degrees of B^{10} burnup.[10] The miniature test plate is illustrated in Fig. 1.23.

The samples were examined after irradiation for dimensional stability and microstructural changes as a function of the burnup of the B^{10} atoms. Since the irradiation temperature was only about 66°C, the irradiated composites were heat treated in air for 312 hr at 260 or 315°C to more closely simulate APPR-1 temperature conditions. The results of the post-irradiation examinations are presented in Table 1.8. The only dimensional change observed was in the thickness. No dimensional changes were noted after heat treatment for 312 hr at 315°C of the specimens irradiated to a burnup of 4 at. % B^{10}. A 2.6% increase in thickness was noted after irradiation of specimens to 11.5 at. % burnup, which increased to 11.5% followed by cladding separation and bulging during the heat treatment at 315°C. Similar but increased damage was found for the specimens irradiated

[10] C. F. Leitten, Phase II Absorber Rod Sample Irradiation – Irradiation Request ORNL-MTR-28, ORNL CF 56-9-118 (Sept. 27, 1956).

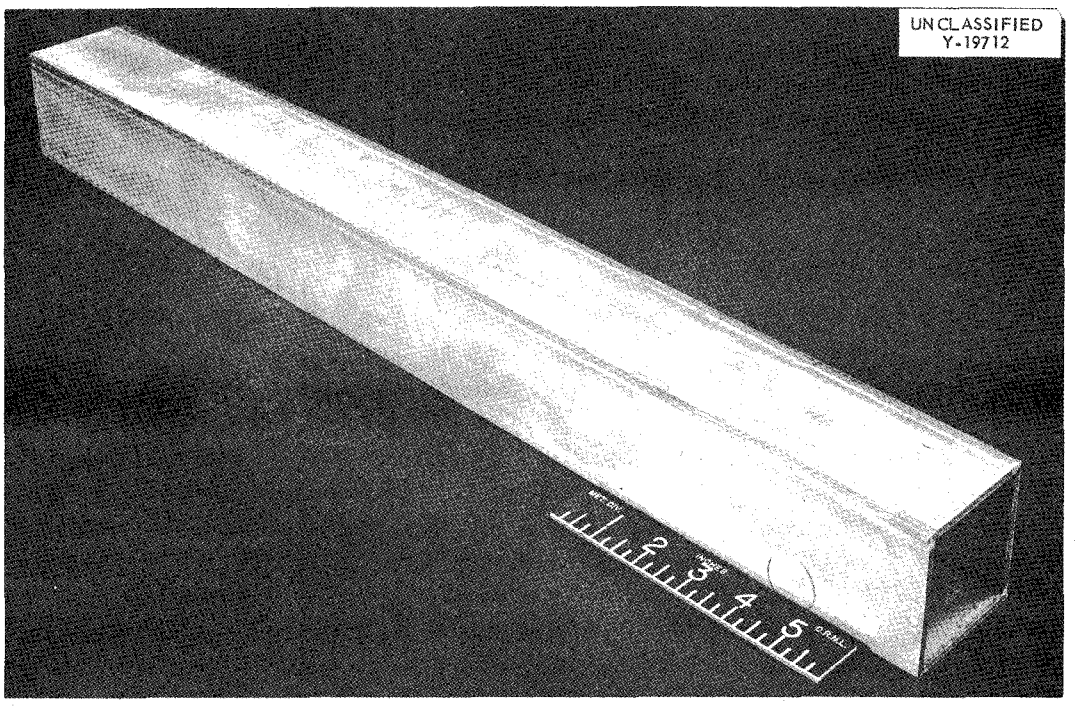

Fig. 1.22. Completed Absorber Section of an APPR-1 Control Assembly.

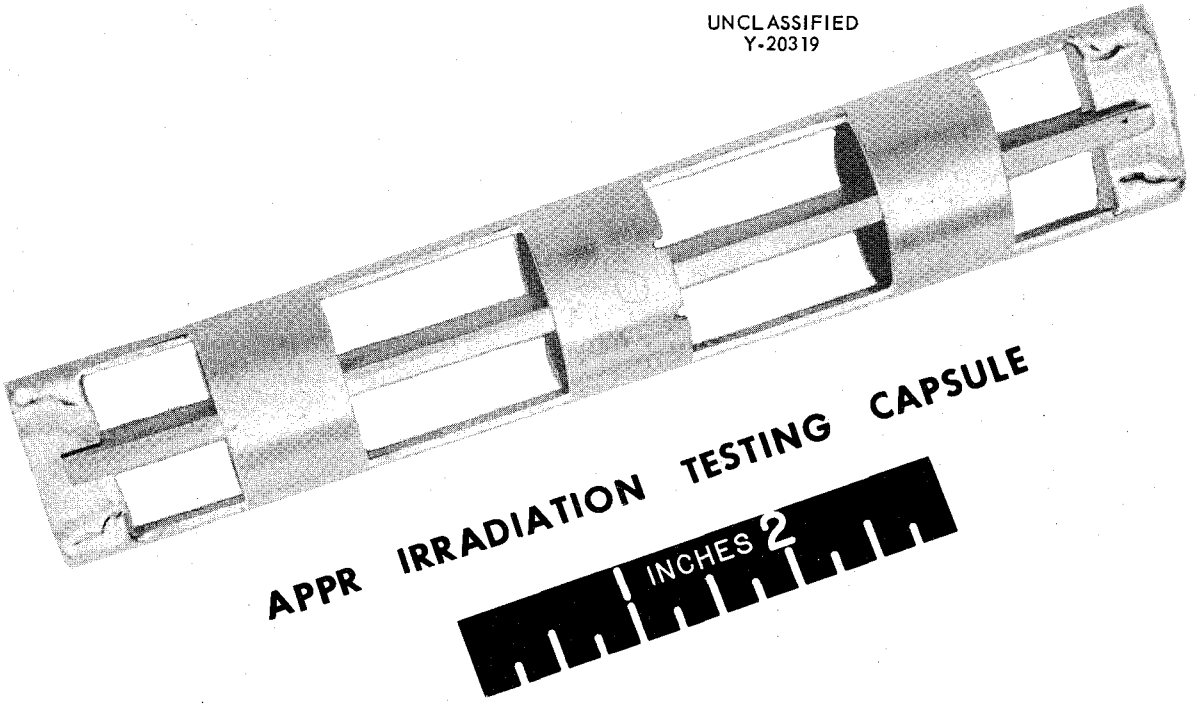

Fig. 1.23. Assembled Test Capsule for Irradiation of Miniature Absorber Samples.

Table 1.8. Effects of Irradiation on Stainless Steel-Clad Plates Containing a Dispersion of Enriched Boron in Iron

Sample No.	Boron Concentration (wt % B^{10})	Burnup* (% of B^{10} atoms)	Thickness Increase (%)**		Heat-Treatment Temperature (°C)
			After MTR Irradiation at 66°C	After 312-hr Heat Treatment	
6	2.81	4	0	0	315
7	2.81	11.5	2.6	10.9	315
8	2.81	17.6	4.5	21.2	315
1	2.81	32.9	34	72.4	315
5	2.81	37	30.1		
60A	1.67	9.3	1.3	3.2	260
60B	1.67	14.7	2.6	7.7	260
120A	3.50	8.9	10.3	18.6	260
120B	3.50	3.4	1.9	3.8	260

*Burnup based on lithium analysis.

**Nominal cladding thickness, 0.033 in.; nominal core thickness, 0.090 in.; sample dimensions, 6 1/2 x 1 x 0.156 in.

to a burnup of 17.5 at. % B^{10}, which approaches the maximum burnup expected in the APPR-1. After irradiation to a burnup of 33 at. % B^{10}, failure of the bond between core and cladding occurred in the reactor. There were also indications that slight increases in the B^{10} concentration would increase the irradiation damage effects. For example, in sample 120A, which contained 3.5 wt % B^{10}, significant damage apparently occurred in the reactor after 8.9% burnup, whereas the 1.7 and 2.8 wt % boron dispersions showed much smaller changes under similar circumstances. This effect is believed to be due to the additional neutron absorption and subsequent damage near the bonded region because of the higher concentration of boron atoms. The dimensional changes are attributed to the helium generated by the boron (n,α) reaction. Helium was identified as a product of irradiation by analyzing the gas extracted from the samples with the highest burnup of B^{10} atoms.

The bonded interface of the composite that was irradiated to a burnup of 4 at. % B^{10} and treated for 312 hr at 315°C is shown in Fig. 1.24; no separation can be observed at the interface. The depth of burnup can be seen as a function of the shading caused by the etchant. It is significant that the highest burnup occurs adjacent to the bonded interface. Separation typical of that which occurred in the composite subjected to a burnup of 11.5 at. % and heat treated for 312 hr at 315°C is shown in Fig. 1.25. The separation gap is 0.005 in. The brittle nature of the irradiated material is indicated by the cracks in the boron-iron dispersion adjacent to the separation gap. The core material adjacent to the separation gap is shown at a higher magnification in Fig. 1.26; microcracks are visible in the grain boundaries between the heavily damaged boron particles. The core material at the center of the sample, shown in Fig. 1.27, was the same as for all other irradiated composites. It is apparent in comparing the microstructures in Figs. 1.26 and 1.27 that the self-shielding effect of the boron confined the burnup to the layer of material adjacent to the interface.

The irradiation results indicate that a composite containing 2.8 wt % B dispersed in iron can withstand 4 at. % B^{10} burnup without cladding

UNCLASSIFIED
PHOTO 46148

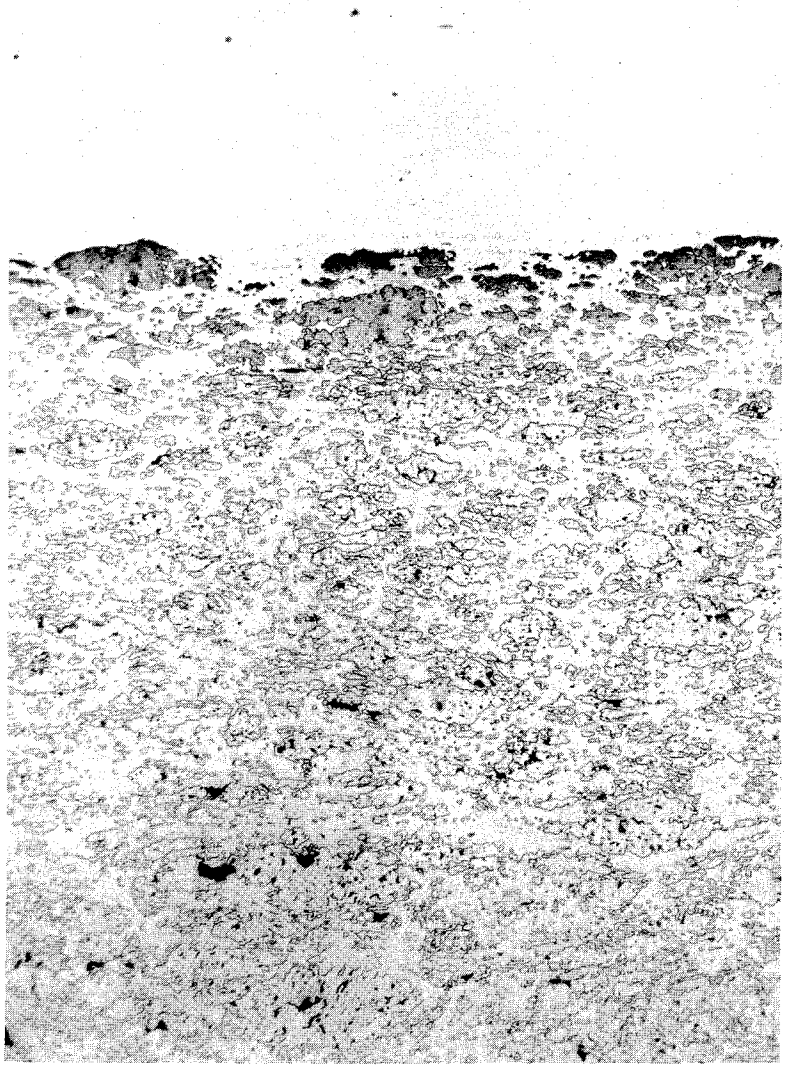

Fig. 1.24. Interface of Core and Cladding in Specimen Irradiated to a Burnup of 4 at. % B^{10} Heat Treated for 312 hr at 600°F. Nital etch. 100X.

UNCLASSIFIED
PHOTO 46149

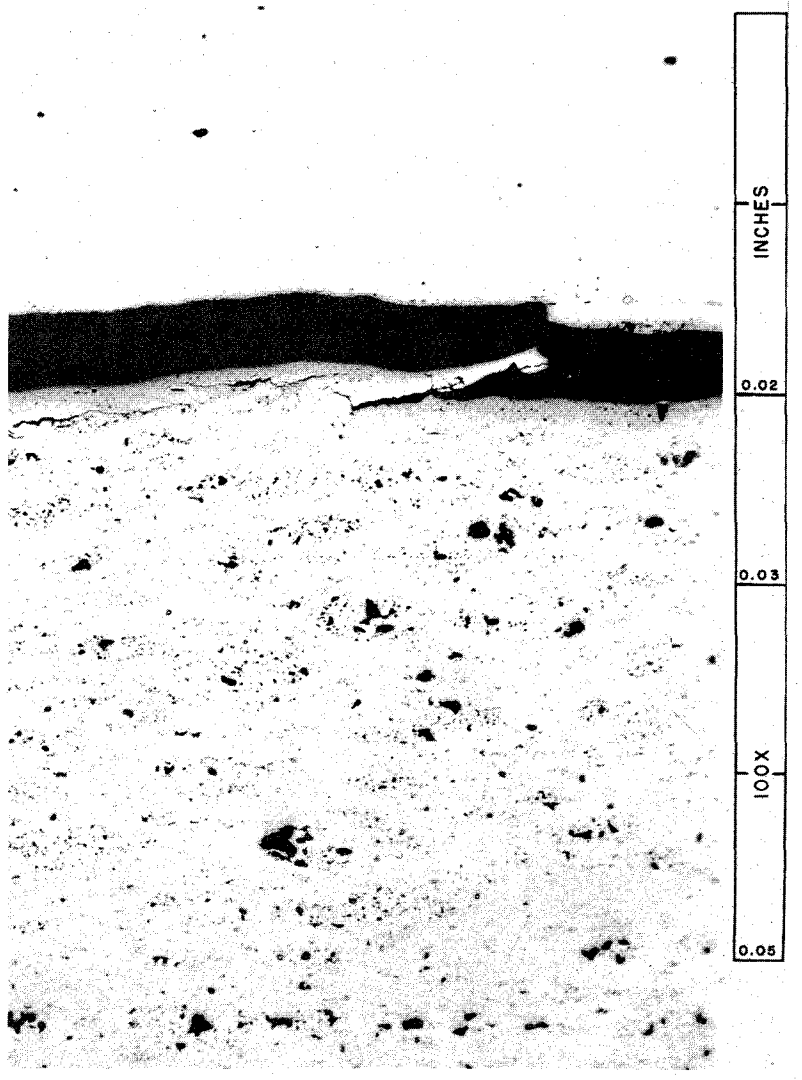

Fig. 1.25. Interface Between Core and Cladding of Specimen Irradiated to a Burnup of 11 at. % B^{10} and Heat Treated for 312 hr at 600°F.

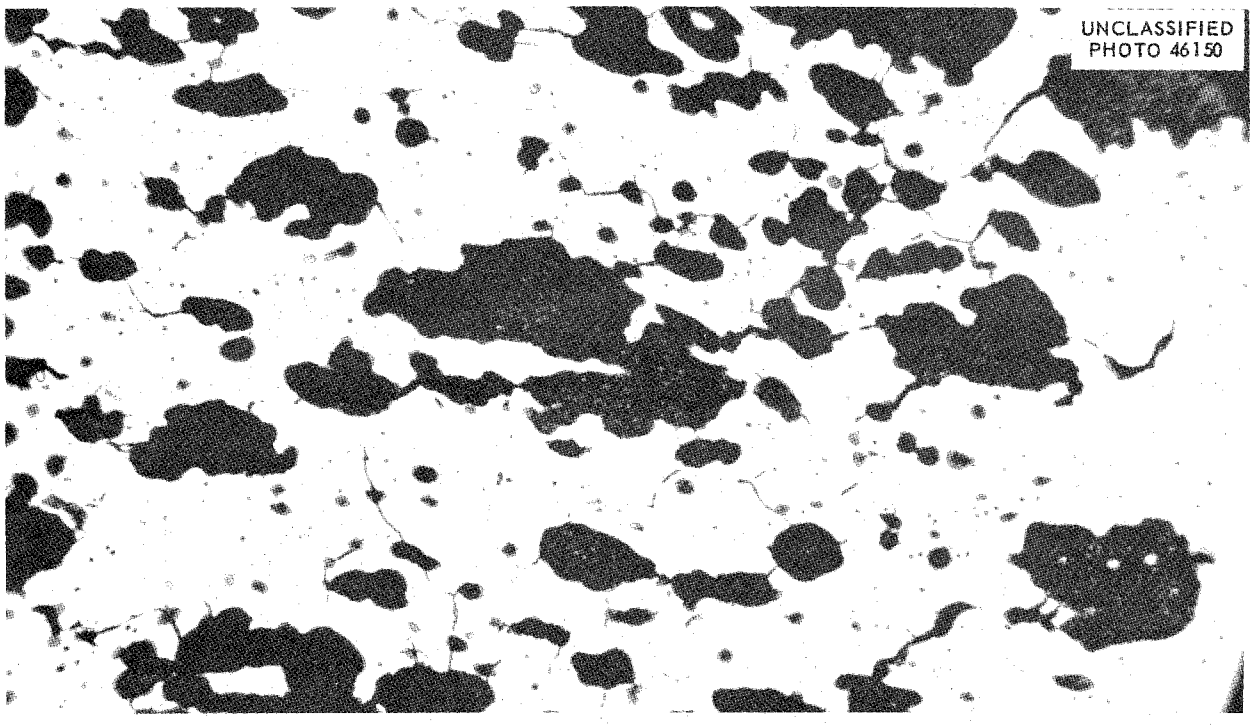

Fig. 1.26. Core Material Adjacent to Separation Gas Shown in Fig. 1.25 at a Higher Magnification. 500X.

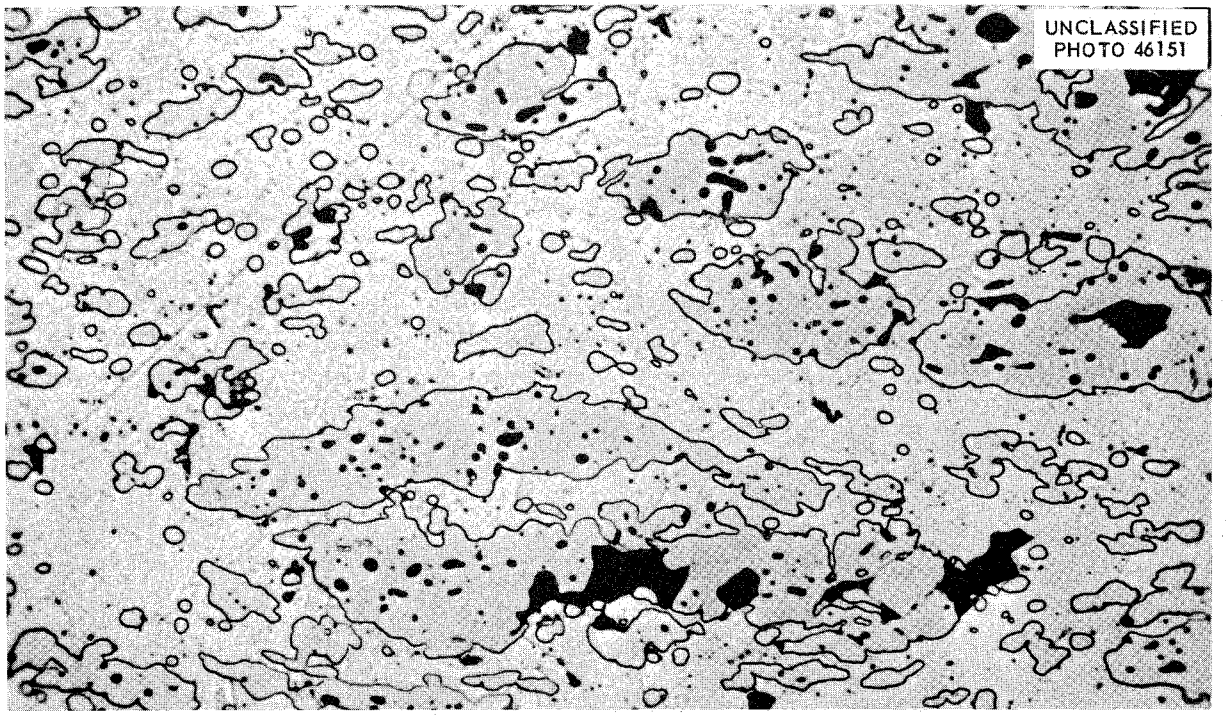

Fig. 1.27. Microstructure at Center of Core Shown in Fig. 1.25. 500X.

separation. On the other hand, swelling and deleterious blistering are likely to occur during irradiation at 150°F to a burnup of between 18 and 33 at. % B^{10}. It is felt that the postirradiation heat treatments at 260°C and 315°C under atmospheric pressure are too severe a test for a pressurized-water application, since the 1200-psi pressure in APPR-1 may well act as a restraint to the blistering observed in the heat-treatment tests. Additional tests are in progress to determine the damage effects at burnups of 5 to 25 at. % B^{10} as a function of pressure and temperature.[11]

A test on a full-size APPR absorber section which was substituted for an MTR control rod revealed no operational difficulty after five reactor cycles.[12] The estimated burnup at the top was 20 at. % B^{10}. Unfortunately, the tip of the absorber section was inadvertently destroyed by MTR operations personnel, and, although the results were favorable as a demonstration test at the burnup conditions anticipated in the APPR-1, destruction of the tip prevented pertinent post-irradiation evaluation. It is noteworthy to report that, after 11.5 Mwy of operation in core I of the APPR-1, the control rod containing the boron-iron absorber section is still functioning satisfactorily.

Core II Absorber Section. Because of the susceptibility of boron-bearing materials to irradiation damage, a backup program was initiated to develop an absorber section containing a rare-earth oxide. Since helium is not formed during neutron bombardment of rare-earth oxides, damage from the evolution and expansion of helium would be eliminated.

Europium was selected for this application on the basis of screening tests because its burnout characteristics most nearly suited the requirements of the APPR-1. It was proposed to incorporate 30 to 40 wt % Eu_2O_3 in type 304 stainless steel by powder-metallurgy

---

[11] C. F. Leitten, Phase III Absorber Rod Sample Irradiation, Irradiation Request ORNL-MTR-28, ORNL CF 57-7-19 (July 5, 1957).

[12] E. E. Gross and L. D. Schaffer, Interim Report of APPR Irradiation Test Program at MTR, ORNL CF 57-1-65 (Jan. 21, 1957).

techniques and to clad the dispersion with wrought type 304 stainless steel by roll-bonding.[13] Because of the high cost of Eu_2O_3, an inexpensive rare-earth oxide mixture of Sm_2O_3 and Gd_2O_3 (Lindsay oxide, Mix 921), which was believed to have chemical properties similar to those of Eu_2O_3, was selected as a substitute for Eu_2O_3 in the initial studies.

The various rare-earth oxides, as procured from the vendors, are of low density and extremely fine particle size. Since such conditions could lead to segregation, a series of experiments was undertaken in an effort to conglomerate the oxide to increase both the particle size and density. Small compacts were sintered in air and under hydrogen at various temperatures ranging from 1500 to 1900°C and times ranging from 1 to 5 hr. Upon completion of each test, the conglomerated oxide was crushed to a desired particle size and examined macroscopically. Compacts containing 30 to 45 wt % dispersions of Lindsay Mix 921 in stainless steel were then prepared by standard powder-metallurgy procedures. The dry powders were blended on an oblique blender for 2 hr, cold-pressed in a compacting die at a pressure of 33 tsi pressure, sintered under hydrogen at 1230°C for 1 1/4 hr, and coined at a pressure of 33 tsi. Variables such as initial oxide preparation method and particle size were investigated during preparation of the compacts. Billets were assembled by using the "picture-frame" technique, evacuated, and hot-rolled at 1150°C to a total reduction in thickness of 90% with a reduction in thickness per mill pass of 10%. Acceptable core end effects were achieved by employing a single rolling direction. Metallographic examination of the various plates indicated that severe stringering and fragmentation of the oxide occurred during hot-rolling when large oxide particles were used and when the oxide was conglomerated at temperatures below 1600°C. A longitudinal section from a plate containing 30 wt % Lindsay oxide prefired at 1500°C in air and crushed to -100 + 325 mesh particle size is shown in Fig. 1.28. Extensive stringering and fragmentation may

[13] D. T. Bourgette, Minutes of Meeting Held at ORNL On May 1 and 2, 1958 Concerning Core II Loading for APPR-1, ORNL CF 58-9-65 (Sept. 9, 1958).

be observed. A similar section of plate which contained oxide prefired at 1700°C under hydrogen and crushed to -325 mesh particle size is shown in Fig. 1.29. Very little fragmentation and stringering occurred. An over-all cross section of this plate is shown in Fig. 1.30. Thin bands of stainless steel foil may be observed between each of the three rare-earth compacts. It was found that the foil was necessary to ensure good bonding when small particles of oxide were used. A typical end effect obtained in hot-rolling the rare-earth oxide composites is illustrated in Fig. 1.31. The blunt end is a prerequisite and is quite similar to that found at the trailing end of the APPR-1 absorber plates containing compacts of boron in iron.

Upon completion of these fabrication experiments, a Eu_2O_3-stainless steel compact was prepared. The oxide was prefired at 1700°C under hydrogen and crushed to a -325 mesh particle size prior to being incorporated into -325 mesh type 304B stainless steel. During the sintering of this compact, a volume increase was observed, and the compact material became covered with a yellowish-green film. These events indicated that a reaction had occurred between the Eu_2O_3 and the stainless steel.

In subsequent compatibility tests of Eu_2O_3 with a number of the important elements of stainless steel, it was found that silicon was associated with the reaction. Small compacts containing 30 wt % Eu_2O_3 oxide which were sintered under hydrogen at various temperatures were used for this investigation. All compacts made with commercial, prealloyed type 304B stainless steel showed about a 7 vol % increase when sintered at temperatures from 1100 to 1230°C. Compacts containing matrices of Fe, Ni, and elemental stainless steel of low silicon content showed volume decreases characteristic of nonreactive compacts. Both the silicon-and the chromium-containing compacts exhibited significant volume increases. It was found that the chromium used contained 1.2 wt % Si, and the reaction was attributed primarily to the presence of the silicon. The data obtained in these tests are summarized in Table 1.9.

Electronmicroscopy confirmed the presence of a reaction product in compacts containing Eu_2O_3 and type 304B stainless steel which were

Fig. 1.28. Core of Composite Plate Containing 30 wt % Lindsay Oxide Mix Prefired at 1500°C and Crushed to −100 +325 Mesh Particle Size. Plate hot rolled at 1150°C.

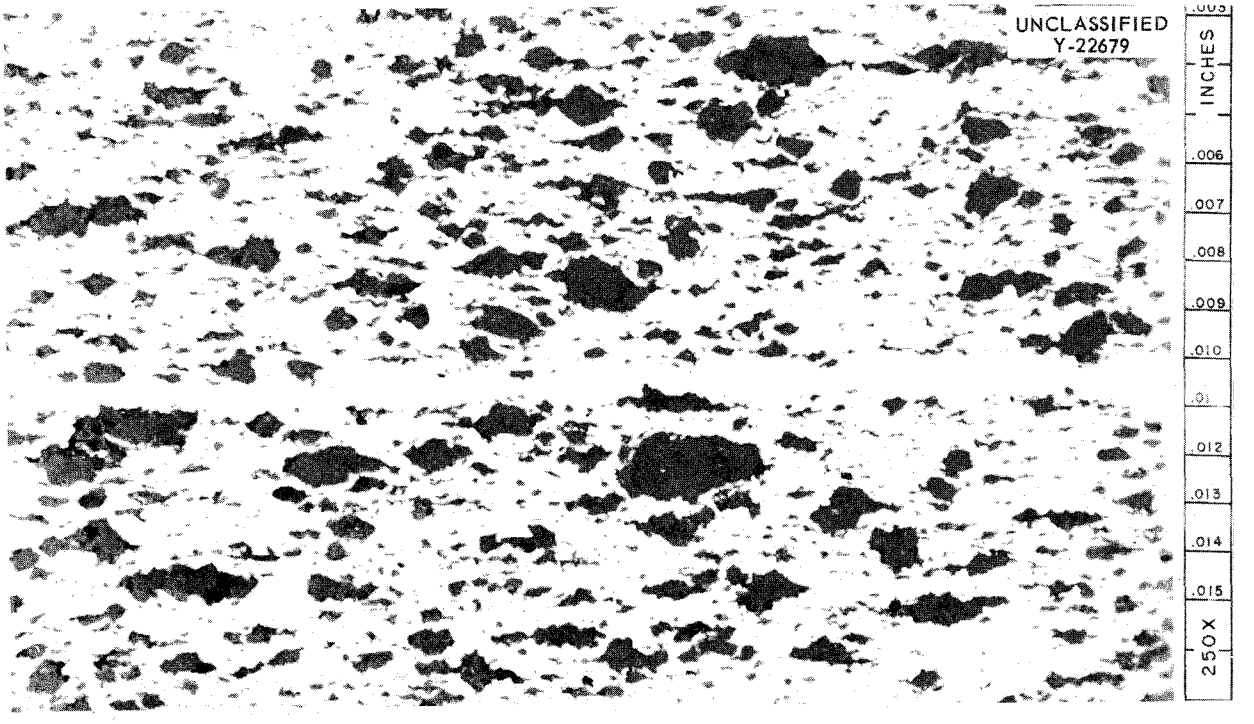

Fig. 1.29. Core of Composite Plate Containing 30 wt % Lindsay Oxide Mix Prefired at 1700°C and Crushed to −325 Mesh Particle Size. Plate hot rolled at 1150°C.

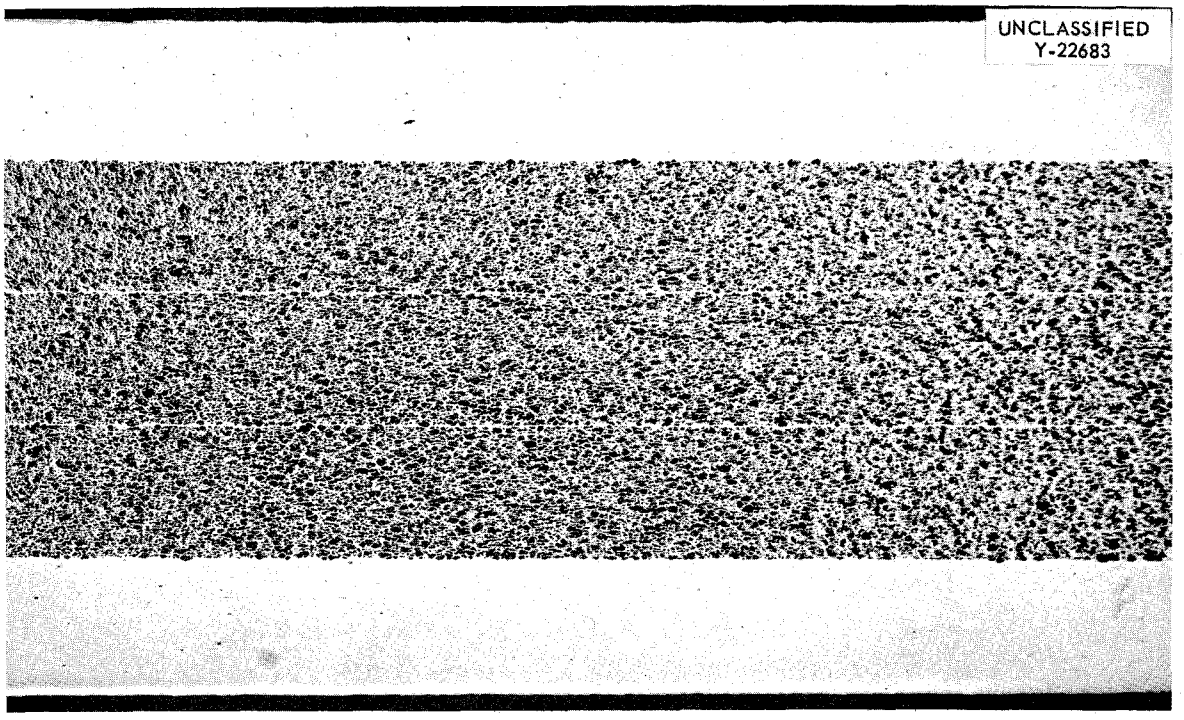

Fig. 1.30. Cross Section of a Composite Plate Containing 30 wt % Lindsay Oxide Prefired at 1700°C and Crushed to −325 Mesh Size. Plate hot rolled at 1150°C. 20X.

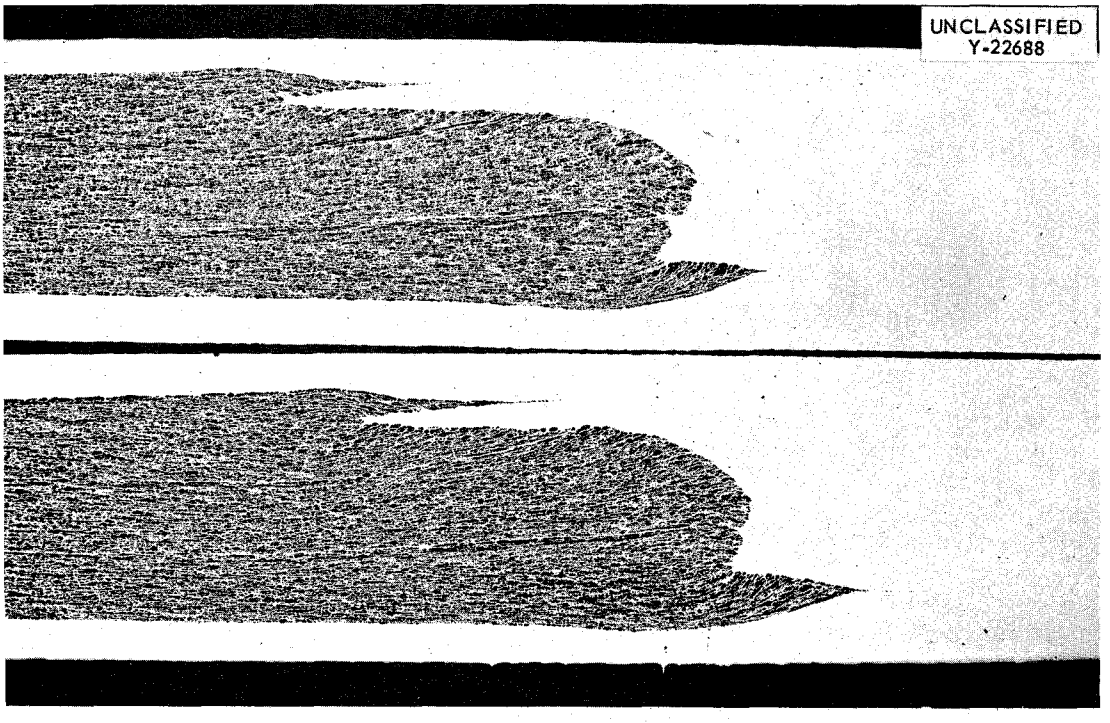

Fig. 1.31. Trailing End of Core Containing a Dispersion of 30 wt % Rare-Earth Oxide in Stainless Steel. Composite plate rolled at 1150°C to total reduction in thickness of 92% using single rolling direction.

Table 1.9. Results of Compatibility Studies of 30 wt % Dispersions of Eu_2O_3 in Stainless Steel and its Elements

Matrix Material	Sintering Temperature (°C)	Volume Change (%)
Type 304B stainless steel	1230	+7.7
Type 304B stainless steel	980	0
Iron	1150	-2.1
Nickel	1150	-1.5
Chromium	1150	+2.2
Silicon	1200	+6.2
Elemental powder*	1150	+1.3
Elemental powder**	1200	-4.4

*Composition: 74% Fe, 18% Cr, 8 % Ni

**Silicon content of Cr, <0.03%.

sintered in hydrogen at 1230°C. As illustrated in Fig. 1.32, a layer existed around the periphery of the stainless steel particles which was absent in the similarly treated Eu_2O_3-iron specimen shown in Fig. 1.33. The reaction product has not been identified because no x-ray diffraction standards exist for europium compounds. The compatibility tests indicate that materials which have a high silicon content (> 1%) are more reactive than materials of low silicon content (< 1%); materials with essentially no silicon content (< 0.03%) showed no reaction.

Because of difficulties inherent in the procurement of prealloyed stainless steel powder with a silicon content of less than 0.03 wt %, low-silicon-content iron, nickel, and chromium elemental powders corresponding in composition to that of type 304 stainless steel were selected as the matrix material. Although small (1/2-in.-dia) experimental compacts containing Eu_2O_3 in elemental powders were stable at the 1230°C

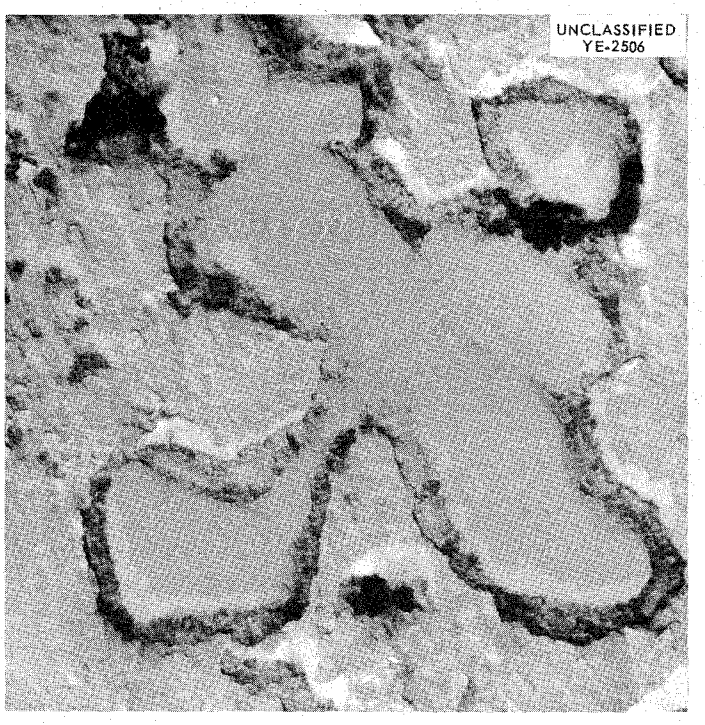

Fig. 1.32. Reaction Layer in a Compact Containing 30 wt % Eu_2O_3 and High-Silicon-Content Type 304 Stainless Steel Sintered at 1230°C Under Hydrogen. Formvar-Au-Manganin replication. 5600X. Reduced 20.5%.

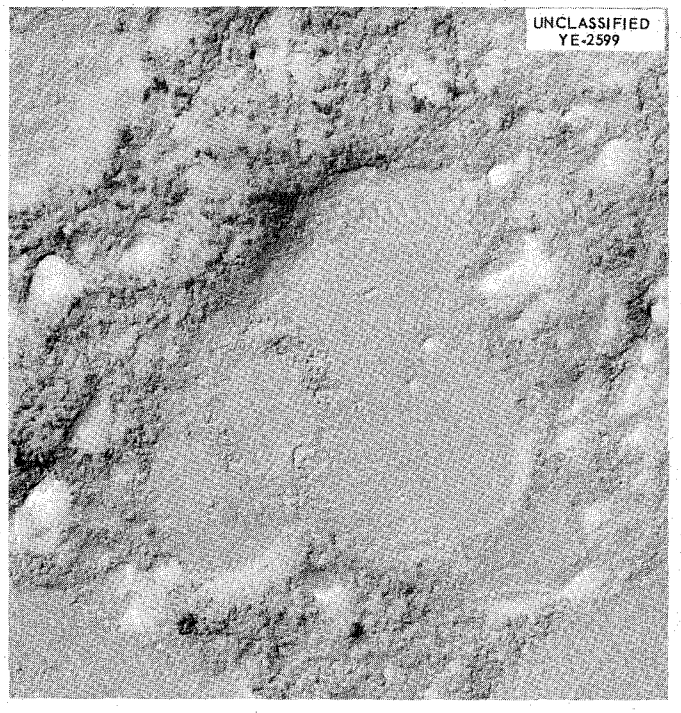

Fig. 1.33. Compact Containing 30 wt % Eu_2O_3 and Electrolytic Iron Sintered at 1230°C Under Hydrogen. Formvar-Au-Manganin replication. 8200X. Reduced 22%.

sintering temperature, significant volume increases occurred while sintering the 2 x 2.25 x 0.3-in. compacts required for full-scale composite plates. This condition prevented coining of the sintered compacts. The difficulty was attributed to the expansion of entrapped gases during sintering. Experimentation revealed that cold-compacting under a light pressure, followed by sintering, repressing, resintering, and coining, resulted in acceptable compacts. The process developed for preparing compacts containing up to 45 wt % Eu_2O_3 in the elemental powders of stainless steel consisted of the following:

1. cold-pressing of the blended powders at a pressure of 9.4 tsi,
2. sintering under hydrogen for 1 1/2 hr at 1230°C,
3. repressing at a pressure of 31 tsi,
4. resintering for 1 1/2 hr under hydrogen at 1230°C,
5. coining under a pressure of 31 tsi.

Compacts prepared in this manner were found to be comparable in densification to the previously developed compacts consisting of Lindsay Mix and prealloyed stainless steel.

Metallographic examination of the Eu_2O_3-stainless steel compacts after hot-rolling at 1150°C into composite plates failed to reveal reactions between the materials. A slight reaction occurred, however, between the Eu_2O_3 and the wrought stainless steel framing and the cladding stainless steel. Encasing the Eu_2O_3-stainless steel compacts in stainless steel foil prepared with elemental powders of low silicon content effectively prevented the reaction between the Eu_2O_3 and the wrought stainless steel.

This developmental work was concluded with the manufacture of a full-size absorber section for core II of the APPR-1. Each side of this absorber section consisted of roll-clad stainless steel composite plate containing a dispersion of 38 wt % Eu_2O_3 in stainless steel. Other than the change in composition of the core material, the core II absorber section is a replica of the core I component.

2. CORRELATION OF FUEL ELEMENT IRRADIATION EXPERIENCE AT VARIOUS AEC INSTALLATIONS

Irradiation experiments with fuel plates of the same general design as that of the APPR-1 fuel elements have been conducted at several AEC installations. Pratt & Whitney Aircraft conducted an irradiation program at the MTR with fuel plates consisting of a 30 wt % UO_2 dispersion in a stainless steel matrix clad with type 347 stainless steel. The Nuclear Development Corporation of America (NDA) has irradiated similar plates consisting of a 30 wt % UO_2 dispersion in a type 310 or 316 stainless steel matrix clad, in each case, with the same type of stainless steel as that used in the matrix. The fuel plates investigated by NDA were produced by the General Electric Company in connection with the ANP program, and similar studies were conducted by GE. Irradiated fuel plates containing 5 to 30 wt % UO_2 in types 347 or 310 stainless steel have also been studied at the Knolls Atomic Power Laboratory (KAPL).

The results of all these experiments and of the experiments at ORNL have been studied in order to correlate burnup and temperature with irradiation damage to such elements.[14] In assessing the data, a fuel element was considered to have failed if swelling, cracking, or fission-product release resulted from the irradiation. Moderate swelling or the appearance of blisters without other indications of failure were considered to be a slight failure, since further irradiation or a higher temperature would undoubtedly have caused complete failure. A plot of the data, as presented in Fig. 2.1, indicated that a curve could be drawn to separate failure from nonfailure conditions relative to burnup and temperature. Two failures appear on the nonfailure side of the curve. Since there are almost eight times as many nonfailure tests at higher temperatures and higher burnup, it appears that factors other than

[14] V. O. Haynes, F. H. Neill, and L. D. Schaffer, Summary of UO_2-Stainless Steel Dispersion Element Irradiation Experiments, ORNL CF-58-2-71 (March 18, 1958).

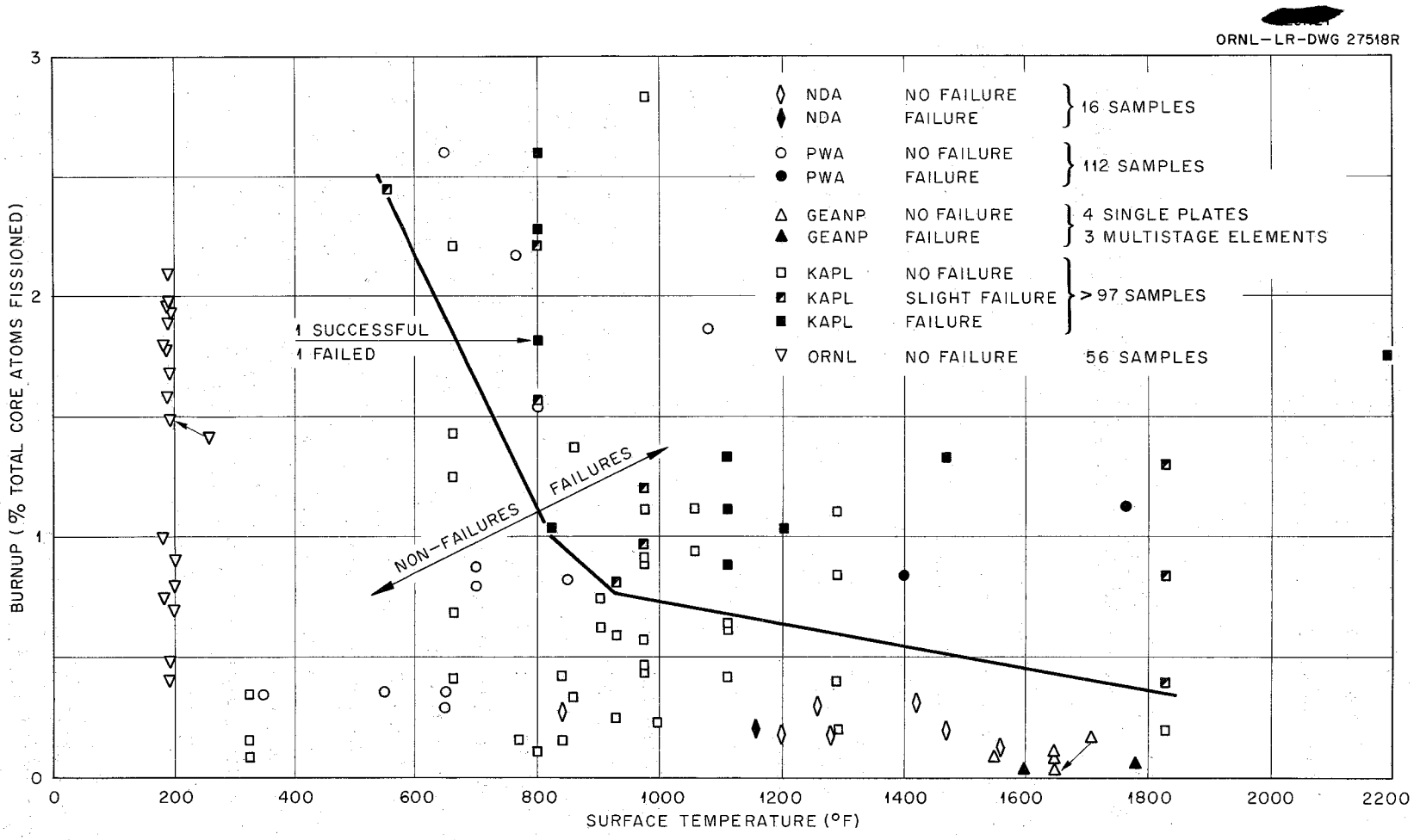

Fig. 2.1. Correlation of Burnup and Fuel Element Surface Temperature with Irradiation Damage to Fuel Elements Consisting of a 30 wt % UO_2 Dispersion in a Stainless Steel Matrix Clad with Stainless Steel.

burnup and temperature or inaccurate test control caused these failures. The correlation presented in Fig. 2.1 provides useful guide lines in the design of fuel plates of the type used in APPR-1.

3. EXPERIMENTAL DETERMINATION OF FISSION-PRODUCT RELEASE AS A RESULT OF MELTDOWN OF AN APPR-1 FUEL ELEMENT

Experiments in the controlled melting of irradiated fuel of the APPR, STR, and MTR types under conditions simulating the loss-of-coolant accident have been performed.[15] The results indicate that a moderate amount of heating in air or steam sufficient only to melt a specimen results in the partial volatilization of the rare gases, the halogens, and the alkali metals. In the presence of air or steam, little of the strontium and other fission products are released. In this type of experiment the only particulate activity observed was cesium.

An attempt has been made recently to relate variations in the quantity of fission-product release to the melting, or preheating time, since the fuel is molten only long enough to permit detection of the fission products. The values observed ranged from 16 to 50% release of the rare gases and from 3.7 to 17.6% release of the iodine with preheating times ranging from 19 to 72 sec. The cesium release values ranged from 15.7 to 72% for preheating times of 6 to 42 sec.

The effect of the preheating time, which has been observed thus far only with samples punched from material irradiated to burnups of 15 to 30%, cannot be explained without considering a possible dependence on the exposed fuel edge of the punched sample. Therefore experiments with clad, miniature coupons are planned.

---

[15] G. E. Creek, W. J. Martin, and G. W. Parker, Experiments on the Release of Fission Products from Molten Reactor Fuels, ORNL-2616 (Dec. 23, 1958).

A complementary and possibly equally important cause of the time effect may be that certain chemical reactions require a finite time and a high temperature for initiation. For example, reactions may occur between UO_2 and silicon or boron in the form of a thermite type of reaction.

An examination of the off-gas obtained during the melting of an APPR-1 fuel plate failed to show any significant particulate activity other than from cesium or iodine. The cesium was readily and quantitatively filtered, but the iodine was only partially retained by filters. Some information on the iodine state present under the oxidizing conditions of the melting is indicated by a preference for absorption in reducing solutions, as expected with free iodine. This does not imply that part of the iodine is not carried on inactive solid particles. This possibility remains to be investigated.

In melting slightly irradiated samples, up to 33% of the iodine was released, along with about 11% of the cesium. For samples irradiated to a burnup of 25%, the cesium release averaged about 40% and the average iodine release declined to 12%. Since this was the only instance in which the release was not proportional to the burnup, these results must be regarded as tentative until they can be checked under different conditions.

The spontaneous release of rare gases at temperatures below the melting point from punched disks of material irradiated to a burnup of 30% suggests significant radiation damage to crystalline UO_2. Again the effect of mechanical stress on the punched samples may have contributed to release of the gases. The planned experiments with clad coupons will provide a basis for further analysis of these observations.

4. CALCULATION OF TANTALUM AND COBALT ACTIVATION IN TYPE 347 STAINLESS STEEL

Preliminary estimates of the activation products expected from the use of stainless steel as cladding material for APPR-1 fuel elements did not reveal significant quantities of long-lived activation products. In making the estimates, reactions whose cross sections were unknown were neglected and, of course, reactions with stainless steel impurities whose concentrations were too small to be reported by the manufacturer were not considered. Measurements made after 700 full-power hours of reactor operation revealed, however, significant quantities of long-lived (greater than 50 days) activation products in the water stream and in the demineralizer. It was found that the manufacturer had not included cobalt in the impurity analysis because non-nuclear customers are not usually interested in this impurity. Subsequent analysis revealed that the type 304L stainless steel cladding used for the core I fuel plates contained about 0.05 wt % cobalt.

Following the realization of the importance of the long-lived activation products from stainless steel, a further evaluation of type 347 stainless steel proposed on the basis of metallurgical properties (see chap. 1) for use as the cladding material for the core II fuel elements was undertaken. Type 347 stainless steel was found to contain, in addition to cobalt (0.05 wt %), a small amount of tantalum (0.2 wt %), which produces a long-lived activation product (Ta^{182}).

An estimate was made of the activity that would be built up in the core in 1.5 years of operation if the stainless steel used contained equal quantities (wt %) of tantalum and cobalt.[16] The results of this study, presented in Fig. 4.1, indicated that the use of type 347 stainless steel would produce an even more serious activation problem than that found with the use of type 304L stainless steel.

---

[16] E. E. Gross, Estimate of the Ratio of Ta^{182} to Co^{60} Activity Expected in the APPR-1 Core, ORNL CF 58-2-32 (Feb. 10, 1958).

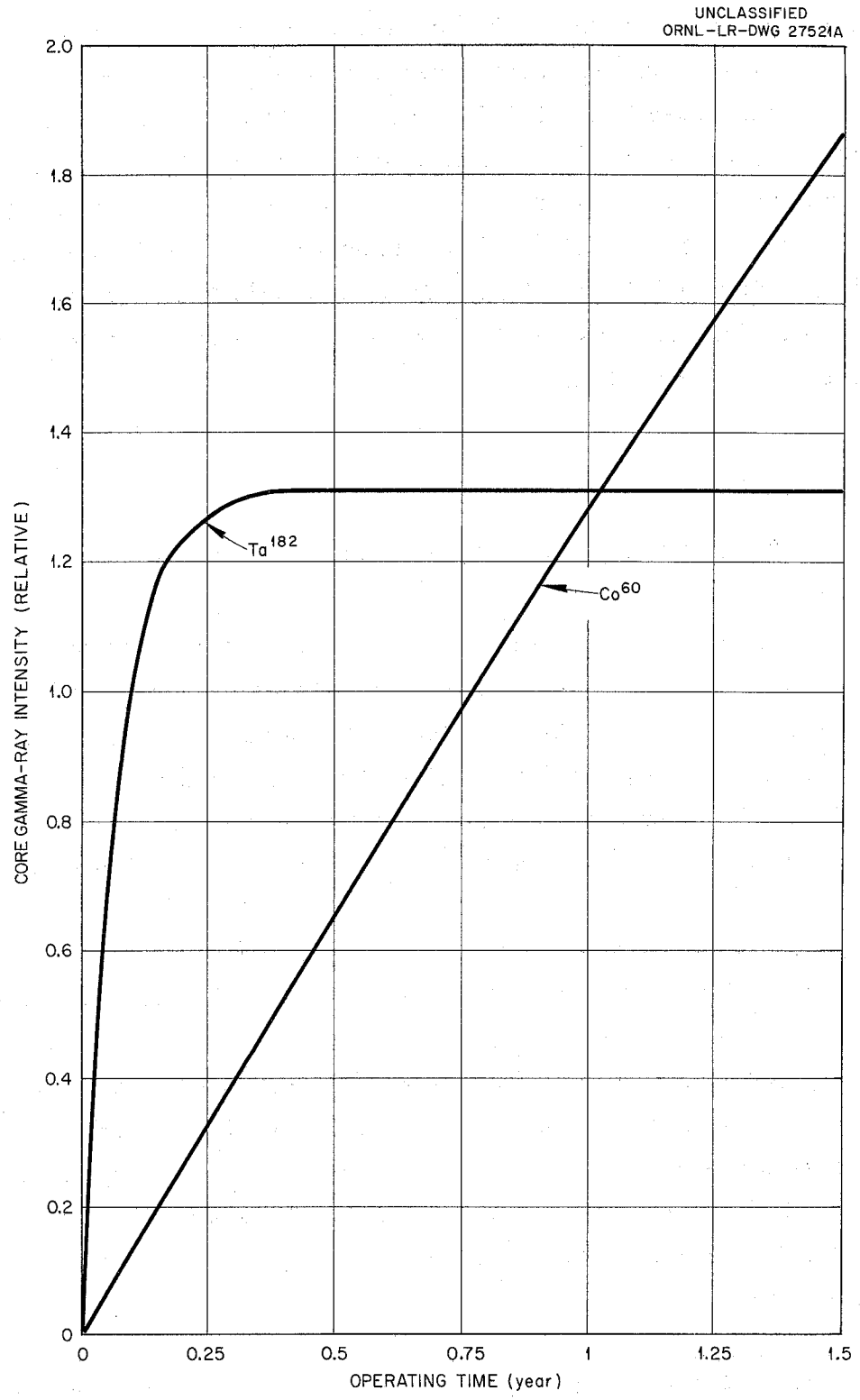

Fig. 4.1. Relative Gamma-Ray Intensity as a Function of Operating Time for Stainless Steel APPR Core Containing Equal Quantities of Co^{59} and Ta^{181}.

In the interest of reducing the buildup of long-lived activation products, it was therefore recommended that the APPR-1 core II be fabricated from low-cobalt (0.005 wt %) type 304L stainless steel (see chap. 1). The decrease in the cobalt content from 0.05 to 0.005 wt % will reduce the production of Co^{60} by a factor of 10. The buildup of Co^{58} as a result of the $Ni^{58}(n,p)Co^{58}$ reaction will remain the same, however; and if the buildup of Co^{58} is troublesome from the standpoint of plant maintenance, consideration may have to be given to the removal of nickel from future cores.

5. CORRELATION OF APPR CRITICAL EXPERIMENTS

The Martin Company, in July 1958, began critical experiments that were designed to investigate methods of flattening the power profile and increasing the reactivity lifetime of the APPR-1 type of core. ORNL personnel were requested to advise the Army Reactor's Branch on The Martin Company work, inasmuch as they were familiar with the original ORNL critical experiment,[17] as well as the Alco Products, Inc. zero power experiment.[18]

The fuel used in the Martin critical experiments is very similar to that used in the ORNL experiment. It consists of 0.002-in.-thick stainless steel. The boron is in the form of 0.0066-in.-thick boron steel foil; and the remaining stainless steel is added by the use of 0.001-, 0.002-, and 0.005-in.-thick stainless steel foils loosely laminated with the uranium foil and the boron foil to mockup an APPR-1 core I fuel plate. The APPR-1 core I fuel plate consists of a homogeneous matrix of B_4C, stainless steel, and UO_2 clad in 0.005-in.-thick stainless steel.

---

[17] D. V. P. Williams et al., Army Package Power Reactor Critical Experiment, ORNL-2128 (Aug. 21, 1956).

[18] J. W. Noaks and W. R. Johnson, Army Package Power Reactor Zero Power Experiments, ZPE-1, APAE-8 (Feb. 8, 1957).

The first experiment assembled by The Martin Company consisted of fuel elements that mocked up the composition of the final APPR-1 core I loading. In contrast to the Alco Products zero power experiment in which the matrix type fuel elements became critical upon the insertion of 17 fuel elements, The Martin Company foil-type elements did not become critical until 27 elements had been inserted. If it is assumed that The Martin Company fuel element is an "exact" mockup of the APPR fuel element, the discrepancy between The Martin Company critical experiment and the zero power experiments could be explained by an almost complete loss of boron during the fabrication of the matrix-type fuel plates. In order to resolve the apparent discrepancy it was decided to assemble a Martin Company critical experiment with 45 elements and no boron to compare with a similar experiment at ORNL and to reanalyze the matrix-type fuel plates for boron, with the analysis normalized to the analysis of a known boron mixture.

Although the reanalysis has not been concluded, the results of The Martin Company clean, cold, critical experiment indicated that the discrepancy in critical mass between a foil type of element and a homogeneous-matrix type of element can be explained to a large extent as a heterogeneous effect. The clean, cold, critical mass results for foil- and matrix-type fuel elements are listed below:

	Critical Mass (kg)
Martin Company foil element[19]	10.1
ORNL foil element	10.35
ORNL homogeneous-matrix substitution	9.04

The clean, cold critical mass for a matrix type of fuel element was obtained by substituting a matrix type of element for a foil element in the ORNL critical experiment.

[19] Information obtained from J. F. O'Brien of The Martin Company.

Further strong evidence that the discrepancy between The Martin Company results and the zero power experiment results is due mainly to heterogeneous effects rather than to the loss of boron is presented in Fig. 5.1. The solid curve in Fig. 5.1 presents the variation in critical mass with boron loading for the ORNL foil-type elements. The broken curve presents the similar data for matrix-type fuel elements. Two of the points on the broken curve were obtained from the substitution measurement made in the ORNL experiment.[17] The other two points came from the insertion of boron steel strips and the worth of fuel in the zero power experiment. In obtaining the points for the broken curve, it was assumed that the amount of boron contained in the form of matrix material was as specified before fabrication. Although it would be desirable to have more points on the broken curve, the consistency of the available data is convincing evidence that even at a loading of 250 g of natural boron there is a significant difference in critical mass between matrix fuel plates and foil fuel plates.

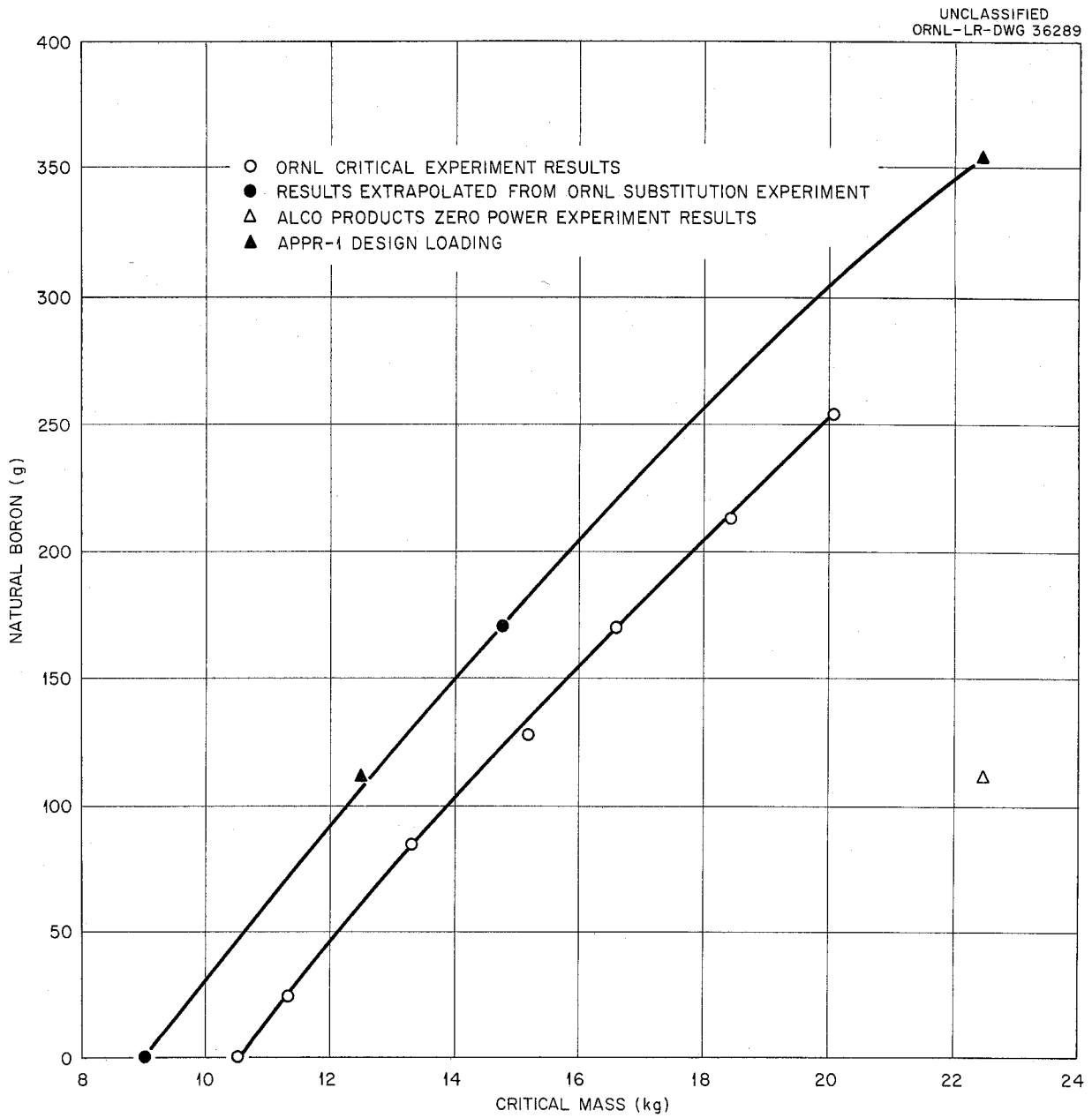

Fig. 5.1. Effect of Boron Loading of APPR-1 Fuel Plates on Critical Mass.

PART II. GAS-COOLED REACTOR PROGRAM

6. GAS-COOLED IN-PILE TEST LOOP

DESIGN CRITERIA

The gas-cooled in-pile test loop for insertion in the ORR was designed[1] to operate with various coolant gases, including N_2, He, CO_2, and air, at temperatures and pressures up to 1500°F and 300 psia. A maximum gas velocity over the fuel specimens of 350 fps was to be achievable to remove up to 60 kw of fission and gamma-ray heat. Initial tests were to be conducted with N_2 as the coolant; the maximum loop temperature was to be 1200°F; the gas pressure was to be 200 psia; and the gas velocity was to be commensurately lower than the 350 fps maximum. The compressors, in-pile section, and other equipment were sized for tests of assemblies of from one to eight fuel plates; each fuel plate was to be 1 in. wide and 10 in. long. Typical assemblies are described in Table 6.1.

The in-pile section of the loop was designed originally to occupy the two adjacent lattice positions, A-1 and A-2; later, it was decided to utilize lattice positions B-1 and B-2. The ORR core-reflector assemblies were to be replaced by an aluminum casing which would space the loop properly and fill the core structure. Preheated gas was to enter the hairpin-shaped in-pile piping above the core, flow to the bottom of the piping, and return through the adjacent pipe leg to the external section of the loop piping above the core. Both legs of the loop were to be utilized for irradiation of specimens. The in-pile loop section was to extend through a rectangular-shaped access in the reactor tank cover, directly above the A-1 and A-2 positions. The later plans for the utilization of positions B-1 and B-2 called for offset pipes to the reactor core flange V-10. Access was to be available from above the reactor tank for insertion and removal of specimens with the use of a specimen retraction mechanism. Side

---

[1] A. L. Boch, F. Neill, and H. C. McCurdy, Proposed Gas-Cooled Loop for the Oak Ridge Research Reactor - A Preliminary Description, ORNL CF 56-8-74 (Aug. 27, 1956).

Table 6.1. Features of Reference Test Specimens for ORR Gas-Cooled Test Loop

Specimen Designation	Sample Cross Section Dimensions (in.)	Flow Area (ft^2)	Gas Flow Rate (ft^3/sec)		Heat Generation (kw)
			Minimum	Maximum	
Fuel Assembly*	1.76 OD	0.00876	1.5	3.1	54
Fuel Assembly**	1.030 x 1.058	0.0040	0.68	1.4	62
Flat plate samples in holder (1 to 8 plates)	1.00 x 0.062	0.005 to 0.010	0.85	3.5	0 to 60

*C. J. Heindl et al., Portable Trailer-Mounted Power Reactor System, ORNL CF 55-8-192 (Aug. 1955)

**H. Raab et al., Nuclear Powered Snow-Train, ORNL CF 55-8-196 (Aug. 1955).

connections to the external loop piping were also to be above the tank but below the vertical access flange. Pipe routing to the equipment room in the basement was to be through the reactor pool water, the south standpipe and the pipe chase below it, and a trench for a subfloor run to the shielded equipment room. The total pipe run between the in-pile section and the equipment room in Bay 1-2, C-D, would have been approximately 125 ft one way, with most of the route utilizing existing shielding.

Gas returning from the in-pile section to the equipment room was to first pass through a hot-gas filter for removal of any particulate matter which might have entered the system. The filtered gas was to be cooled by passing it successively through regenerative and water-cooled heat exchangers. The cooled gas was to be compressed in a carbon-ring reciprocating blower and then passed through a cold-gas filter for removal of particulate matter that might have been added in the blower. The gas was then to be reheated by passing it first through the economizer and then through the preheater. Variable controls would have enabled the preheater to add an appropriate amount of energy to the gas to obtain the desired temperatures in the specimen region. A sketch of the loop assembly is shown in Fig. 6.1.

MAJOR COMPONENTS AND FEATURES

Compressors. Two 6-in.-bore, 7-in.-stroke, single-stage, water-cooled, double-acting, carbon-ring, reciprocating compressors with carbon-packed shaft seals, Model WGBOL-9, were purchased from the Joy Manufacturing Company. The specified operating conditions for the compressors were the circulation of oil-free, dry (-70°F dew point) nitrogen in the amount of 1.475 lb/sec, with intake temperature and pressure conditions of 260 to 295°F and 255 psia and discharge conditions of 345°F (minimum) and 325 psia. A run-in loop was built to check the compliance of these units with the specified low in-leakage and wear rates. One unit was subjected to preliminary test and shakedown operations in which the leakage and wear rates were found to be excessive. After field servicing by factory representatives was

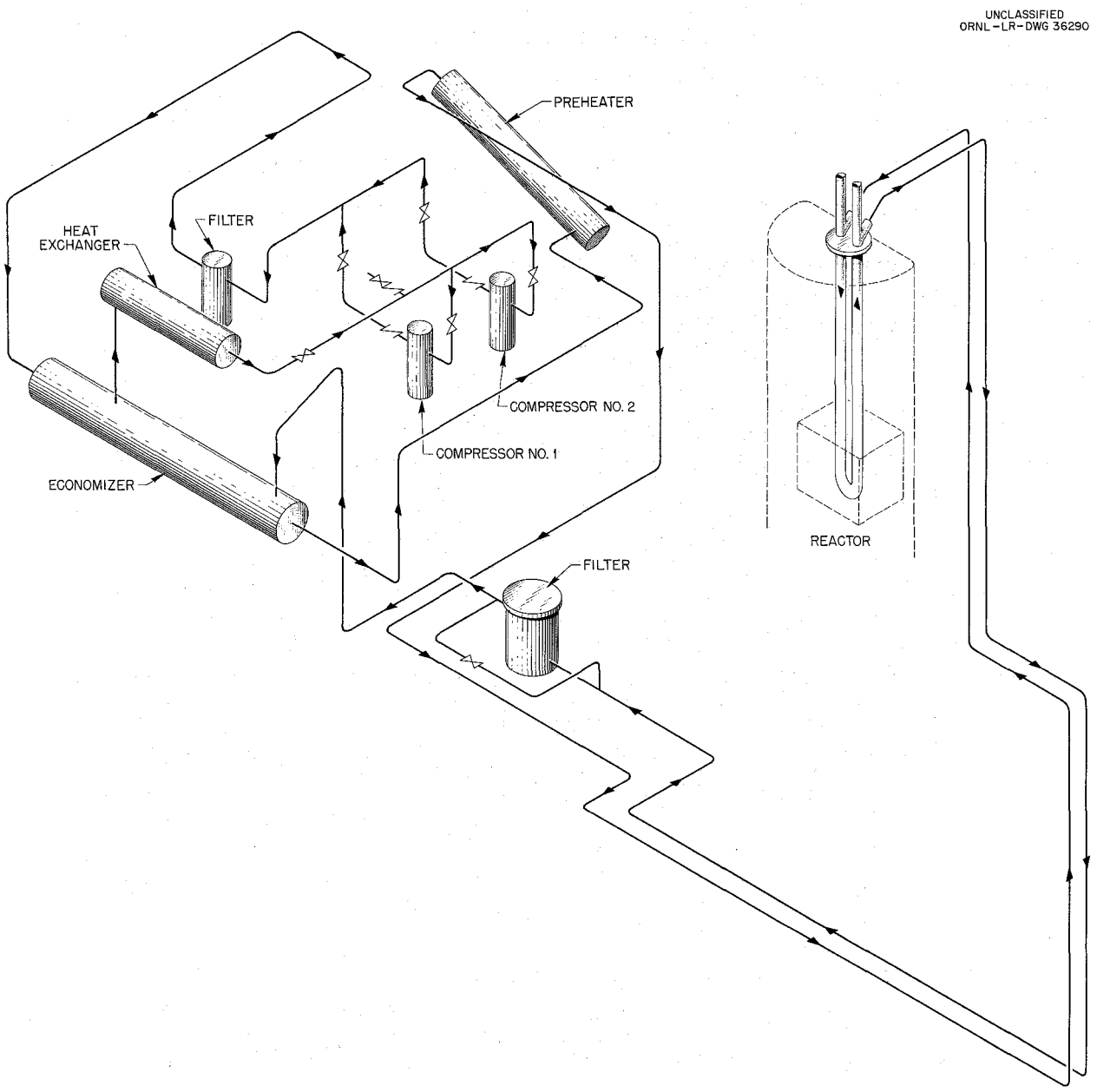

Fig. 6.1. Sketch of ORR Gas-Cooled In-Pile Loop Designed for Army Reactor Program Experiments.

unsuccessful in improving these conditions, both units were returned to the factory. The Joy Manufacturing Company has since reworked the compressors and has reported that performance has been improved.

Economizer. The economizer unit (approximately 350-kw capacity) for nitrogen was designed by ORNL with Inconel specified as the material of construction to accommodate the high operating temperatures and pressures. The design was predicated somewhat on the availability of Inconel stock. The unit was to be made up of 479 tubes, 3/16 in. in outside diameter and 14 1/2 ft long, with 0.025-in. walls, which were brazed into the tube sheets. One tube sheet was to float with tube expansion. When the project was terminated, negotiations were nearly complete on a contract with the Struthers Wells Corp. for the fabrication of this unit.

Preheater. The preheater was to be electrically powered and rated at 145 kw, 240 v. It was to be equipped with Nichrome, radially finned, direct-gas-contact elements. The V-shaped, "bus-bar"-like, fin elements were to be shaped into a cylindrical array approximately 6 in. in diameter and 10 1/2 ft long. Since the design of the preheater was similar to that of the economizer, the preheater was included as a second unit in the fabrication negotiations mentioned above. It was planned to purchase the heating elements as a separate item, and negotiations were essentially completed with the Hynes Electric Heating Div., Turbine Equipment Co. for the two heater elements (one being a spare) and the associated power control equipment.

Cooler. The water-cooled nitrogen heat exchanger was purchased from The Andale Company who designed and fabricated the unit. It is a folded-tube conventional unit capable of removing 80 kw of heat from air or nitrogen at 500°F.

Filters. The hot-gas filter was to be housed in an internally insulated Inconel vessel designed for gas temperatures up to 1500°F. The filter medium was to be a replaceable Fibrefrax unit capable of removing 99% of the particulate material 1 to 2 μ in diameter. The filter vessel cover was flanged for access, and provision was made for remote servicing of the unit, which was to be located in an enlargement

of the shielded trench. The design of the unit by the Buffalo Forge Co. was nearly complete at the time of project termination.

Servicing of the filter was to be accomplished with the use of a lead cask on wheels, which could be rolled over a sliding floor opening to communicate to the trench. The filter flange bolts were to be removable by direct operators extended through the floor plug. The cover could be raised to the under surface of the floor plug which could be rolled away to expose the filter to the carrier. The used filter unit could then be withdrawn into the shielded carrier for later disposal. Adequate shielding was to be available throughout the operation. Provision was to be made in the trench for storage of a new filter unit and remote insertion into the filter housing. After installation of a new filter, the trench cover was to be replaced; the cask was to be removed; and the filter cover was to be replaced and bolted. This procedure, although somewhat complex, would not have been required except in the event of a major fuel plate failure. Filter plugging would be unlikely during normal operation, and, even if the filter plugged, no serious activity problems would be presented. Since the proposed test program was eventually to include tests of advanced fuel elements, it was deemed appropriate to include these somewhat elaborate provisions for filtering. Cotton-felt pad filters manufactured by the Dollinger Corporation were to be installed immediately downstream of the compressor to accumulate carbon wear particles from the rings and seals.

Instrumentation and Controls. The instruments were designed to provide the information required for loop operation and safety. Accurate measurements of both gas and metal temperatures for the portion of the loop in the reactor core were considered to be essential to successful and safe operation. Inconel-sheathed Chromel-Alumel thermocouples were proposed for these and for other temperature measurements, as required. Inlet and outlet gas temperatures, together with gas flow and pressure data, were to be used in determining the power generation of the fuel test piece.

The safety of the loop was to be dependent upon the instrumentation. Loss of flow or gas pressurization could have resulted in inadequate cooling and subsequent failure of test pieces. Reactor shutdown was to be initiated by loop instrumentation for high fuel and loop temperatures, loss of gas circulation, low gas pressure, and high radiation levels. Appropriate alarms were included to give warning of undesirable conditions prior to reactor shutdown for these reasons, as well as to warn of other less hazardous conditions. In the latter category, alarms were planned to warn of heat exchanger cooling-water low temperature, heater high temperature, low gas supply pressure, high radiation levels in the gas ventilation system, and miscellaneous changes of loop temperatures. The instruments were to be located adjacent to the equipment room. Nearly continuous monitoring of loop conditions by loop operators was deemed to be necessary, and the instrumentation was designed on this basis. Operators for this loop, however, would have provided limited service for other experiments in the vicinity. At the time of termination of the project, the design of the instrumentation was essentially complete, and most components had been procured.

Retraction and Withdrawal Devices. Each piping leg into the reactor was to receive a holder carrying the specimens. Each holder was to be suspended through an O-ring seal from a common holder plate above the overhead access flange, which was within a single pipe extension attached to the access flange. The electrically powered mechanism for turning a nonrising lead screw that engaged the common holder plate was to be within a housing atop the pipe extension. By driving the lead screw, the common holder plate with both holders would be raised. Travel of the mechanism was to be sufficient to permit complete retraction of the holders from the reactor lattice. The retraction device was to be removable as a unit from the common access flange. Insertion and removal of specimens were to be accomplished by replacing the retraction device with a specimen servicing device.

The servicing device was to provide for withdrawal, severance, and dry removal for disposal of a specimen holder and subsequent insertion of a replacement holder.

Other Features. Remotely demountable flanges were planned for connecting the in-pile piping to the out-of-pile system. They were to be located near the hairpin piping on the side connection. This feature was to be included to permit removal of the loop piping from the reactor core and reactor tank without disturbing other portions of the loop system.

The out-of-pile piping run from the reactor tank to the equipment room was to be thermally insulated and encased in a helium-tight stainless steel jacket. It was planned to bleed helium through this annulus and past a monitor as a means of leak detection.

ANALOG COMPUTER STUDY

The operation of the proposed gas-cooled loop was carefully studied by means of an analog computer. A system of differential and algebraic equations was derived[2] for various gas flow rates by writing heat balances on the various parts of the loop shown in the diagram of Fig. 6.2. The computer was built up from these equations.

The tests showed that, with nitrogen as the coolant, a flow rate of more than 1.0 lb/sec was necessary to keep the temperature of the fuel at or below 1650°F with design-point power of 57.2 kw being generated in the fuel. A flow rate of 1.5 lb/sec was more than adequate to limit the temperature of the fuel to 1650°F. With the power generated in the fuel limited to 70% of design point, a flow rate of 1.0 lb/sec was enough to limit the fuel temperature to 1650°F. The same limit could be obtained by increasing the capacity of the cooler in tests with a flow rate of 1.0 lb/sec.

The rates at which the temperature of the fuel would rise and fall with flow rates of 1.0 and 1.5 lb/sec are shown in Fig. 6.3.

---

[2] F. P. Green et al., Analog Computer Study of the Operation of the Gas-Cooled Loop of the Oak Ridge Research Reactor, ORNL CF 58-7-48 (July 7, 1958).

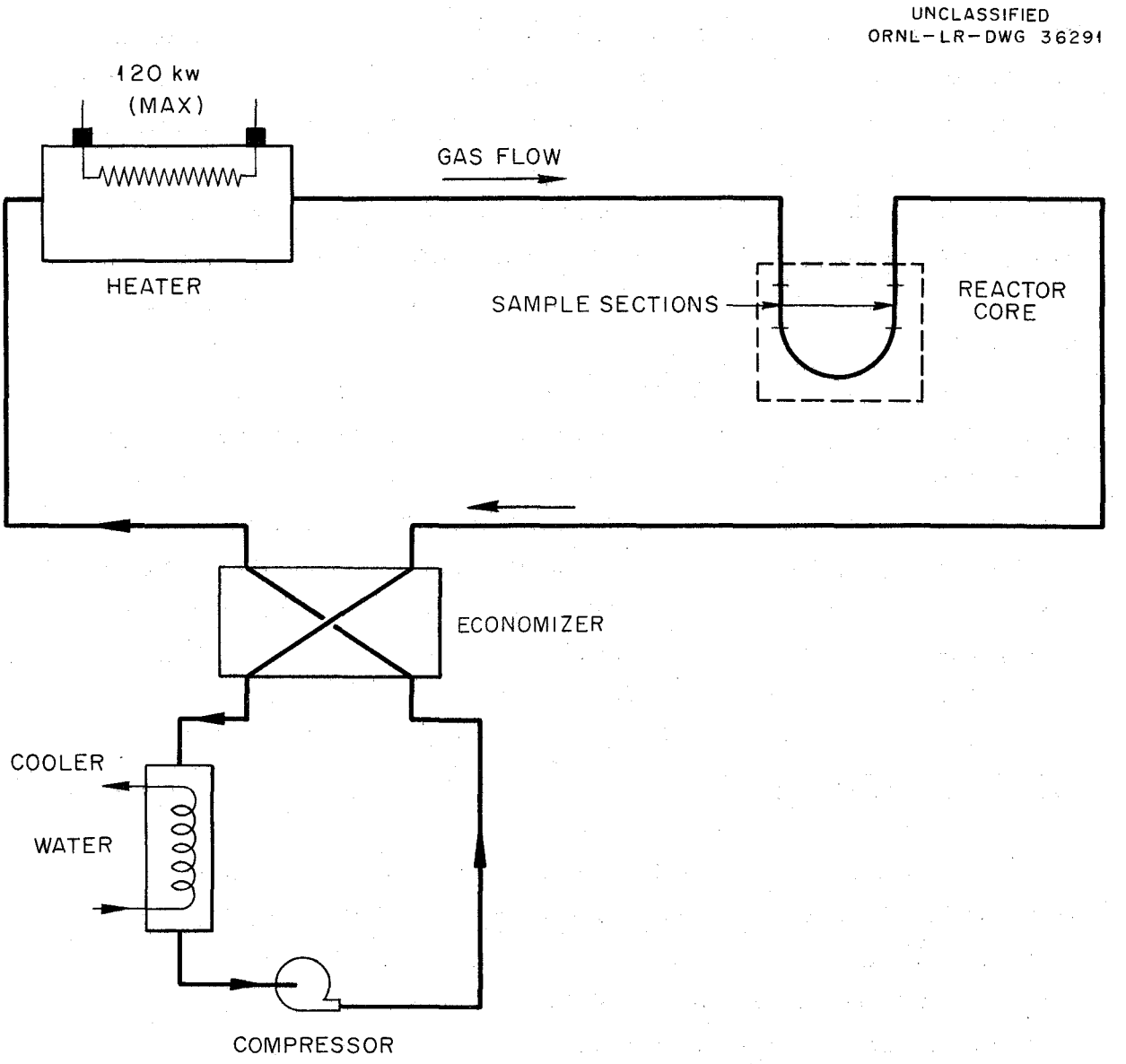

Fig. 6.2. Gas-Cooled In-Pile Loop Schematic Flow Diagram.

Gas temperatures are shown only for the startup case (increasing fuel temperature). For the cases of increasing temperature, it was considered that heat was being added to the system by the heater, by fissioning in the fuel, and, to a small degree, by the compressor. The temperature of the fuel was maintained at design point by controlling the temperature of the gas leaving the heater with a simple on-off controller on the heater. For the cases of decreasing fuel temperatures, the system was considered to have been operating at steady state. At time t = 0, the fission heat was reduced to zero, and the electric heater was turned off.

A step change in the flow rate produced a brief dip in the fuel temperature, which, in turn, caused the heater to supply more heat to the system (Fig. 6.4). The heater was on continuously until the sharp break in the gas temperature curve occurred. After that time, it was on intermittently to hold the gas temperature constant. Since there was no overshoot of the fuel temperature, it was concluded that the simple on-off controller on the heater was adequate to control the fuel temperature.

GAS VELOCITY MEASUREMENTS

A low-temperature, air-flow mockup of the in-pile section of the loop was fabricated, as shown in Fig. 6.5, to study velocity profiles in various sections of the loop. It is important that the coolant flow over all the samples be as uniform as possible in order to simplify the analysis of the radiation damage in the individual samples.

The mockup section was used to determine the effect of various combinations and arrangements of the simulated fuel element samples and the close return bend of the pipe on the flow distribution. The flow distribution was measured in terms of a velocity traverse at four different cross sections in the in-pile section, two representing positions ahead of each sample irradiation position, and the other two being cross sections downstream of each irradiation position, as shown in Fig. 6.6.

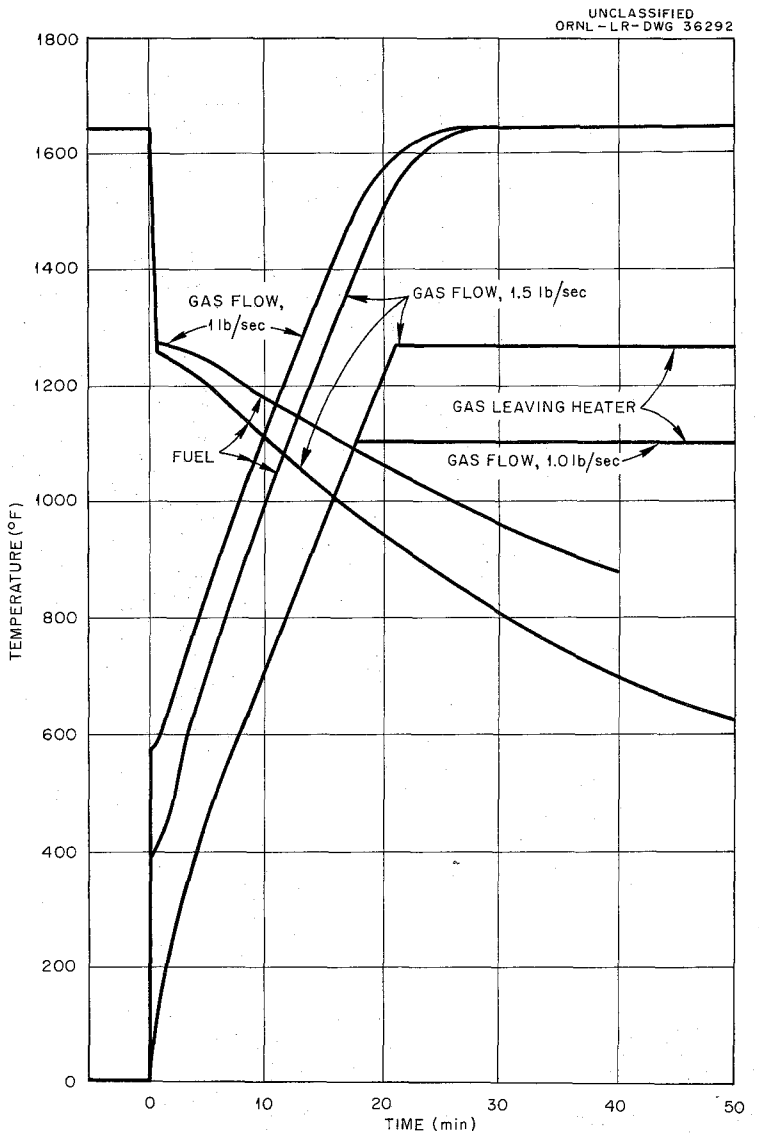

Fig. 6.3. Heating and Cooling Rates in the Proposed ORR Gas-Cooled In-Pile Loop.

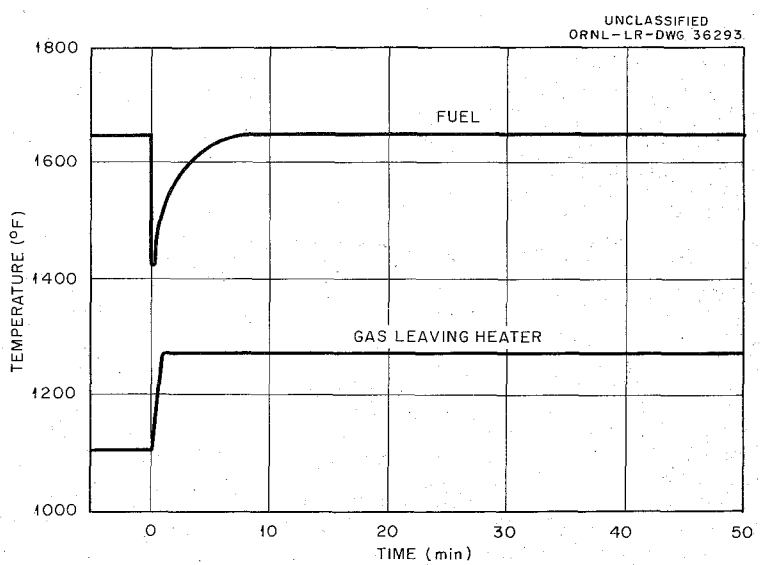

Fig. 6.4. Temperature Changes Produced by Step Changes in Flow Rate from 1.0 lb/sec to 1.5 lb/sec at Time $t = 0$.

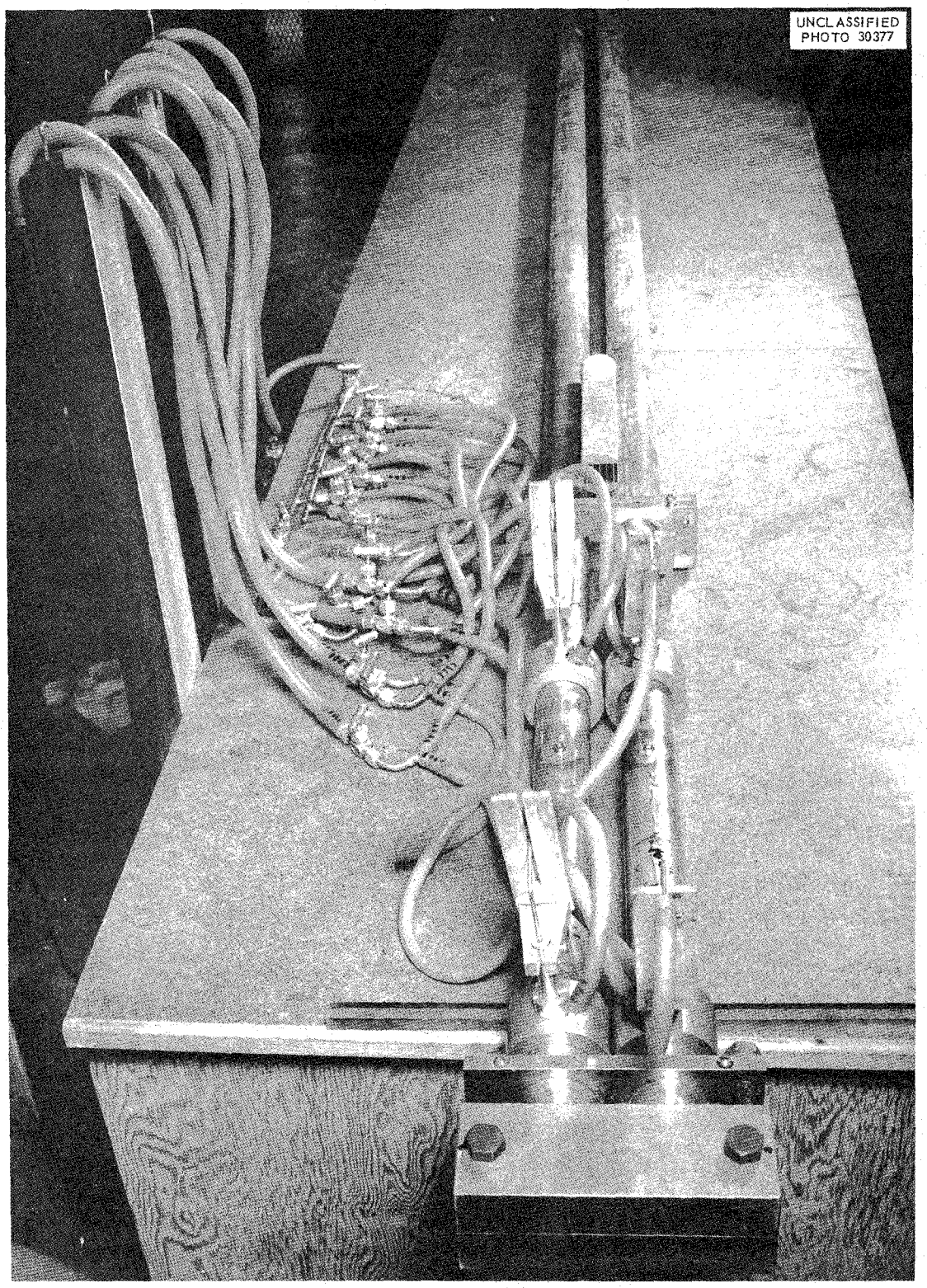

Fig. 6.5. Mockup Fabricated for Gas-Velocity Measurements of In-Pile Section of Gas-Cooled Loop.

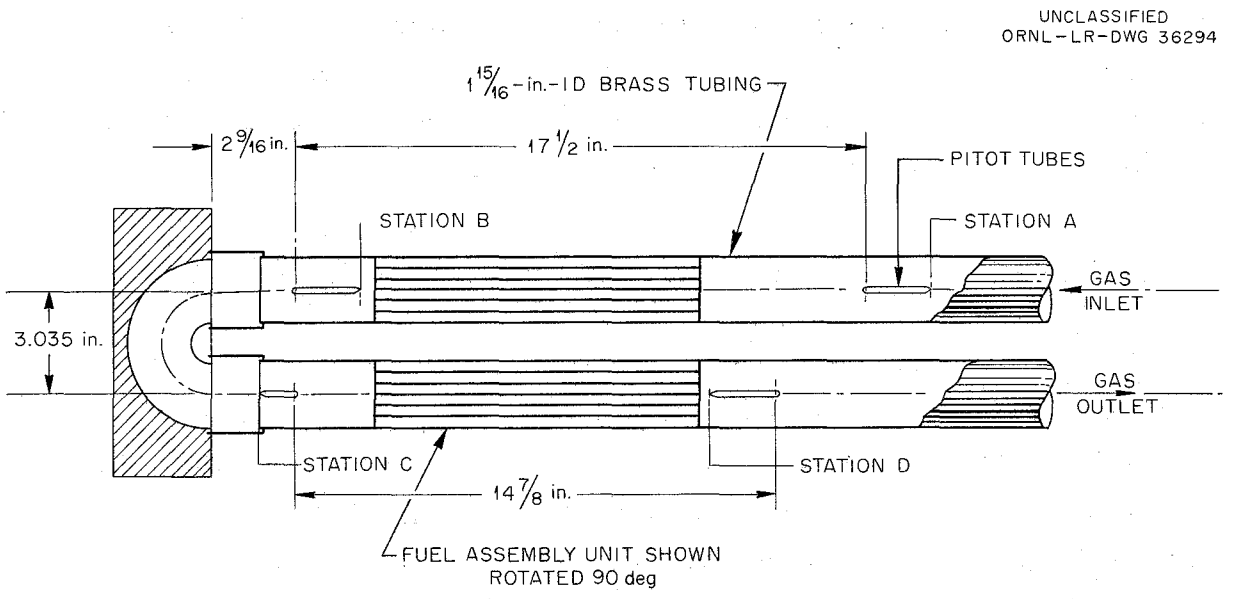

Fig. 6.6. Diagram of In-Pile Section Mockup Showing Positions at Which Velocity Measurements Were Taken.

Typical sets of results obtained for stations A, B, C, and D are shown in Figs. 6.7 and 6.8. Station A indicates the typical turbulent flow-velocity pattern. At station B, the flow pattern was still relatively uniform, even after the gas had passed through the first set of experimental fuel plates. At station C, after passing the return bend in the pipe, the flow was no longer uniform. At station D, with no experimental plates installed in the loop, the flow pattern returned to a uniform pattern; however, with experimental plates in the facility, the flow was very erratic. Several types of flow-correction guide vanes were under study for use in the return bend at the time of termination of the project. One type of guide-vane assembly is shown in Fig. 6.9.

DETERMINATION OF COEFFICIENT OF HEAT TRANSFER IN LOOP INSULATION

The thermal insulation material planned for use around the out-of-pile section of the ORR gas-cooled loop was Thermoflex encased in a 12 x 10-in. stainless steel duct. The unusual geometry and the helium atmosphere in the duct made an experimental determination of the heat loss desirable. The experimental equipment consisted of two 3-ft lengths of 2 1/2-in. pipe wrapped in Thermoflex and placed in a stainless steel duct. The ends were covered and insulated to reduce end heat loss. Thermocouples were appropriately placed on the pipe and insulation. The heating was simulated by Calrod heaters centered in each pipe.

Measurements were made with the insulation in an air atmosphere and in a helium atmosphere. The detailed results of the experiment have been reported[3] and are summarized in Table 6.2.

The results of these tests indicated that the apparent thermal conductivity of the porous material would be increased by a factor of 2.6 to 1.5 in the temperature range of 300 to 1200°F if helium were substituted for air in the voids of the insulation.

---

[3] B. E. Short, F. H. Neill, and R. G. Reinhardt, Heat Loss Experiment for Package Reactor Loop, ORNL CF 57-11-127 (Nov. 14, 1957).

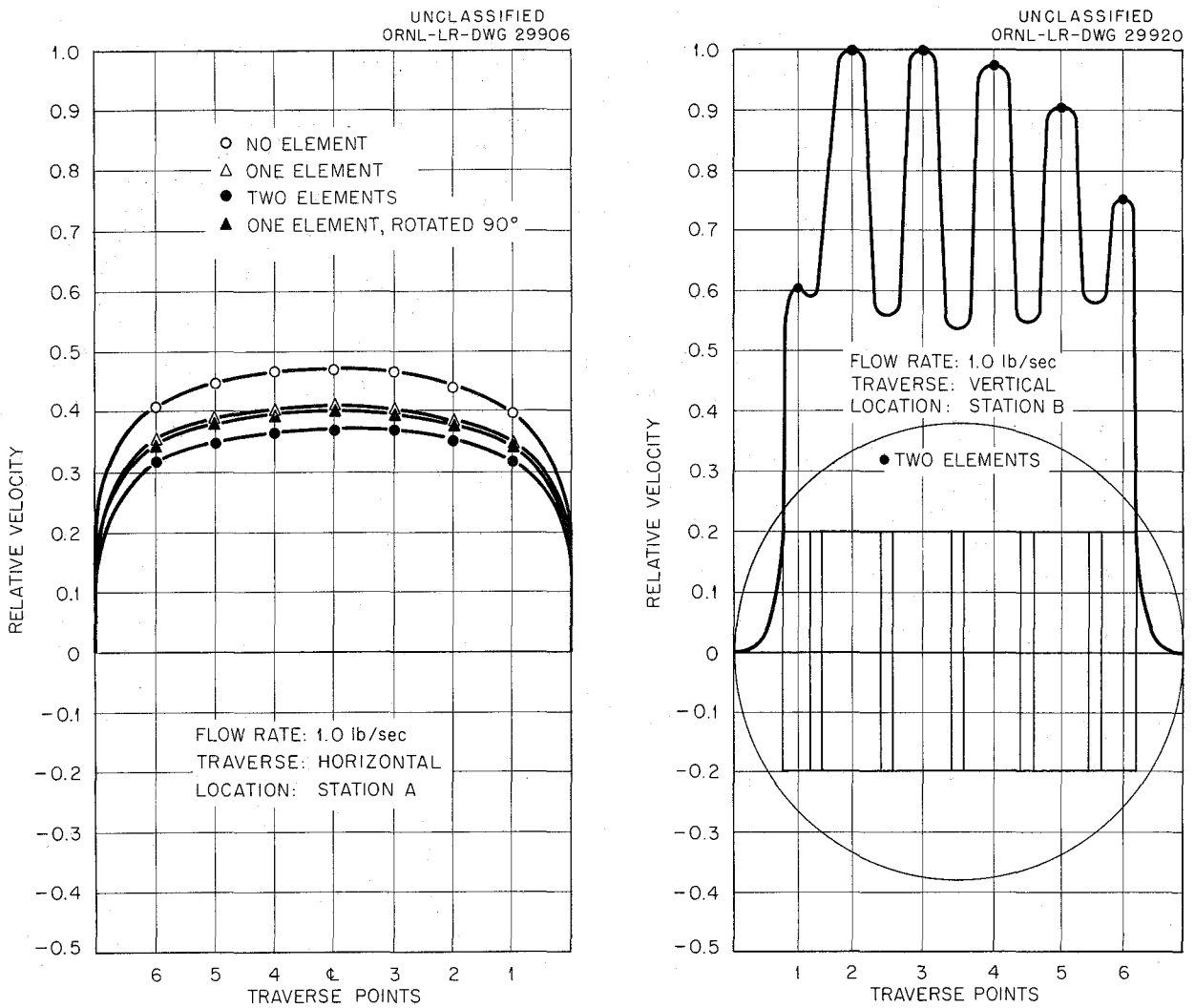

Fig. 6.7. Velocity Traverses at Stations A and B of ORR Gas-Cooled Loop Mockup.

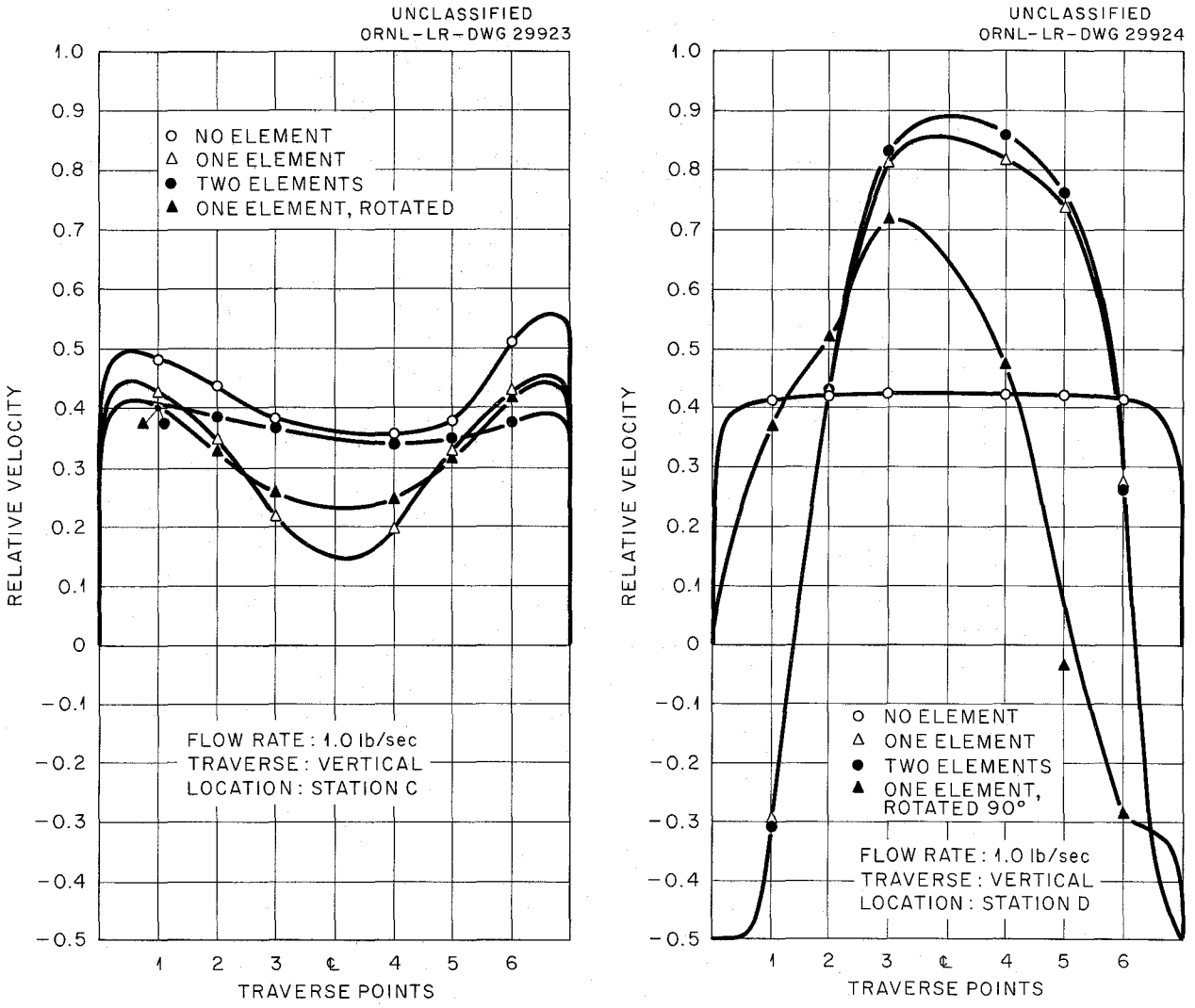

Fig. 6.8. Velocity Traverses at Stations C and D of ORR Gas-Cooled Loop Mockup.

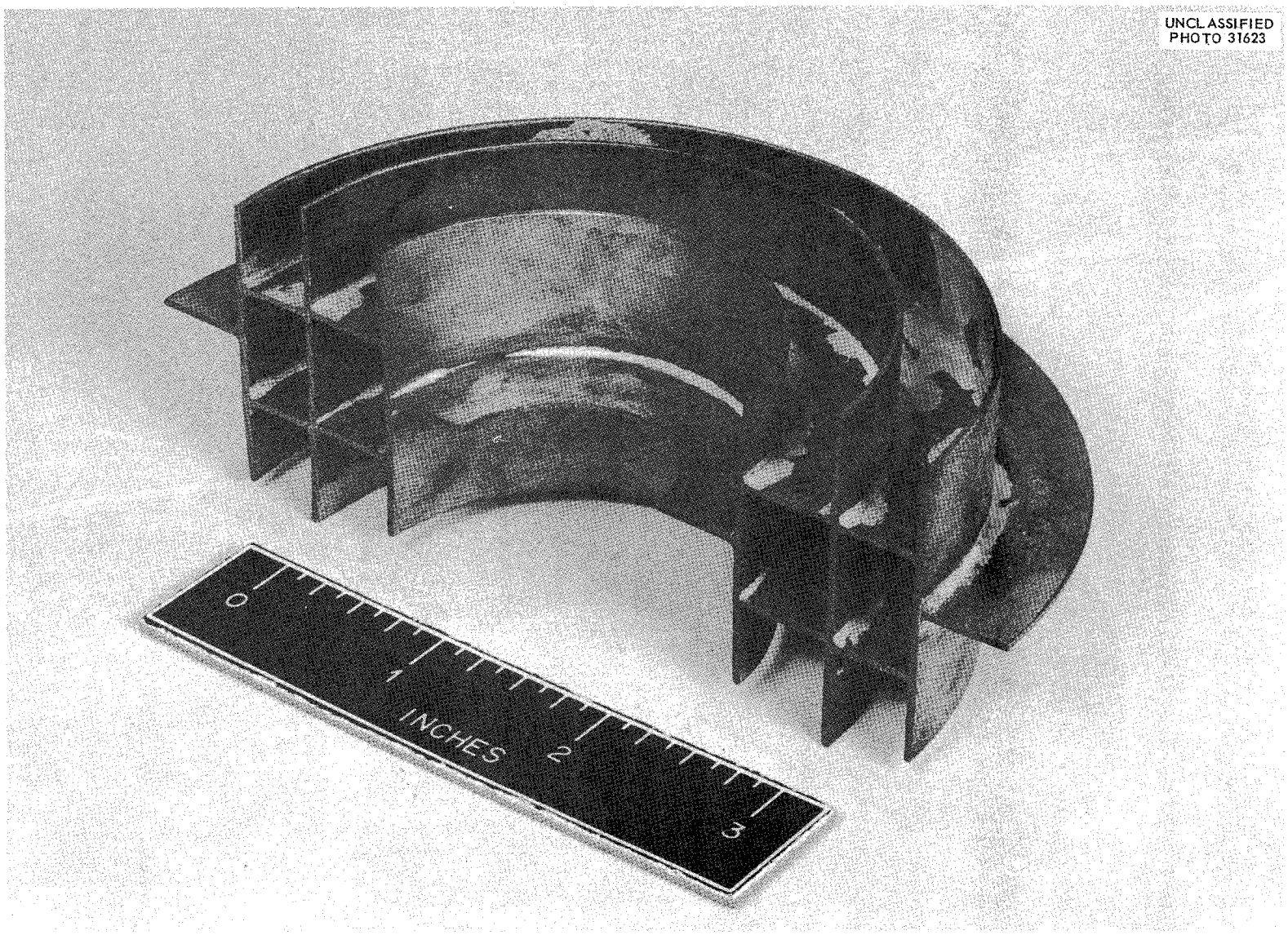

Fig. 6.9. Guide-Vane Assembly for Use in Return Bend of ORR Gas-Cooled Loop.

Table 6.2. Data on Thermal Conductivity of Thermoflex Insulation

Temperature (°F)	Thermal Conductivity of Thermoflex (Btu/hr·ft·°F)		Apparent Thermal Conductivity of Helium in Thermoflex (Btu/hr·ft·°F)	Ratio of Thermal Conductivity of Helium in Thermoflex to the Thermal Conductivity of Air in Thermoflex
	In Air	In Helium		
300	0.021	0.110	0.951	2.60
500	0.025	0.128	1.078	2.40
1000	0.035	0.167	1.387	1.73
1200	0.039	0.182	1.507	1.54

REACTIVITY AND FLUX MEASUREMENTS PERTINENT TO LOOP OPERATION

A nuclear mockup of the in-pile section of the loop was made to obtain reactivity and flux information for hazards evaluation and for experiment planning. The mockup is shown in Fig. 6.10, and a diagram of the cross section of the tubes is shown in Fig. 6.11.

The results of the reactivity measurements made at the ORR may be summarized as follows:

Experiment	Reactivity Effect (% $\delta k/k$)
Insertion of loop mockup	-0.72
Flooding of the loop with water	+0.024
Insertion of fuel sample containing 20 g of U^{235} and 21 g of stainless steel	
In position A-1	+0.12
In position A-2	+0.24

The flux expected within the loop was measured by exposure of aluminum wires containing a known quantity of manganese impurity. The wires were inserted and exposed in the loop by means of an aluminum wire holder (shown being inserted into the loop in Fig. 6.10). After exposure, the wires were cut into 1-in. pieces. Each segment was then weighed and the Mn^{56} activity was measured. It was assumed that the Mn^{56} activity resulted from thermal-neutron absorption. The flux in the loop during the time of the exposure was then calculated based on the assumptions that the flux is constant during the time of exposure, that the mean life of the activity is very much longer than the time interval used to determine the activity, and that the original number of Mn^{55} atoms is not reduced appreciably by the irradiation.

The results of the flux measurements, normalized to 20-Mw ORR operation, are presented in Fig. 6.12. The location of the flux peak and the average value of the flux in positions A-1 and A-2 are in good

UNCLASSIFIED
PHOTO 44821

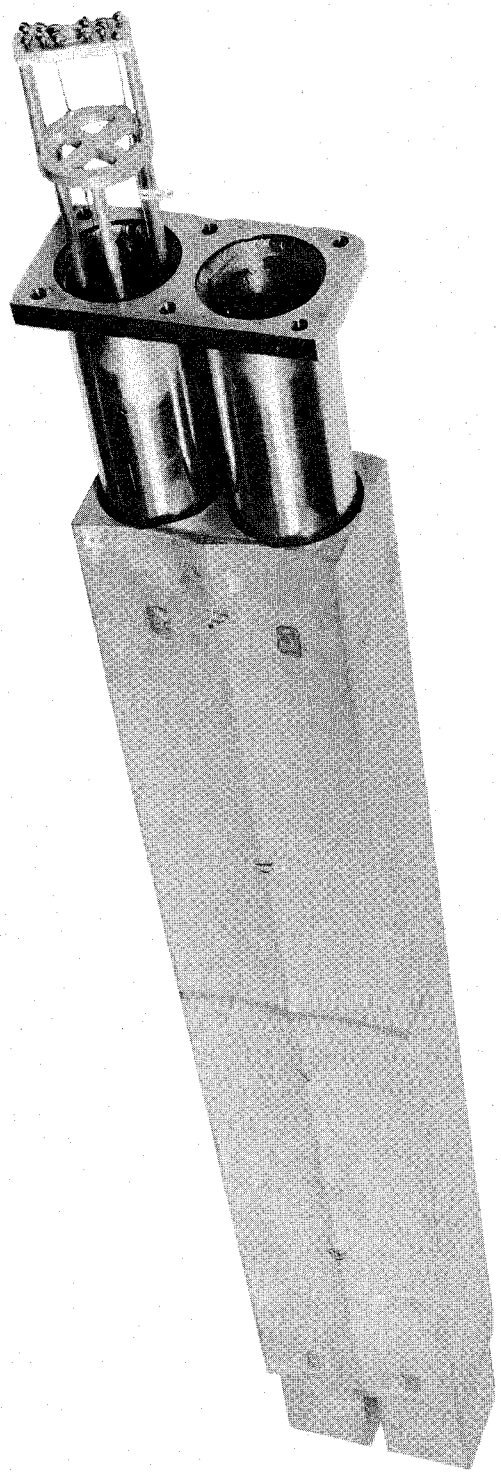

Fig. 6.10. Nuclear Mockup of In-Pile Section of ORR Gas-Cooled Loop for Reactivity and Flux Measurements.

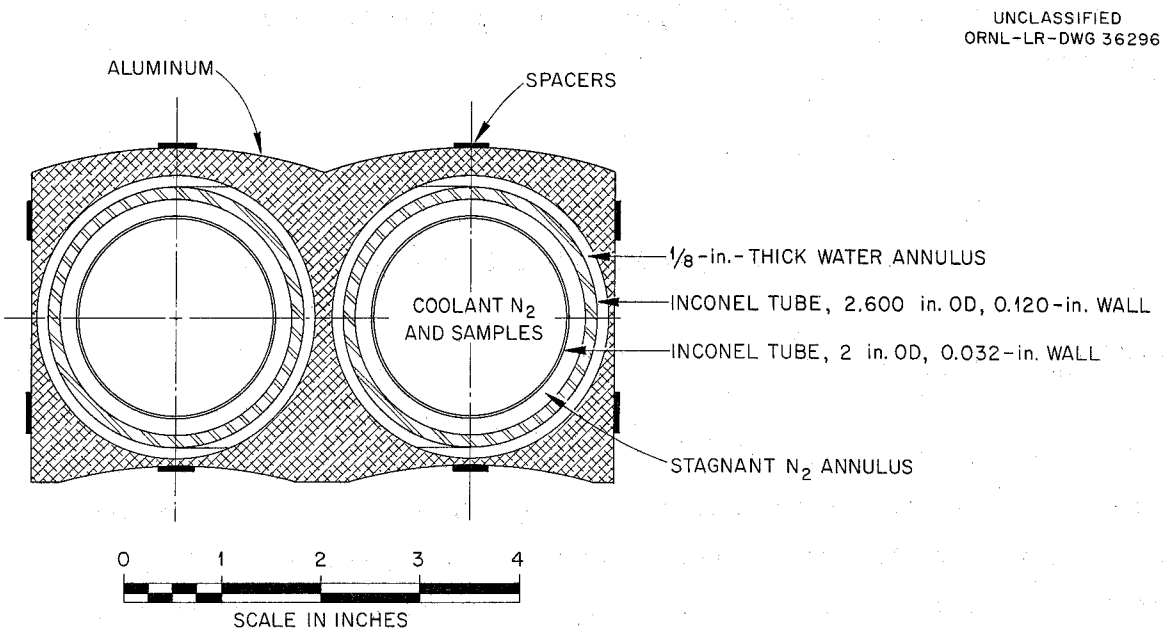

Fig. 6.11. Diagram of Cross Section of In-Pile Section of ORR Gas-Cooled Loop.

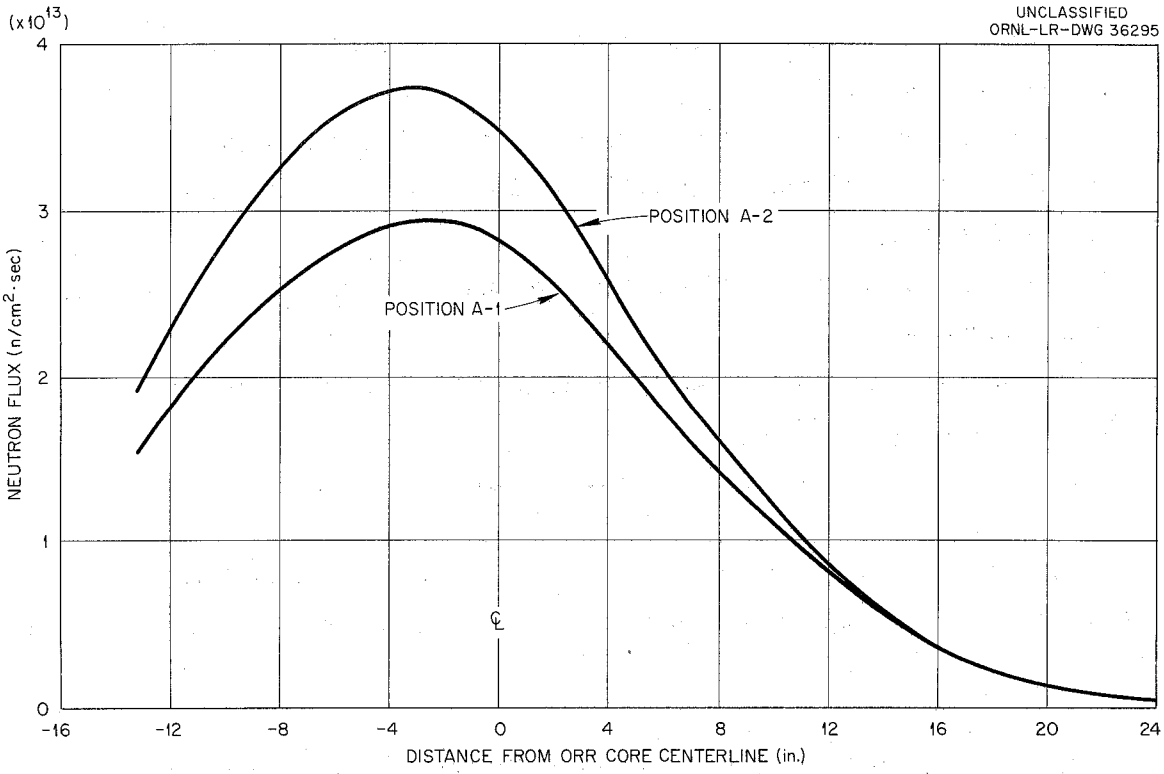

Fig. 6.12. Neutron Flux in Mockup of Gas-Cooled In-Pile Loop Inserted in Lattice Positions A-1 and A-2 of the ORR Normalized to 20-Mw Operation.

agreement with values obtained for other experiments which have been performed in the ORR.[4]

7. GAS-COOLED REACTOR EXPERIMENT SUPPORT

REVIEW OF GCRE DESIGN

A general review of the Army gas-cooled reactor design was made at the request of Aerojet-General Nucleonics. As a result of the review, the review committee, which included consultants selected by Aerojet-General Nucleonics, outlined four critical problem areas in the GCRE design that required further consideration:[5] (1) the "hot-spot" temperature on the fuel element, (2) corrosion, (3) the gas ducting system design, and (4) control rod design.

In order to minimize the hot-spot temperature on the fuel element, it was recommended that:

1. one end of the fuel plate be brazed to the clip assembly,
2. the clip be redesigned to provide a slip fit at the other end of the fuel plate,
3. flutter of the fuel element be investigated in an out-of-pile wind tunnel experiment,
4. experimental results from the GE-ANP experiment be studied for application to the GCRE,
5. effort be made to minimize the radial and axial peak-to-average flux variations.

With respect to the corrosion problem, it was suggested that zirconium not be used for the inner insulation retainer in the fuel

---

[4] C. D. Cagle and R. A. Costner, Initial Post Neutron Measurements in the ORR, ORNL-2559 (to be published).

[5] H. Brown, Summary of Recommendations at Meeting on GCRE at AGN—October 17-18, 1957, AGN-346 (Nov. 5, 1957).

assembly and that the ceramic tube support be replaced with a metallic material. In order to preserve axial symmetry and therefore to achieve more uniform coolant flow through the reactor, it was suggested that, if possible, the gas ducts should enter the reactor parallel to the vertical axes. Also, consideration was to be given to the elimination of the automatic withdrawal of xenon rods so that the reactor operator would have full control of the reactor at all times.

SIMULATOR ANALYSIS

The ORNL analog computer facility was used for a preliminary analysis of the GCRE to determine whether the nuclear closed-loop control system could interfere with the safety system in any way and to investigate the effects of certain component failures.[6] The results of this work were to be used as a basis for further analyses to be made with facilities of the Avionics Division of Aerojet-General Nucleonics.

[6] E. R. Mann, Evaluation of GCRE Reactor and Heat Transfer System by Means of the ORNL Analog Computer Facility, ORNL CF 58-7-2, (July 2, 1958).

[redacted]

ORNL-2703
C-83 - Reactors-Special
Features of Military Package
Power Reactors
M-3679 (22nd ed.)

INTERNAL DISTRIBUTION

1. T. D. Anderson
2. R. J. Beaver
3. D. S. Billington
4. E. P. Blizard
5. A. L. Boch
6. C. J. Borkowski
7. G. E. Boyd
8. E. J. Breeding
9. R. B. Briggs
10. F. R. Bruce
11. C. E. Center (K-25)
12. R. A. Charpie
13. W. B. Cottrell
14. J. A. Cox
15. F. L. Culler
16. H. N. Culver
17. J. E. Cunningham
18. J. C. Ebersole
19. L. B. Emlet (K-25)
20. E. P. Epler
21. A. P. Fraas
22. J. H. Frye, Jr.
23. W. R. Grimes
24. A. Hollaender
25. A. S. Householder
26. W. H. Jordan
27. C. P. Keim
28. M. T. Kelley
29. C. F. Leitten
30. J. A. Lane
31. R. S. Livingston
32. H. G. MacPherson
33. W. D. Manly
34. E. R. Mann
35. H. C. McCurdy
36. H. F. McDuffie
37. F. R. McQuilkin
38. A. J. Miller
39. E. C. Miller
40. K. Z. Morgan
41. J. P. Murray (Y-12)
42. F. H. Neill
43. M. L. Nelson
44. G. W. Parker
45. A. M. Perry
46. M. E. Ramsey
47. P. M. Reyling
48. A. Richt
49. A. F. Rupp
50. H. W. Savage
51. A. W. Savolainen
52. E. D. Shipley
53. M. J. Skinner
54. A. H. Snell
55. J. A. Swartout
56. E. H. Taylor
57. W. C. Thurber
58. D. B. Trauger
59. A. M. Weinberg
60. C. E. Winters
61-64. ORNL Y-12 Technical Library
Document Reference Section
65-76. Laboratory Records Department
77. Laboratory Records, ORNL R. C.
78-80. Central Research Library

[redacted]

[redacted]

EXTERNAL DISTRIBUTION

81. Aerojet-General Nucleonics, San Ramon, California
82-83. AFPR, Lockheed, Marietta
84-85. Air Force Special Weapons Center
86. Air Technical Intelligence Center
87. ANP Project Office, Convair, Fort Worth
88. Alco Products, Inc.
89-93. Argonne National Laboratory
94. Armed Forces Special Weapons Project, Sandia
95. Armed Forces Special Weapons Project, Washington
96. Army Chemical Center
97-106. Atomic Energy Commission, Washington (Army Reactors Branch)
107. Atomics International
108. Battelle Memorial Institute
109-110. Bettis Plant (WAPD)
111. Brookhaven National Laboratory
112. Bureau of Aeronautics
113. Bureau of Medicine and Surgery
114. Bureau of Ordnance (AD-1B)
115. Bureau of Ships
116. Bureau of Yards and Docks
117-118. Chicago Operations Office
119. Chicago Patent Group
120. Combustion Engineering, Inc.
121. Continental Army Command
122. duPont Company, Aiken
123. duPont Company, Wilmington
124. Engineer Research and Development Laboratories
125-126. General Electric Company (ANPD)
127-129. General Electric Company, Richland
130. General Nuclear Engineering Corporation
131. Hartford Aircraft Reactors Area Office
132. Iowa State College
133-134. Knolls Atomic Power Laboratory
135-136. Los Alamos Scientific Laboratory
137. Martin Company
138. National Aeronautics and Space Administration, Cleveland
139. National Aeronautics and Space Administration, Washington
140. Naval Air Development Center
141. Naval Civil Engineering Laboratory
142-143. Naval Research Laboratory
144. New York Operations Office
145. Nuclear Development Corporation of America
146. Oak Ridge Operations Office
147. Office of Naval Research
148. Office of the Chief of Naval Operations
149. Ordnance Tank-Automotive Command

[redacted]

[redacted]

150. Patent Branch, Washington
151-153. Phillips Petroleum Company (NRTS)
154. Pratt and Whitney Aircraft Division
155. Sandia Corporation
156-157. School of Aviation Medicine
158. Sylvania-Corning Nuclear Corporation
159. The Surgeon General
160-163. Union Carbide Nuclear Company (ORNL)
164. USAF Headquarters
165. USAF Project RAND
166. U. S. Naval Postgraduate School
167. U. S. Naval Radiological Defense Laboratory
168. University of California Radiation Laboratory, Berkeley
169. University of California Radiation Laboratory, Livermore
170. Walter Reed Army Medical Center
171-175. Wright Air Development Center
176-200. Technical Information Service Extension

[redacted]

[redacted]

[redacted]

[redacted]